Stony Brook University

Bundle-Forming α-Helical Peptide-Dendron Hybrids

A Dissertation Presented

by

Jeannette Elizabeth Marine

to

The Graduate School

in Partial Fulfillment of the

Requirements

for the Degree of

Doctor of Philosophy

in

Chemistry

Stony Brook University

May 2016

Stony Brook University

The Graduate School

Jeannette Elizabeth Marine

We, the dissertation committee for the above candidate for the

Doctor of Philosophy degree, hereby recommend

acceptance of this dissertation.

Jonathan G. Rudick
Dissertation Advisor
Assistant Professor, Department of Chemistry

Isaac Carrico
Chairperson of Defense
Associate Professor, Department of Chemistry

Melanie Chiu
Third Member of Dissertation Committee
Assistant Professor, Department of Chemistry

Yizhi Meng
Outside Committee Member
Assistant Professor, Department of Materials Science and Engineering

This dissertation is accepted by the Graduate School

Charles Taber
Dean of the Graduate School

Abstract of the Dissertation

Bundle-Forming α-Helical Peptide-Dendron Hybrids

by

Jeannette Marine

Doctor of Philosophy

in

Chemistry

Stony Brook University

2016

Accurate control over the three-dimensional arrangement of atoms in synthetic materials remains a challenge for polymer and supramolecular chemistry. A defined sequence of monomers programs the folding and self-assembly of peptides and proteins, which makes them excellent candidates for materials in which the precise arrangement of atoms is known. The inherent sensitivity of peptides to external stimuli hampers their practical application. Conjugating peptides with synthetic polymers creates biohybrid materials with increased stability and processability. Hybrid biomaterials can retain the folding and self-assembly properties of peptides. Our approach to hybrid biomaterials is to combine helix bundle-forming peptides with a class of structurally perfect polymers called dendrons. These novel peptide-dendron hybrids offer unprecedented control over folding and self-assembly in synthetic materials.

A general synthetic strategy was required to prepare peptides with reactive groups to participate in copper-catalyzed azide-alkyne cycloaddition (CuAAC) reactions. Assembling peptides with hydrophobic amino acids bearing azides and alkynes resulted in difficult sequences. Therefore, an alternative strategy was developed whereby polar lysine residues were used in the assembly of peptides and later transformed to azidonorleucine residues. The

quantitative nature of the diazotransfer reaction with imidazole-1-sulfonyl azide (ISA) was demonstrated through MALDI-TOF and HPLC experiments. This strategy was effective both in solution and on solid-phase to transform large numbers of lysines in a peptide. Orthogonally protected lysines provided a method to site-specifically transform lysine residues on-resin. The reactivity and versatility of the diazotransfer reaction provides a general strategy to site-specifically incorporate multiple azides after chain assembly.

The CuAAC reaction is a bioorthogonal reaction that introduces a small 1,4-triazole linkage to conjugate the dendrons to the peptides in a graft-to manner. Iterative synthesis was used to prepare sequence-defined peptides and second-generation dendrons resulting in monodisperse starting materials. Monodisperse and defect-free products were obtained from CuAAC reactions of dendrons with peptides. The monodisperse nature of the peptide-dendron hybrids was confirmed using MALDI-TOF and HPLC.

The first examples of peptide-dendron hybrids that fold and self-assemble into α-helical bundles have been designed on the basis of hydrophobic patterning of the amino acid sequence. The α-helical secondary structure of the hybrids, which was found to be dependent on the concentration of the hybrid and the ionic strength of the solution, was confirmed from circular dichroism (CD) spectroscopy experiments. Titration studies demonstrated that the hybrids self-assemble into bundles of α-helices with the dendrons on the outside of the bundle. Characterization of several bundle-forming α-helical peptide dendron hybrids has provided initial principles to design synthetic materials that display the structure and function of native peptides.

Table of Contents

List of Figures

Chapter 1

Chapter 2

Chapter 3

Chapter 4

List of schemes

Chapter 4

List of Tables

Chapter 2

Chapter 3

Chapter 4

List of Abbreviations

9-BBN	9-borabicyclo(3.3.1)nonane
α	alpha
β	beta
δ	chemical shift
ε	extinction coefficient
[θ]	mean residue ellipticity
μ	micro- (scale)
Ac	acetyl
Alloc	allyloxycarbonyl
Bn	benzyl
Boc	butoxycarbonyl
Bu	butyl
CD	circular dichroism
CuAAC	copper-catalyzed azide-alkyne cycloaddition
d	doublet (NMR)
Da	dalton
dd	doublet of doublets (NMR)
DMF	*N,N*-dimethylformamide
DMSO	dimethyl sulfoxide
DNA	deoxyribonucleic acid
e.g.	for example
ESI	electrospray ionization

EtOAc	ethyl acetate
Fmoc	9-fluorenylmethoxycarbonyl
g/mol	grams per mole
GPC	gel permeation chromatography
h	hour
HBTU	*O*-(benzotriazol-1-yl)-*N,N,N',N'*-tetramethyluronium hexafluorophosphate
hex	hexane
HPLC	high-performance liquid chromatography
HRMS	high-resolution mass spectrometry
Hz	hertz
IR	infrared
ISA	imidazole-1-sulfonyl azide
J	coupling constant
k	kilo- (scale)
L	liter
m	milli- (scale); multiplet (NMR)
M	molar
m/z	mass-to-charge ratio
MALDI	matrix-assisted laser desorption ionization
MeCN	acetonitrile
mg	milligram
min	minute
M_n	number average molecular weight

mol	mole
MS	mass spectrometry
Ms	mesyl (methanesulfonyl)
M_w	weight average molecular weight
n	nano- (scale)
N_3	azide
NMM	*N*-methylmorpholine
NMR	nuclear magnetic resonance
PEG	polyetheylene glycol
ppm	parts per million
PS	poly(styrene)
R_f	retention factor
RNA	ribonucleic acid
s	singlet (NMR)
SPAAC	strain-promoted azide-alkyne cycloaddition
SPPS	solid-phase peptide synthesis
TFA	trifluoroacetic acid
THF	tetrahydrofuran
TLC	thin layer chromatography
TOF	time-of-flight
Ts	tosyl (4-toluenesulfonyl)
UV	ultraviolet

Acknowledgments

I would like to start by thanking Professor Jonathan G. Rudick, my dissertation advisor for his unparalleled dedication, guidance, and support. I am fortune to have joined such a wonderful research group. You have provided me the opportunity to grow as a scientist and instilled a strong foundation in synthetic and supramolecular chemistry. I would also like to thank my dissertation committee members, Professor Isaac Carrico and Professor Melanie Chiu, for their willingness to serve on my committee and for providing constructive criticism. I would also like to thank Professor Yizhi Meng for taking the time to serve as the outside member.

I am grateful that I have been able to work with so many wonderful people throughout the years, in particular Shuang Song, Xiaoli Liang, Lauren Spagnuolo, Deborah A. Barkley, Maisha Rahman, Oleg Gelman, Kenneth Kan, Yue Wu, and Dr. Jo-Ann Jee. I would like to thank many members of the Department of Chemistry and collaborators at Stony Brook University including Professor Daniel P. Raleigh for serving as the chair of my committee in previous meetings and for use of the Circular Dichorism (CD) instrument; Professor Frank W. Fowler, for serving as committee member in a previous meeting; Matthew D. Watson, for training me on the CD instrument; Dr. Béla Ruzsicska, for training me on mass spectroscopy; Dr. James Marecek and Dr. Francis Picart, for sharing their knowledge of NMR spectroscopy; Katherine Hughes for being the best and most knowledgeable Graduate Student Affairs Coordinator.

Lastly, I would like to thank my friends and family for their unending support throughout the years. To my daughter, Zainab, thank you for giving me the strength to get through the tough times. To my husband, Zeeshan, thank you for being there every step

of the way. Most importantly to my parents, Maria and Domingo, I would not be the person I am if it were not for the both of you.

Chapter 1

Introduction

1.1 Bundle-forming α-Helical Peptide-Dendron Hybrids

Inspired by the structural features and functions of peptides and proteins, there has been significant interest in creating materials in which the three-dimensional arrangement of atoms is precisely known.[1-3] Gaining control over hierarchical self-assembly processes that span multiple length scales has been especially challenging in soft materials.[4,5] Synthetic polymers are assembled through statistical reactions that lead to a distribution of polymer chain lengths (i.e., polydispersity) and poor control over the sequence of monomers in copolymers. Peptides and proteins, macromolecules whose molecular structure can be precisely controlled, are attractive alternatives to synthetic polymers. Folding and self-assembly of peptides and proteins are programmable through the sequence of amino acid monomers. However, the precisely defined three-dimensional structure that results from folding and self-assembly of peptides and proteins is restricted to a narrow range of conditions.[2,6] Additional strategies are needed to control the structure of soft materials.

Hybrid materials exploit the advantages of the individual components while minimizing their disadvantages.[1,2,6-12] Conjugating peptides with synthetic polymers is of interest for creating hybrid biomaterials that combine the precise and programmable three-dimensional structure of proteins with the diverse physical properties available to synthetic polymers.[8,13] In order to have complete control over the structure of peptide-polymer hybrid materials, monodisperse polymers are needed. Dendrons are a class of structurally perfect polymers composed of branched monomers. A fundamental

understanding of how the dendron (or polymer) influences the folding and self-assembly of the peptide component in these hybrids will allow us to rationally design synthetic materials with tailored properties.[14,15]

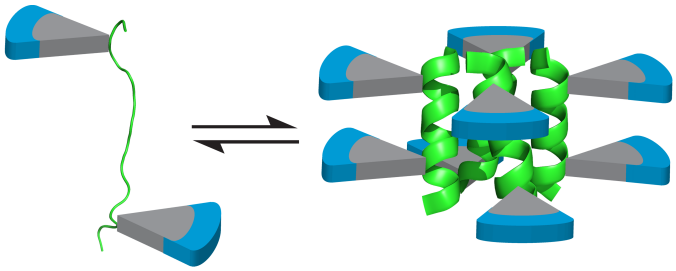

Figure 1.1 Folding and assembly of a peptide (green ribbon) with two dendritic side-chains (wedges) to form a dendronized bundle of α-helices. Reproduced with permission from ref 17. Copyright 2015 American Chemical Society.

Our approach to hybrid biomaterials is to combine helix bundle-forming peptides with dendrons (Figure 1.1). Patterning of polar and non-polar residues in the amino acid sequences was used to create amphipathic α-helices that self-assemble into bundles.[16] Bundle-forming α-helical peptide-dendron hybrids were prepared by site-specifically introducing hydrophilic dendrons to the exterior residues of the bundle assembly. The bioorthogonal CuAAC reaction[17,18] was employed as a graft-to approach that would be suitable for a wide-range of peptides. Assembling peptides with hydrophobic amino acids bearing azides and alkynes suitable for CuAAC resulted in difficult sequences. Therefore, an alternative strategy was developed whereby polar lysine residues were used in the assembly of peptides and later transformed to azidonorleucine residues.[19] The first examples of peptide-dendron hybrids that fold and self-assembly into α-helical bundles with the dendrons on the outside of the bundle were synthesized and characterized.[20,21]

1.2 Peptides as Modules for Programming Function in Hybrid Materials

The variety of architectures that are readily available among peptide building blocks has drawn significant interest for the design of peptide-dendron hybrids (Figure 1.2). Cyclic peptides have been used to generate cylindrical nanostructures due to stacking of the dendronized peptide macrocycles (Figure 1.2c).[22,23] Linear peptides of various lengths have also been investigated. On one end of the spectrum, dendritic dipeptides have been extensively studied as supramolecular materials.[24-34] At the other end of the spectrum, dendronized polymers (Figure 1.2b) have been prepared from polypeptides of relatively high molecular weight. These dendronized polymers are of interest because of the rigid α-helical rodlike conformation of the polymer backbone,[35,36] and because high molecular weight monodisperse polypeptides can be obtained by genetic engineering.[35] A series of peptide-dendron hybrids based on sequence-defined peptide oligomers have also been studied (Figure 1.2a).[22,37,38]

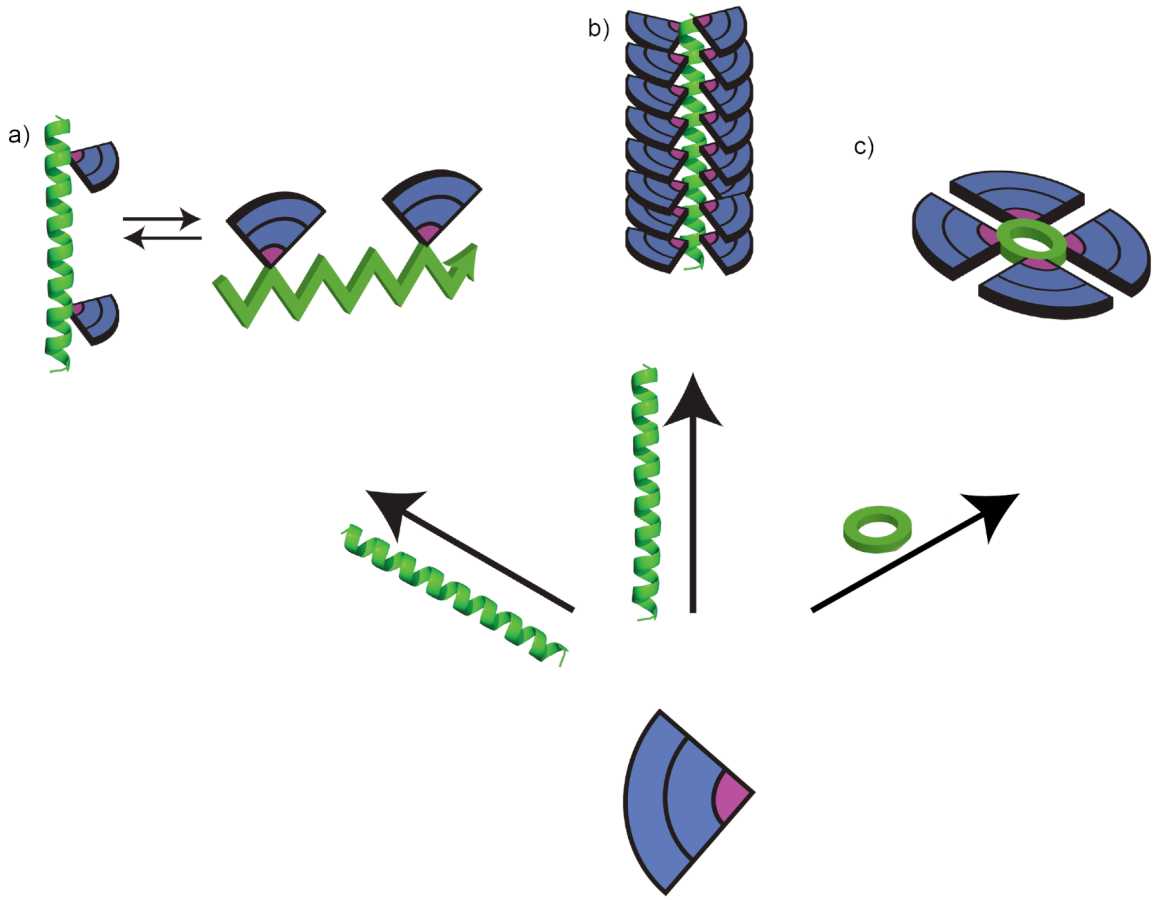

Figure 1.2 Diverse architectures found in peptide-dendron hybrids: a) dendronized peptide that undergoes an α-helical to β-sheet transition b) dendronized peptides with high grafting density and c) dendronized cyclic peptides.

The number of amino acids between dendrons (i.e., grafting density) and size of the dendrons have a tremendous impact on the conformation of the peptide in the hybrids. Dendronized polypeptide polymers have a very high grafting density with one dendron per repeat unit of the polymer backbone (Figure 1.2b). Lee and Fréchet grafted dendrons to an α-helical polypeptide.[36] When smaller (i.e., low generation) dendrons were grafted to the polymer, the dendronized polymers remained α-helical. Sufficiently large dendrons, however, induced a conformational transition from α-helix to random coil. It

was speculated that the steric bulk of the dendrons was responsible for the change in backbone conformation. Parquette and coworkers examined the effect of dendrons on the conformation of a short, sequence-defined α-helical peptide oligomer.[37] An overall low grafting density (i.e., one dendron per eight residues) was used, but the distance between the dendrons was varied. While most hybrids adopted the designed α-helical conformation, two peptide-dendron hybrids adopted β-sheet conformations (Figure 1.2a). The transition from α-helix to β-sheet could not be correlated with the distance between the dendrons. In a related study, Parquette showed that a higher grafting density (i.e., one dendron per two residues) on a β-sheet peptide resulted in peptide-dendron hybrids that were unstructured.[39] Hybrids with lower grafting density display greater fidelity to the conformation of the peptide without any dendrons.

Peptide-dendron hybrids have been used to create functional porous architectures that mimic the structure of porous proteins. Percec has reported a general strategy using dipeptide hybrids that undergo a supramolecular polymerization to create helical columnar assemblies featuring functional pores[24-26,30,33] capable of transporting protons.[24] The hydrogen bond network of the dipeptides drives the assembly into helical columns[29] and the helical sense of the supramolecular assembly is programed by the stereochemistry of the dipeptides.[25] Naturally occurring peptide macrocycles that adopt a bowl-shaped conformation inspired the design of dendronized cyclic peptides.[22]

Dynamic hybrid biomaterials with programmable responses to external stimuli have been accessed using peptide-dendron hybrids. Monomeric α-helical peptides functionalized with two dendrons undergo a solvent dependent transition to β-sheet structures with increased stability.[37] In a β-sheet conformation, the peptide-dendron

hybrids self-assemble into either fibrillar or nanotubular structures. The dendronized peptides are able to convert from soluble fibrillar networks to insoluble nanotubular aggregates as a function of ionic strength or pH.[40] Cyclic peptides functionalized with dendrons self-assemble into columnar assemblies with uniform diameters.[22,23,38] The dendronized peptides can undergo a unidirectional orientation as a response to an electric field.[22]

The hydrogen bonding ability of peptides can be used to design static hybrid structures. Hybrid biomaterials prepared from sequence-defined oligopeptides retain the ability to hydrogen bond and adopt programed secondary structures after dendronization.[35,37] Nanotubes with uniform diameters have been created using cyclic peptides (Figure 1.2c). The hydrogen bonding ability of these peptides is robust enough to program columnar assembly into tubular structures.[22,38] The programmable self-assembly of peptides can be used to design materials with diverse architectures and function.

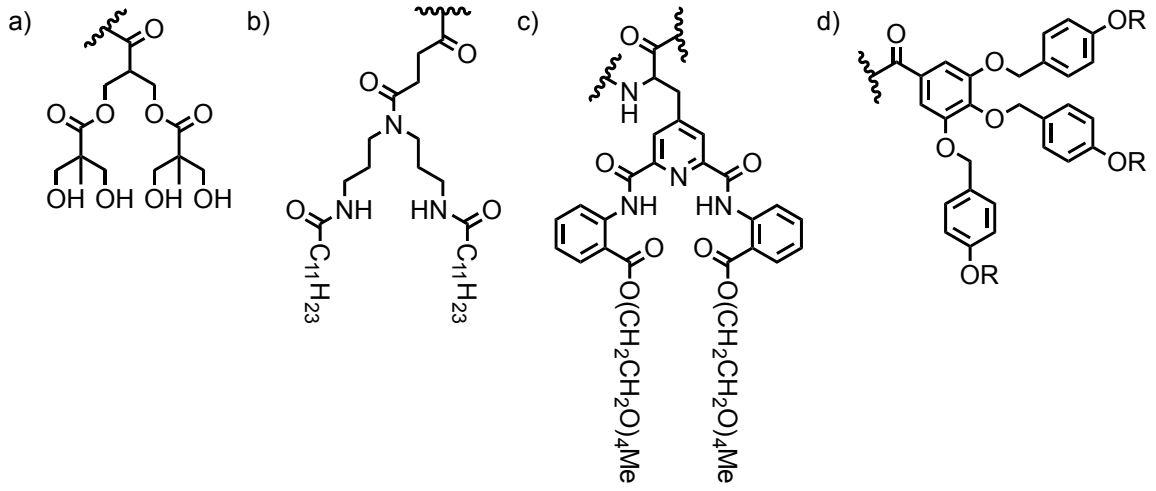

Figure 1.3 Common dendritic blocks grafted onto peptides are a) polyester, b) polyamide, c) Parquette-polyamide, and d) poly(benzyl ether).

The dendritic building blocks are strategically chosen to confer physical properties like solubility and mesomorphic behavior to the peptide-dendron hybrids. When grafted to peptides, hydrophilic polyester[36] (Figure 1.3a) and polyamide[37,39,41] (Figure 1.3b,c) dendrons yield water-soluble peptide-dendron hybrids. Self-assembling amphiphilic poly(benzyl ether) mesogenic dendrons (Figure 1.3d) have been conjugated to cyclic peptides[22,38] and dipeptides.[24-34] All the resulting hybrids display solubility in organics and liquid crystalline properties similar to the promesogenic dendrons. A drawback common to these peptide-dendron hybrids is that the UV absorption properties of the dendrons makes characterization of the peptide conformations in CD spectroscopy experiments difficult.

1.3 Strategies for the Synthesis of Peptide-Dendron Hybrids

Three strategies have been developed for the synthesis of peptide-dendron hybrids: the graft-to approach, the graft-from approach, and the macromonomer route (Figure 1.4). In the graft-to approach, preformed peptide and dendron starting materials are conjugated to form the hybrid biomaterial.[22-36,38,41-43] In the graft-from approach, the generation of a peptide-dendron hybrid is increased through iterations of divergent dendritic growth. In the macromonomer approach, a dendritic amino acid monomer is employed in iterative peptide synthesis. These same strategies have been followed for the synthesis of dendronized polymers[35,36] and bottlebrush polymers.[44]

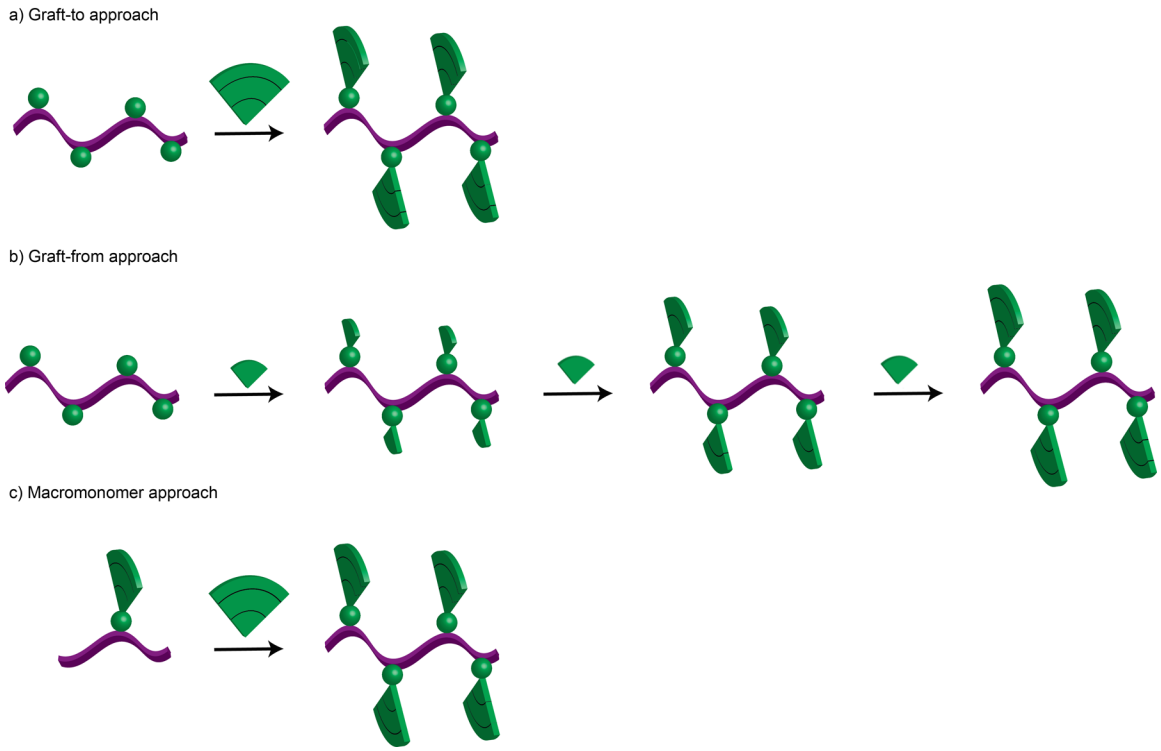

Figure 1.4 Synthetic strategies for the synthesis of peptide-dendron hybrids.

The graft-to approach employs starting materials that are free of structural defects and impurities, which should minimize the impurities in the product. Etherification, esterification, and amidation reactions have been used to graft dendrons to peptides (Figure 1.5). Etherification reactions have been successfully employed in the synthesis of singly dendronized peptides (Figure 1.5a).[24-34] Increasing the number of dendrons in a peptide-dendron hybrid concomitantly increases the likelihood of incomplete reactions, resulting in hybrids with structural imperfections. A great deal of precaution (e.g., prolonged reaction times) was taken to ensure reactions went to completion in the synthesis of cyclic peptides bearing three dendrons.[22,23,38] Creating monodisperse peptide-dendron hybrids with high grafting densities (e.g., 1 dendron per repeat unit) is even more challenging due to the steric bulk associated with dendrons, resulting in

polydisperse materials.[35,36] Despite the challenges of grafting dendrons at higher density, several chemistries have proven up to the task.

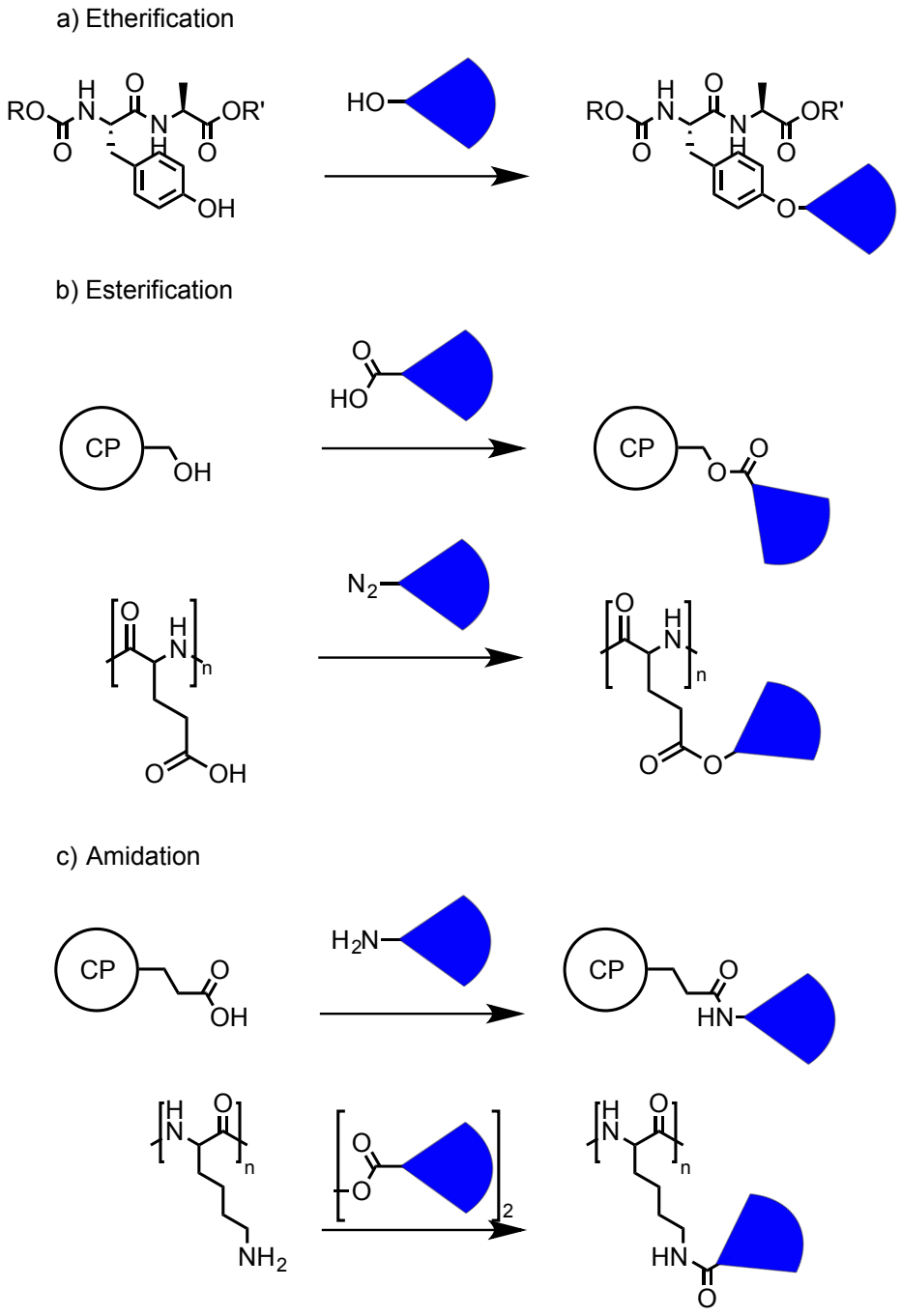

Figure 1.5 Chemistries used to graft dendrons to peptides.

Like the graft-to approach, the macromonomer[37] and graft-from[45,46] approaches can

yield monodisperse peptide-dendron hybrids. A potential drawback of the macromonomer route is that the chain assembly process consumes a lot of precious, dendritic macromonomer, and it can require substantial optimization to yield the desired product. It can be very challenging to separate defective hybrids that might only differ from the target hybrid by a single amino acid. The graft-from strategy is expected to yield some defective branching points as the dendrons become larger. These defective hybrids are unlikely to be removed by any purification method. The graft-to approach is the most reliable strategy by which structurally perfect peptide-dendron hybrids can be synthesized.

The previous graft-to approaches to prepare peptide-dendron hybrids reported in literature are not amenable to site-specific conjugation of dendrons to deprotected peptides.[22-36,38,41-43] For example, peptides containing deprotected glutamic acids and aspartic acid would undergo reaction with alcohols in an indiscriminant fashion. In order to attain complete control over the macromolecular architecture of peptide dendron hybrids, a synthetic strategy is required in which the molecular weight, polydispersity, and functional group placement can be fine-tuned.

1.4 Bioorthogonal Reactions for Conjugating Peptides with Dendrons

Chemoselective reactions that are quantitative under mild conditions and yield few byproducts are required for covalently grafting dendrons to deprotected peptides. Bioorthogonal click reactions such as the copper-catalyzed azide-alkyne cycloaddition (CuAAC),[47,48] strain-promoted azide-alkyne cycloaddition (SPAAC),[49] Staudinger ligation,[50,51] tetrazine ligation,[52] and thiol-ene[53,54] reactions meet these stringent requirements.[55,56] While all of these reactions are highly efficient, the CuAAC reaction

had been shown to be tolerant of the steric bulk of dendrons and efficient for grafting-to polymers and dendrimers.

CuAAC Reactions are especially attractive due the quantitative coupling efficiencies of the reaction. As mentioned above, the graft-to strategy is essentially the same for synthesizing dendronized polymers, bottlebrush polymers, and peptide-dendron hybrids. Dendronized linear polymers were accessed by exhaustive addition of highly branched dendritic azides to the side-chains of a poly(vinylacetylene) using CuAAC. This methodology was successfully employed to synthesize high generation polymers with quantitative grafting densities.[44] Bottlebrush polymers were prepared by grafting poly(etheylene glycol) of varying molecular weight (750 D - 5 kD) to poly(γ-propargy-L-glutamate). These examples demonstrate that the CuAAC reaction tolerates the severe steric demands of grafting polymers and dendrimers at high densities on linear chain molecules.

Unprotected peptides have been conjugated to the peripheral groups of dendrons via the CuAAC reaction.[57-60] Multivalent displays presenting up to four copies of peptides or proteins have been prepared in this manner.[57,58,61] The groups of Liskamp and Becker have each shown that linear peptides can be conjugated to the peripheral groups of dendrons. Liskamp took advantage of microwave-assisted CuAAC to quantitatively functionalize the dendron,[62] whereas Becker used hexaethylene glycol spacers to achieve quantitative reactions at room temperature.[58] Full-length proteins have also been conjugated to the peripheral groups of dendrons and dendrimers.[61] These examples demonstrate that the bioorthogonal CuAAC reaction is robust enough to prepare multivalent macromolecules.

CuAAC Reactions are robust and quantitatively proceed in a wide range of reaction conditions (e.g., solvent, catalyst, and ligands). Similar to many chemical reactions the rate of the CuAAC is dependent on concentration. Reactions employing low concentrations of starting materials tend to suffer from slowed reaction kinetics.[63] Ligands are usually employed to compensate for the slowed reaction kinetics.[18,64,65] The copper catalyst is also especially susceptible to oxidation generating inactive copper(II) species. Incorporating reducing agents (e.g., sodium ascorbate) and ligands helps stabilize the copper(I) species as an alternative to excluding oxygen. [17,63,65,66] High concentrations of starting materials affords fast reactions that circumvent the use of ligands.

1.5 Helix Bundle Design

Coiled-coil motifs consist of two or more amphipathic α-helices forming bundles of peptides that wrap around each other and supercoil. Helix bundle motifs are ubiquitous in nature, and support functions such as catalysis in water-soluble enzymes[67] and ion/small-molecule transport among transmembrane proteins.[68] This motif has been used as building blocks for self-assembling hybrid biomaterials.[15] Helix bundles have been conjugated to polymers[12,13,69-76] and nanoparticles.[77,78]

Protein design seeks to create synthetic proteins whose structure and function are precisely encoded by the sequence of amino acids.[67,79] Protein redesign takes advantage of amino acid sequences that are known to adopt a particular fold or perform a particular function and mutates the amino acids to create new proteins with tailored stability or altered functionality.[80] De novo protein design approaches the same goals by assigning the amino acid sequence from first principles. Amino acid sequences large enough to match the structural or functional complexity of full-length proteins present challenges

for the design and chemical synthesis of the proteins. Shorter peptides that can self-assemble into structures that closely resemble the structures of full-length proteins have been investigated as minimalist models for protein structure and function.[15] Designed peptides circumvent the issues associated with designing and synthesizing full-length proteins.

Helix bundles are typically described by of heptad repeat (*abcdefg*). General rules to obtain an amphipathic α-helix require placing nonpolar residues three to four residues apart, which is referred to as hydrophobic patterning.[80] Sequestration of the nonpolar residues in the core of the bundle provides the driving force for the assembly of α-helical peptides into bundles. Following the lettered notation of the heptad repeat, positions *a* and *d* make up the non-polar face, residues *b*, *c*, and *f* are solvent exposed, and residues *e* and *g* are involved in interhelical interactions (Figure 1.6). The number of heptads present in a sequence is also of critical importance. Meier et al.[81] and Burkhard et al.[82] have reported two-heptad repeat sequences that fold into α-helical peptides but lack oligomer-state specificity. Peptides with as few as three and four heptads happen to display discreet stable bundles.[83-85] Additionally, specific rules can be incorporated in the design to improve upon the specificity of the design. For example, in a coil-coiled system residues *a* and *d* are typically aliphatic hydrophobic residues (Ala, Ile, Leu, Met, Val).[86] Salt bridge interactions can be exploited in bundles by placing complementary charged at the *e* and *g* positions.[87,88] More elaborate rules can be used to rationally design principles can be used to elegantly create peptides with specific oligomeric states, helix selectivity and stabilities.

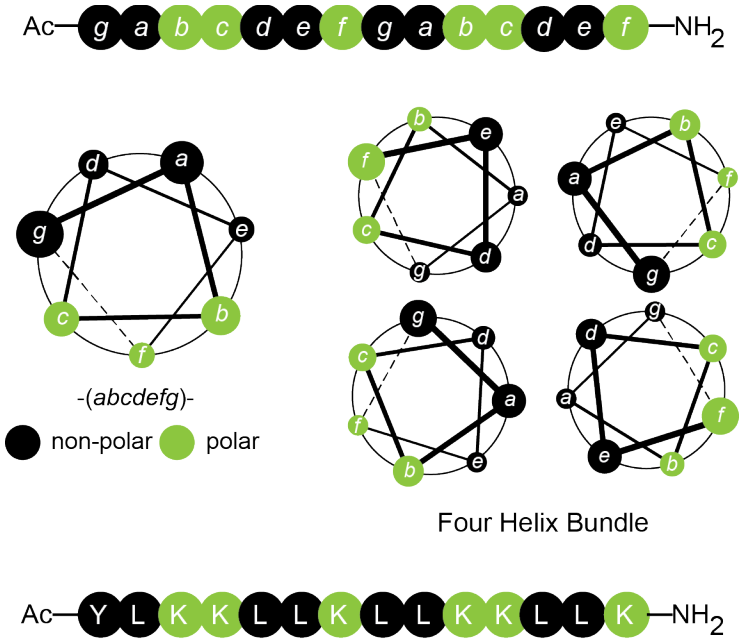

Figure 1.6 Non-polar and polar patterning of linear sequences (top) to adopt an α-helix that self-assembles into helix bundles. Redesigned "LK" sequence (bottom). Y = tyrosine, K = lysine, and L = leucine

DeGrado and Lear have shown that hydrophobic patterning is sufficient to determine the secondary structure of a peptide.[16] By arranging hydrophobic residues to match the 3.6-residues-per-turn periodicity of the α-helix, amino acid sequences following $(HPPHHPH)_n$ form amphipathic helices upon folding. For sequences in which $n \geq 2$, the self-assembly into bundles is driven by the presence of nonpolar amino acids on the hydrophobic face of the peptide. Polar amino acids on the solvent-exposed face of the bundle make the self-assembled structure hydrophilic. Compared to the designs mentioned above, peptides have a higher content of hydrophibic residues, lower sequence diversity, and shorter in overall length. Short peptides comprised of leucine-lysine ("LK") residues have been reported to form bundles comprised of either four or five α-helices.[16,89] Folding and self-assembly of LK peptides are dependent on ionic strength

and concentration.[16] Amino acids on the exterior of the bundle are amenable to modification without disrupting folding and self-assembly processes. Shaw and coworkers have coupled a metal catalyst to the *N*-terminus of a 14-residue "LK" peptide. After coupling the peptide remains helical however the catalytic activity is reduced compared to free catalyst.[90] Additionally, "LK" peptides have maintained their well defined secondary structures after absorption onto hydrophobic[91,92] and hydrophilic[92] surfaces. The robust design of LK peptides was found to be tolerant to modifications, which makes them attractive sequences for hybrid materials.

1.6 Safe, Mild, and Efficient Diazotransfer Reactions with Peptides

Peptides containing clickable groups[93] (e.g., azide or alkyne) have garnered much attention due to the success of CuAAC chemistry.[48,94] Azides and alkynes are functional groups that are not present in nature, which makes cycloaddition reactions between azides and alkynes (e.g., CuAAC[48,94] or SPAAC[49]) promising bioorthogonal reactions. Azide- and alkyne-containing peptides are generally synthesized by solid phase peptide synthesis (SPPS), which allows for site-specific placement of clickable groups.[95-97] The azide functionality is usually introduced utilizing non-natural amino acids with azide groups on the side chain (e.g., azidonorleucine,[98,99] azidonorvaline,[99] azidohomoalanine,[99] and azidoalanine[100]) or by coupling azidocarboxylic acids to the *N*-terminus.[101,102] Azide-containing amino acids are prepared following the traditional routes of either nucleophilic substitution of a leaving group by the azide anion[103-105] or by direct conversion of an amine via a diazotransfer reaction.[106] Diazotransfer reactions offer an avenue to directly convert amino groups in assembled peptides to azide groups.

Imidazole-1-sulfonyl azide hydrochloride (ISA•HCl, Figure 1.7) has been shown to be an efficient diazotransfer agent that is also shelf-stable, cost efficient, low shock sensitivity, and crystalline.[107,108] Trifluoromethanesulfonyl azide (TfN_3, Figure 1.7) has been the traditional reagent for diazotransfer reactions. The Liskamp group successfully converted the *N*-terminal amine of a peptide to an azide using TfN_3 as a diazotransfer agent.[109] Neat TfN_3, however, is shock sensitive, costly and requires fresh preparation prior to use with varying yields. Imidazole-1-sulfonate displays similar reactivity to trifluoromethanesulfonates. Goddard-Borger and Stick prepared imidazole-1-sulfonyl azide hydrochloride (ISA•HCl) with reproducible yields.[107] Löwik and coworkers have shown that they are able to achieve 98% conversion of a resin bound amine to its corresponding azide using ISA•HCl.[110] The van Hest group showed that they could introduce azide moieties into proteins using ISA•HCl.[111] ISA•HCl has also been used to convert amines to azides in a variety of substrates including aminoglycosides,[112] polymers,[113] and dendrimers.[114] These results indicate that ISA•HCl is suitable to create peptides with a high degree of site-specific reactive groups.

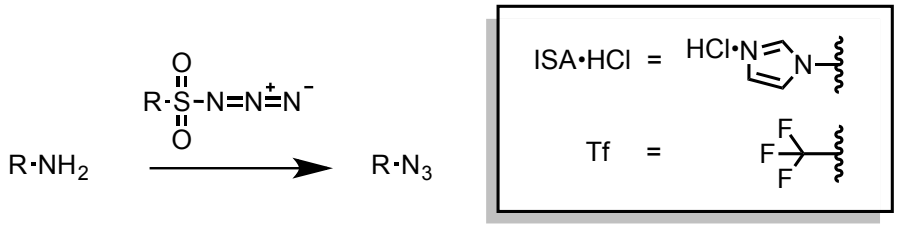

Figure 1.7 Diazotransfer reaction using imidazole-1-sulfonyl azide hydrochloride or triflyl azide.

Although diazotransfer reactions have provided a facile route to convert amines to azides with retention of stereochemistry, a mechanism has yet to be established. In the late 1960s, Fisher and Anselme provided the first mechanistic proposal for the

diazotransfer reaction. The proposed reaction mechanism required an aromatic amine anion to react with tosyl azide to afford a tetrazine intermediate that later decomposed into the corresponding azide (Figure 1.8).[115,116] However, these reports did not include experiments to confirm the mechanism of the reaction or the source of each nitrogen atom in the product.

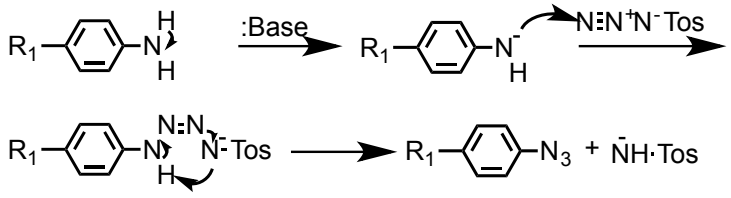

Figure 1.8 Diazotransfer reaction mechanism postulated by Fisher and Anselme

The efficiency of the diazotransfer reaction was found to be dependent on the electronic properties of the diazo group. Incorporating a strong electron-withdrawing group like trifluoromethanesulfonyl (triflyl) azide (TfN_3) increases the efficiency of the reaction.[106] The presence of metal catalyst was also found to increase the rate and efficiency of the reaction.[117] Wong and coworkers postulated the mechanism of the metal catalyzed diazotransfer reaction (Figure 1.9). Under basic conditions the amine complexed to the metal catalyst. Nucleophilic attack by the amine on the terminal nitrogen of the azide provided a tetrazene intermediate, which undergoes deprotonation and cyclization. The cyclic tetrazene can then undergo decomposition to afford the azide.[118]

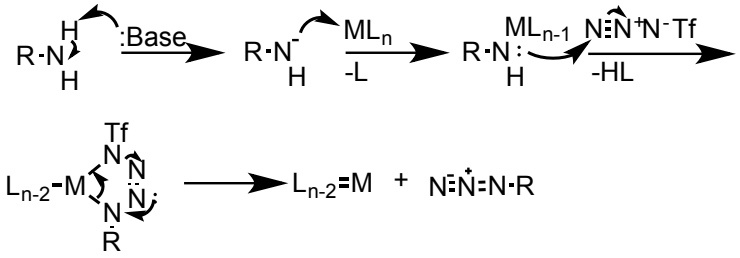

Figure 1.9 Wong and coworkers postulated metal-catalyzed diazotransfer reaction mechanism.

Odell and coworkers utilized ^{15}N isotopic labeling to investigate the mechanism of ISA·HCl. The studies confirmed that diazo (N_2) transfer to an amine affords the azide. Furthermore, the position of the ^{15}N labeled amine was tracked and found to be at N1 position of the product confirming the diazo transfer pathway (Figure 1.10).[119] The work of Samuelson and coworkers also corroborates the attack by the amine on the terminal position of the azidating reagent.[120]

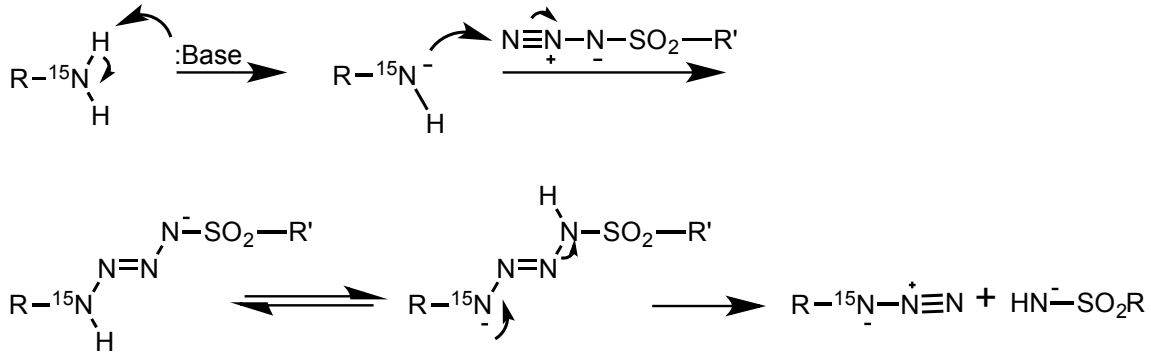

Figure 1.10 Reaction mechanism proposed by Odell and coworkers.

1.7 Overview of the Thesis

Peptide-dendron hybrids offer the ability to design materials and control hierarchical self-assembly over multiple length scales. Rational design can be used to create peptide-dendron hybrids with tailored functions, stability and processability. Helix bundle motifs are attractive candidates for materials due to their ability to support function and ability to precisely arrange atoms.

In chapter 2, the diazotransfer reaction is used as a general synthetic strategy to prepare peptides with reactive groups suitable to participate in CuAAC reactions. Assembling peptides with hydrophobic amino acids bearing azides and alkynes resulted

in difficult sequences. Therefore, an alternative strategy was developed whereby polar lysine residues were used in the assembly of peptides and later transformed to azidonorleucine residues using imidazole-1-sulfonyl azide (ISA) as a diazotransfer agent. In addition, a site-specific strategy to incorporate azidonorleucines was developed using orthogonally protected lysines.

Chapter 3 describes the first example of a peptide-dendron hybrid that folds and self-assembles into an α-helical bundle. The hybrid was designed by hydrophobic patterning of polar and non-polar residues such that an amphipathic α-helix would form. Two polar solvent exposed residues were replaced with hydrophilic dendrons using bioorthogonal CuAAC reaction. Folding and assembly properties programed into the amino acid sequence propagated into the hybrid resulting in dendronized bundle forming α-helical peptides.

A detailed account of the first peptide-dendron hybrids that fold and self-assemble into α-helical bundles is presented in Chapter 4. Sequential changes to the peptide are made to improve the stability of the conjugates. Characterization of several bundle-forming α-helical peptide dendron hybrids has provided initial principles to design synthetic materials that display the structure and function of native peptides. The novel peptide-dendron hybrids reported offer unprecedented control over folding and self-assembly in synthetic materials.

1.8 References

1. Aida, T.; Meijer, E. W.; Stupp, S. I., Functional Supramolecular Polymers. *Science* **2012,** *335*, 813-817.

2. Shu, J. Y.; Panganiban, B.; Xu, T., Peptide-polymer conjugates: from fundamental science to application. *Annu. Rev. Phys. Chem.* **2013,** *64*, 631-57.

3. Collie, G. W.; Pulka-Ziach, K.; Lombardo, C. M.; Fremaux, J.; Rosu, F.; Decossas, M.; Mauran, L.; Lambert, O.; Gabelica, V.; Mackereth, C. D.; Guichard, G., Shaping quaternary assemblies of water-soluble non-peptide helical foldamers by sequence manipulation. *Nat Chem* **2015,** *7*, 871-878.

4. Ulijn, R. V.; Smith, A. M., Designing peptide based nanomaterials. *Chem. Soc. Rev.* **2008,** *37*, 664-675.

5. Hentschel, J.; Krause, E.; Börner, H. G., Switch-Peptides to Trigger the Peptide Guided Assembly of Poly(ethylene oxide)−Peptide Conjugates into Tape Structures. *J. Am. Chem. Soc.* **2006,** *128*, 7722-7723.

6. Klok, H.-A., Peptide/Protein−Synthetic Polymer Conjugates: Quo Vadis. *Macromolecules* **2009,** *42*, 7990-8000.

7. Harris, J. M.; Chess, R. B., Effect of pegylation on pharmaceuticals. *Nat. Rev. Drug Discov.* **2003,** *2*, 214-221.

8. Duncan, R., The dawning era of polymer therapeutics. *Nat. Rev. Drug Discov.* **2003,** *2*, 347-360.

9. Klok, H. A.; Vandermeulen, G. W.; Nuhn, H.; Rosler, A.; Hamley, I. W.; Castelletto, V.; Xu, H.; Sheiko, S. S., Peptide mediated formation of hierarchically organized solution and solid state polymer nanostructures. *Faraday Discuss.* **2005,** *128*, 29-41.

10. Nowak, A. P.; Breedveld, V.; Pakstis, L.; Ozbas, B.; Pine, D. J.; Pochan, D.; Deming, T. J., Rapidly recovering hydrogel scaffolds from self-assembling diblock copolypeptide amphiphiles. *Nature* **2002,** *417*, 424-428.

11. Deming, T. J., Polypeptide Materials: New synthetic methods and applications. *Adv. Mater.* **1997,** *9*, 299-311.

12. Petka, W. A.; Harden, J. L.; McGrath, K. P.; Wirtz, D.; Tirrell, D. A., Reversible Hydrogels from Self-Assembling Artificial Proteins. *Science* **1998,** *281*, 389-392.

13. Shu, J. Y.; Tan, C.; DeGrado, W. F.; Xu, T., New Design of Helix Bundle Peptide−Polymer Conjugates. *Biomacromolecules* **2008,** *9*, 2111-2117.

14. Xu, T.; Shu, J., Coiled-coil helix bundle, a peptide tertiary structural motif toward hybrid functional materials. *Soft Matter* **2010,** *6*, 212-217.

15. Apostolovic, B.; Danial, M.; Klok, H.-A., Coiled coils: attractive protein folding motifs for the fabrication of self-assembled, responsive and bioactive materials. *Chem. Soc. Rev.* **2010,** *39*, 3541-3575.

16. DeGrado, W. F.; Lear, J. D., Induction of peptide conformation at apolar/water interfaces. 1. A study with model peptides of defined hydrophobic periodicity. *J. Am. Chem. Soc.* **1985,** *107*, 7684-7689.

17. Chan, T. R.; Hilgraf, R.; Sharpless, K. B.; Fokin, V. V., Polytriazoles as Copper(I)-Stabilizing Ligands in Catalysis. *Org. Lett.* **2004,** *6*, 2853-2855.

18. Wang, Q.; Chan, T. R.; Hilgraf, R.; Fokin, V. V.; Sharpless, K. B.; Finn, M. G., Bioconjugation by Copper(I)-Catalyzed Azide-Alkyne [3 + 2] Cycloaddition. *J. Am. Chem. Soc.* **2003,** *125*, 3192-3193.

19. Marine, J. E.; Liang, X.; Song, S.; Rudick, J. G., Azide-Rich Peptides Via an On-Resin Diazotransfer Reaction. *Biopolymers* **2015,** *104*, 419-426.

20. Marine, J. E.; Song, S.; Liang, X.; Watson, M. D.; Rudick, J. G., Bundle-forming α-helical peptide-dendron hybrid. *Chem. Commun.* **2015,** *51*, 14314-14317.

21. Marine, J. E.; Song, S.; Liang, X.; Rudick, J. G., Synthesis and Self-Assembly of Bundle-Forming α-Helical Peptide–Dendron Hybrids. *Biomacromolecules* **2015**, Accepted.

22. Sato, K.; Itoh, Y.; Aida, T., Columnarly Assembled Liquid-Crystalline Peptidic Macrocycles Unidirectionally Orientable over a Large Area by an Electric Field. *J. Am. Chem. Soc.* **2011,** *133*, 13767-13769.

23. Sato, K.; Itoh, Y.; Aida, T., Homochiral supramolecular polymerization of bowl-shaped chiral macrocycles in solution. *Chem. Sci.* **2014,** *5*, 136-140.

24. Percec, V.; Dulcey, A. E.; Balagurusamy, V. S. K.; Miura, Y.; Smidrkal, J.; Peterca, M.; Nummelin, S.; Edlund, U.; Hudson, S. D.; Heiney, P. A.; Duan, H.; Magonov, S. N.; Vinogradov, S. A., Self-Assembly of Amphiphilic Dendritic Dipeptides into Helical Pores. *Nature* **2004,** *430*, 764-768.

25. Percec, V.; Dulcey, A.; Peterca, M.; Ilies, M.; Miura, Y.; Edlund, U.; Heiney, P. A., Helical Porous Protein Mimics Self-Assembled from Amphiphilic Dendritic Dipeptides. *Aust. J. Chem.* **2005,** *58*, 472-482.

26. Percec, V.; Dulcey, A. E.; Peterca, M.; Ilies, M.; Ladislaw, J.; Rosen, B. M.; Edlund, U.; Heiney, P. A., The internal structure of helical pores self-assembled from dendritic dipeptides is stereochemically programmed and allosterically regulated. *Angew. Chem., Int. Ed.* **2005,** *44*, 6516-6521.

27. Percec, V.; Dulcey, A. E.; Peterca, M.; Ilies, M.; Sienkowska, M. J.; Heiney, P. A., Programming the internal structure and stability of helical pores self-assembled from dendritic dipeptides via the protective groups of the peptide. *J. Am. Chem. Soc.* **2005,** *127*, 17902-17909.

28. Percec, V.; Dulcey, A. E.; Peterca, M.; Ilies, M.; Nummelin, S.; Sienkowska, M. J.; Heiney, P. A., Principles of self-assembly of helical pores from dendritic dipeptides. *Proc. Natl. Acad. Sci. U. S. A.* **2006,** *103*, 2518-2523.

29. Peterca, M.; Percec, V.; Dulcey, A. E.; Nummelin, S.; Korey, S.; Ilies, M.; Heiney, P. A., Self-assembly, structural, and retrostructural analysis of dendritic dipeptide pores undergoing reversible circular to elliptical shape change. *J. Am. Chem. Soc.* **2006,** *128*, 6713-6720.

30. Kaucher, M. S.; Peterca, M.; Dulcey, A. E.; Kim, A. J.; Vinogradov, S. A.; Hammer, D. A.; Heiney, P. A.; Percec, V., Selective transport of water mediated by porous dendritic dipeptides. *J. Am. Chem. Soc.* **2007,** *129*, 11698-11699.

31. Percec, V.; Dulcey, A. E.; Peterca, M.; Adelman, P.; Samant, R.; Balagurusamy, V. S. K.; Heiney, P. A., Helical pores self-assembled from homochiral dendritic dipeptides based on L-Tyr and nonpolar alpha-amino acids. *J. Am. Chem. Soc.* **2007,** *129*, 5992-6002.

32. Percec, V.; Peterca, M.; Dulcey, A. E.; Imam, M. R.; Hudson, S. D.; Nummelin, S.; Adelman, P.; Heiney, P. A., Hollow spherical supramolecular dendrimers. *J. Am. Chem. Soc.* **2008,** *130*, 13079-13094.

33. Kim, A. J.; Kaucher, M. S.; Davis, K. P.; Peterca, M.; Imam, M. R.; Christian, N. A.; Levine, D. H.; Bates, F. S.; Percec, V.; Hammer, D. A., Proton Transport from

Dendritic Helical-Pore-Incorporated Polymersomes. *Adv. Funct. Mater.* **2009,** *19*, 2930-2936.

34. Rosen, B. M.; Peterca, M.; Morimitsu, K.; Dulcey, A. E.; Leowanawat, P.; Resmerita, A.-M.; Imam, M. R.; Percec, V., Programming the supramolecular helical polymerization of dendritic dipeptides via the stereochemical information of the dipeptide. *J. Am. Chem. Soc.* **2011,** *133*, 5135-5151.

35. Zhuravel, M. A.; Davis, N. E.; Nguyen, S. T.; Koltover, I., Dendronized Protein Polymers: Synthesis and Self-Assembly of Monodisperse Cylindrical Macromolecules. *J. Am. Chem. Soc.* **2004,** *126*, 9882-9883.

36. Lee, C. C.; Fréchet, J. M. J., Synthesis and Conformations of Dendronized Poly(l-lysine). *Macromolecules* **2006,** *39*, 476-481.

37. Shao, H.; Lockman, J. W.; Parquette, J. R., Coupled Conformational Equilibria in β -Sheet Peptide−Dendron Conjugates. *J. Am. Chem. Soc.* **2007,** *129*, 1884-1885.

38. Amorin, M.; Perez, A.; Barbera, J.; Ozores, H. L.; Serrano, J. L.; Granja, J. R.; Sierra, T., Liquid crystal organization of self-assembling cyclic peptides. *Chem. Commun.* **2014,** *50*, 688-690.

39. Shao, H.; Bewick, N. A.; Parquette, J. R., Intramolecular chiral communication in peptide-dendron hybrids. *Org. Biomol. Chem.* **2012,** *10*, 2377-2379.

40. Shao, H.; Parquette, J. R., Controllable Peptide–Dendron Self-Assembly: Interconversion of Nanotubes and Fibrillar Nanostructures. *Angew. Chem., Int. Ed.* **2009,** *48*, 2525-2528.

41. Lee, J.; Kim, J. M.; Yun, M.; Park, C.; Park, J.; Lee, K. H.; Kim, C., Self-organization of amide dendrons with focal dipeptide units. *Soft Matter* **2011,** *7*, 9021-9026.

42. Jang, W.-D.; Jiang, D.-L.; Aida, T., Dendritic physical gel: Hierarchical self-organization of a peptide-core dendrimer to form a micrometer-scale fibrous assembly. *J. Am. Chem. Soc.* **2000,** *122*, 3232-3233.

43. Jang, W.-D.; Aida, T., Dendritic Physical Gels: Structural Parameters for Gelation with Peptide-Core Dendrimers. *Macromolecules* **2003,** *36*, 8461-8469.

44. Helms, B.; Mynar, J. L.; Hawker, C. J.; Fréchet, J. M. J., Dendronized linear polymers via "click chemistry". *J. Am. Chem. Soc.* **2004,** *126*, 15020-15021.

45. Tomalia, D. A.; Kirchhoff, P. M., Rod-shaped dendrimer. Google Patents1987.

46. Yin, R.; Zhu, Y.; Tomalia, D. A.; Ibuki, H., Architectural Copolymers: Rod-Shaped, Cylindrical Dendrimers. *J. Am. Chem. Soc.* **1998,** *120*, 2678-2679.

47. Rostovtsev, V. V.; Green, L. G.; Fokin, V. V.; Sharpless, K. B., A Stepwise Huisgen Cycloaddition Process: Copper(I)-Catalyzed Regioselective "Ligation" of Azides and Terminal Alkynes. *Angew. Chem., Int. Ed.* **2002,** *41*, 2596-2599.

48. Tornøe, C. W.; Christensen, C.; Meldal, M., Peptidotriazoles on Solid Phase: [1,2,3]-Triazoles by Regiospecific Copper(I)-Catalyzed 1,3-Dipolar Cycloadditions of Terminal Alkynes to Azides. *J. Org. Chem.* **2002,** *67*, 3057-3064.

49. Baskin, J. M.; Prescher, J. A.; Laughlin, S. T.; Agard, N. J.; Chang, P. V.; Miller, I. A.; Lo, A.; Codelli, J. A.; Bertozzi, C. R., Copper-free click chemistry for dynamic in vivo imaging. *Proc. Natl. Acad. Sci. U. S. A.* **2007,** *104*, 16793-16797.

50. Saxon, E.; Bertozzi, C. R., Cell Surface Engineering by a Modified Staudinger Reaction. *Science* **2000,** *287*, 2007-2010.

51. Saxon, E.; Armstrong, J. I.; Bertozzi, C. R., A "Traceless" Staudinger Ligation for the Chemoselective Synthesis of Amide Bonds. *Org. Lett.* **2000,** *2*, 2141-2143.

52. Blackman, M. L.; Royzen, M.; Fox, J. M., Tetrazine Ligation: Fast Bioconjugation Based on Inverse-Electron-Demand Diels−Alder Reactivity. *J. Am. Chem. Soc.* **2008,** *130*, 13518-13519.

53. Lowe, A. B., Thiol-ene "click" reactions and recent applications in polymer and materials synthesis. *Polym. Chem.* **2010,** *1*, 17-36.

54. Hoyle, C. E.; Bowman, C. N., Thiol–Ene Click Chemistry. *Angew. Chem., Int. Ed.* **2010,** *49*, 1540-1573.

55. Sletten, E. M.; Bertozzi, C. R., From Mechanism to Mouse: A Tale of Two Bioorthogonal Reactions. *Acc. Chem. Res.* **2011,** *44*, 666-676.

56. Sletten, E. M.; Bertozzi, C. R., Bioorthogonal Chemistry: Fishing for Selectivity in a Sea of Functionality. *Angew. Chem., Int. Ed.* **2009,** *48*, 6974-6998.

57. Wan, J.; Huang, J. X.; Vetter, I.; Mobli, M.; Lawson, J.; Tae, H.-S.; Abraham, N.; Paul, B.; Cooper, M. A.; Adams, D. J.; Lewis, R. J.; Alewood, P. F., α-Conotoxin Dendrimers Have Enhanced Potency and Selectivity for Homomeric Nicotinic Acetylcholine Receptors. *J. Am. Chem. Soc.* **2015,** *137*, 3209-3212.

58. Tang, W.; Ma, Y.; Xie, S.; Guo, K.; Katzenmeyer, B.; Wesdemiotis, C.; Becker, M. L., Valency-Dependent Affinity of Bioactive Hydroxyapatite-Binding Dendrons. *Biomacromolecules* **2013,** *14*, 3304-3313.

59. Schellinger, J. G.; Danan-Leon, L. M.; Hoch, J. A.; Kassa, A.; Srivastava, I.; Davis, D.; Gervay-Hague, J., Synthesis of a Trimeric gp120 Epitope Mimic Conjugated to a T-Helper Peptide To Improve Antigenicity. *J. Am. Chem. Soc.* **2011,** *133*, 3230-3233.

60. Rijkers, D. T.; van Esse, G. W.; Merkx, R.; Brouwer, A. J.; Jacobs, H. J. F.; Pieters, R. J.; Liskamp, R. M. J., Efficient microwave-assisted synthesis of multivalent dendrimeric peptides using cycloaddition reaction (click) chemistry. *Chem. Commun.* **2005**, 4581-4583.

61. Gupta, K.; Singh, S.; Gupta, K.; Khan, N.; Sehgal, D.; Haridas, V.; Roy, R. P., A Bioorthogonal Chemoenzymatic Strategy for Defined Protein Dendrimer Assembly. *ChemBioChem* **2012,** *13*, 2489-2494.

62. Rijkers, D. T. S.; van Esse, G. W.; Merkx, R.; Brouwer, A. J.; Jacobs, H. J. F.; Pieters, R. J.; Liskamp, R. M. J., Efficient microwave-assisted synthesis of multivalent dendrimeric peptides using cycloaddition reaction (click) chemistry. *Chem. Commun.* **2005**, 4581-4583.

63. Hong, V.; Presolski, S. I.; Ma, C.; Finn, M. G., Analysis and Optimization of Copper-Catalyzed Azide-Alkyne Cycloaddition for Bioconjugation. *Angew. Chem., Int. Ed.* **2009,** *48*, 9879-9883.

64. Gupta, S. S.; Kuzelka, J.; Singh, P.; Lewis, W. G.; Manchester, M.; Finn, M. G., Accelerated Bioorthogonal Conjugation: A Practical Method for the Ligation of Diverse Functional Molecules to a Polyvalent Virus Scaffold. *Bioconjugate Chem.* **2005,** *16*, 1572-1579.

65. Soriano del Amo, D.; Wang, W.; Jiang, H.; Besanceney, C.; Yan, A. C.; Levy, M.; Liu, Y.; Marlow, F. L.; Wu, P., Biocompatible Copper(I) Catalysts for in Vivo Imaging of Glycans. *J. Am. Chem. Soc.* **2010,** *132*, 16893-16899.

66. Kumar, A.; Li, K.; Cai, C., Anaerobic conditions to reduce oxidation of proteins and to accelerate the copper-catalyzed "Click" reaction with a water-soluble bis(triazole) ligand. *Chem. Commun.* **2011,** *47*, 3186-3188.

67. Yu, F.; Cangelosi, V. M.; Zastrow, M. L.; Tegoni, M.; Plegaria, J. S.; Tebo, A. G.; Mocny, C. S.; Ruckthong, L.; Qayyum, H.; Pecoraro, V. L., Protein Design: Toward Functional Metalloenzymes. *Chem. Rev.* **2014,** *114*, 3495-3578.

68. MacKenzie, K. R., Folding and Stability of α-Helical Integral Membrane Proteins. *Chem. Rev.* **2006,** *106*, 1931-1977.

69. Danial, M.; van Dulmen, T. H. H.; Aleksandrowicz, J.; Pötgens, A. J. G.; Klok, H.-A., Site-Specific PEGylation of HR2 Peptides: Effects of PEG Conjugation Position and Chain Length on HIV-1 Membrane Fusion Inhibition and Proteolytic Degradation. *Bioconjugate Chem.* **2012,** *23*, 1648-1660.

70. Vandermeulen, G. W. M.; Tziatzios, C.; Duncan, R.; Klok, H.-A., PEG-Based Hybrid Block Copolymers Containing α-Helical Coiled Coil Peptide Sequences: Control of Self-Assembly and Preliminary Biological Evaluation. *Macromolecules* **2005,** *38*, 761-769.

71. Pechar, M.; Kopečková, P.; Joss, L.; Kopeček, J., Associative diblock copolymers of poly(ethylene glycol) and coiled-coil peptides. *Macromol. Biosci.* **2002,** *2*, 199-206.

72. Vandermeulen, G. W. M.; Tziatzios, C.; Klok, H.-A., Reversible Self-Organization of Poly(ethylene glycol)-Based Hybrid Block Copolymers Mediated by a

De Novo Four-Stranded α-Helical Coiled Coil Motif. *Macromolecules* **2003,** *36*, 4107-4114.

73. Dube, N.; Presley, A. D.; Shu, J. Y.; Xu, T., Amphiphilic Peptide–Polymer Conjugates with Side-Conjugation. *Macromol. Rapid Commun.* **2011,** *32*, 344-353.

74. Presley, A. D.; Chang, J. J.; Xu, T., Directed co-assembly of heme proteins with amphiphilic block copolymers toward functional biomolecular materials. *Soft Matter* **2011,** *7*, 172-179.

75. Lund, R.; Shu, J.; Xu, T., A Small-Angle X-ray Scattering Study of α-helical Bundle-Forming Peptide–Polymer Conjugates in Solution: Chain Conformations. *Macromolecules* **2013,** *46*, 1625-1632.

76. Shu, J. Y.; Lund, R.; Xu, T., Solution Structural Characterization of Coiled-Coil Peptide–Polymer Side-Conjugates. *Biomacromolecules* **2012,** *13*, 1945-1955.

77. Mahmoud, Z. N.; Gunnoo, S. B.; Thomson, A. R.; Fletcher, J. M.; Woolfson, D. N., Bioorthogonal dual functionalization of self-assembling peptide fibers. *Biomaterials* **2011,** *32*, 3712-3720.

78. Mahmoud, Z. N.; Grundy, D. J.; Channon, K. J.; Woolfson, D. N., The non-covalent decoration of self-assembling protein fibers. *Biomaterials* **2010,** *31*, 7468-7474.

79. Nanda, V.; Koder, R. L., Designing artificial enzymes by intuition and computation. *Nat Chem* **2010,** *2*, 15-24.

80. Woolfson, D. N., The design of coiled-coil structures and assemblies. *Adv. Protein Chem.* **2005,** *70*, 79-112.

81. Meier, M.; Lustig, A.; Aebi, U.; Burkhard, P., Removing an Interhelical Salt Bridge Abolishes Coiled-Coil Formation in a de Novo Designed Peptide. *J. Struct. Biol.* **2002,** *137*, 65-72.

82. Burkhard, P.; Meier, M.; Lustig, A., Design of a minimal protein oligomerization domain by a structural approach. *Protein Sci.* **2000,** *9*, 2294-2301.

83. Talbot, J. A.; Hodges, R. S., Tropomyosin: a model protein for studying coiled-coil and α-helix stabilization. *Acc. Chem. Res.* **1982,** *15*, 224-230.

84. Lumb, K. J.; Carr, C. M.; Kim, P. S., Subdomain Folding of the Coiled Coil Leucine Zipper from the bZIP Transcriptional Activator GCN4. *Biochemistry* **1994,** *33*, 7361-7367.

85. Su, J. Y.; Hodges, R. S.; Kay, C. M., Effect of Chain Length on the Formation and Stability of Synthetic α-Helical Coiled Coils. *Biochemistry* **1994,** *33*, 15501-15510.

86. Woolfson, D. N.; Alber, T., Predicting oligomerization states of coiled coils. *Protein Sci.* **1995,** *4*, 1596-1607.

87. O'Shea, E. K.; Rutkowski, R.; Stafford, W. F., 3rd; Kim, P. S., Preferential heterodimer formation by isolated leucine zippers from fos and jun. *Science* **1989,** *245*, 646-8.

88. O'Shea, E. K.; Rutkowski, R.; Kim, P. S., Mechanism of specificity in the Fos-Jun oncoprotein heterodimer. *Cell* **1992,** *68*, 699-708.

89. Buchko, G. W.; Jain, A.; Reback, M. L.; Shaw, W. J., Structural characterization of the model amphipathic peptide Ac-LKKLLKLLKKLLKL-NH_2 in aqueous solution and with 2,2,2-trifluoroethanol and 1,1,1,3,3,3-hexafluoroisopropanol. *Can. J. Chem.* **2013,** *91*, 406-413.

90. Jain, A.; Buchko, G. W.; Reback, M. L.; O'Hagan, M.; Ginovska-Pangovska, B.; Linehan, J. C.; Shaw, W. J., Active Hydrogenation Catalyst with a Structured, Peptide-Based Outer-Coordination Sphere. *ACS Catal.* **2012,** *2*, 2114-2118.

91. Long, J. R.; Oyler, N.; Drobny, G. P.; Stayton, P. S., Assembly of α-helical Peptide Coatings on Hydrophobic Surfaces. *J. Am. Chem. Soc.* **2002,** *124*, 6297-6303.

92. Mermut, O.; Phillips, D. C.; York, R. L.; McCrea, K. R.; Ward, R. S.; Somorjai, G. A., In situ adsorption studies of a 14-amino acid leucine-lysine peptide onto hydrophobic polystyrene and hydrophilic silica surfaces using quartz crystal microbalance, atomic force microscopy, and sum frequency generation vibrational spectroscopy. *J. Am. Chem. Soc.* **2006,** *128*, 3598-3607.

93. Johansson, H.; Pedersen, D. S., Azide- and Alkyne-Derivatised α-Amino Acids. *Eur. J. Org. Chem.* **2012,** *2012*, 4267-4281.

94. Kolb, H. C.; Finn, M. G.; Sharpless, K. B., Click Chemistry: Diverse Chemical Function from a Few Good Reactions. *Angew. Chem., Int. Ed.* **2001,** *40*, 2004-2021.

95. Palomo, J. M., Solid-phase peptide synthesis: an overview focused on the preparation of biologically relevant peptides. *RSC Adv.* **2014,** *4*, 32658-32672.

96. Chan, W. C.; White, P. D., *Fmoc Solid Phase Peptide Synthesis: A Practical Approach*. Oxford University Press: New York, NY, 2004.

97. Kates, S. A.; Albericio, F., *Solid-Phase Synthesis: A Practical Guide*. Marcel Dekker, Inc.: New York, NY, 2000.

98. Canalle, L. A.; Vong, T.; Adams, P. H. H. M.; van Delft, F. L.; Raats, J. M. H.; Chirivi, R. G. S.; van Hest, J. C. M., Clickable Enzyme-Linked Immunosorbent Assay. *Biomacromolecules* **2011,** *12*, 3692-3697.

99. Le Chevalier Isaad, A.; Barbetti, F.; Rovero, P.; D'Ursi, A. M.; Chelli, M.; Chorev, M.; Papini, A. M., N^{α}-Fmoc-Protected ω-Azido- and ω-Alkynyl-L-amino Acids as Building Blocks for the Synthesis of "Clickable" Peptides. *Eur. J. Org. Chem.* **2008**, 5308-5314.

100. Torres, O.; Yüksel, D.; Bernardina, M.; Kumar, K.; Bong, D., Peptide tertiary structure nucleation by side-chain crosslinking with metal complexation and double "click" cycloaddition. *ChemBioChem* **2008,** *9*, 1701-1705.

101. Meldal, M.; Juliano, M. A.; Jansson, A. M., Azido Acids in a Novel Method of Solid-Phase Peptide Synthesis. *Tetrahedron Lett.* **1997,** *38*, 2531-2534.

102. Tulla-Puche, J.; Bayó-Puxan, N.; Moreno, J. A.; Francesch, A. M.; Cuevas, C.; Álvarez, M.; Albericio, F., Solid-Phase Synthesis of Oxathiocoraline by a Key Intermolecular Disulfide Dimer. *J. Am. Chem. Soc.* **2007,** *129*, 5322-5323.

103. Curtius, T.; Darapsky, A., III. Ueber Benzylazid. *J. Prakt. Chem.* **1901,** *63*, 428-444.

104. Levene, P. A.; Rothen, A.; Kuna, M., The Mechanism of the Reaction of Substitution and Walden Inversion. *J. Biol. Chem.* **1937,** *120*, 777-797.

105. Boyer, J. H.; Canter, F. C., Alkyl and Aryl Azides. *Chem. Rev.* **1954,** *54*, 1-57.

106. Cavender, C. J.; Shiner, V. J., Trifluoromethanesulfonyl azide. Its reaction with alkyl amines to form alkyl azides. *J. Org. Chem.* **1972,** *37*, 3567-3569.

107. Goddard-Borger, E. D.; Stick, R. V., An Efficient, Inexpensive, and Shelf-Stable Diazotransfer Reagent: Imidazole-1-sulfonyl Azide Hydrochloride. *Org. Lett.* **2007,** *9*, 3797-3800.

108. Fischer, N.; Goddard-Borger, E. D.; Greiner, R.; Klapötke, T. M.; Skelton, B. W.; Stierstorfer, J., Sensitivities of Some Imidazole-1-sulfonyl Azide Salts. *J. Org. Chem.* **2012,** *77*, 1760-1764.

109. Rijkers, D. T. S.; van Vugt, H. H. R.; Jacobs, H. J. F.; Liskamp, R. M. J., A convenient synthesis of azido peptides by post-assembly diazo transfer on the solid phase applicable to large peptides. *Tetrahedron Lett.* **2002,** *43*, 3657-3660.

110. Hansen, M. B.; van Gurp, T. H. M.; van Hest, J. C. M.; Löwik, D. W. P. M., Simple and Efficient Solid-Phase Preparation of Azido-peptides. *Org. Lett.* **2012,** *14*, 2330-2333.

111. Schoffelen, S.; van Eldijk, M. B.; Rooijakkers, B.; Raijmakers, R.; Heck, A. J. R.; van Hest, J. C. M., Metal-free and pH-controlled introduction of azides in proteins. *Chem. Sci.* **2011,** *2*, 701-705.

112. Bastian, A. A.; Warszawik, E. M.; Panduru, P.; Arenz, C.; Herrmann, A., Regioselective Diazo-Transfer Reaction at the C^3-Position of the 2-Desoxystreptamine Ring of Neamine Antibiotics. *Chem.–Eur. J.* **2013,** *19*, 9151-9154.

113. Kulbokaite, R.; Ciuta, G.; Netopilik, M.; Makuska, R., *N*-PEG'ylation of chitosan via "click chemistry" reactions. *React. Funct. Polym.* **2009,** *69*, 771-778.

114. Tosh, D. K.; Yoo, L. S.; Chinn, M.; Hong, K.; Kilbey, S. M., II; Barrett, M. O.; Fricks, I. P.; Harden, T. K.; Gao, Z. G.; Jacobson, K. A., Polyamidoamine (PAMAM) dendrimer conjugates of "clickable" agonists of the A3 adenosine receptor and coactivation of the P2Y14 receptor by a tethered nucleotide. *Bioconjugate Chem.* **2010,** *21*, 372-84.

115. Fischer, W.; Anselme, J. P., Reaction of amine anions with p-toluenesulfonyl azide. Novel azide synthesis. *J. Am. Chem. Soc.* **1967,** *89*, 5284-5285.

116. Anselme, J. P.; Fischer, W., The reaction of anions of primary amines and hydrazones with p-toluenesulfonyl azide. *Tetrahedron* **1969,** *25*, 855-859.

117. Alper, P. B.; Hung, S.-C.; Wong, C.-H., Metal catalyzed diazo transfer for the synthesis of azides from amines. *Tetrahedron Lett.* **1996,** *37*, 6029-6032.

118. Nyffeler, P. T.; Liang, C.-H.; Koeller, K. M.; Wong, C.-H., The Chemistry of Amine−Azide Interconversion: Catalytic Diazotransfer and Regioselective Azide Reduction. *J. Am. Chem. Soc.* **2002,** *124*, 10773-10778.

119. Stevens, M. Y.; Sawant, R. T.; Odell, L. R., Synthesis of Sulfonyl Azides via Diazotransfer using an Imidazole-1-sulfonyl Azide Salt: Scope and ^{15}N NMR Labeling Experiments. *J. Org. Chem.* **2014,** *79*, 4826-4831.

120. Pandiakumar, A. K.; Sarma, S. P.; Samuelson, A. G., Mechanistic studies on the diazo transfer reaction. *Tetrahedron Lett.* **2014,** *55*, 2917-2920.

Chapter 2

2. Azide-Rich Peptides via an On-Resin Diazotransfer Reaction

Adapted with permission from Marine, J. E.; Liang, X.; Song, S.; Rudick, J. G. *Biopolymers* **2014**, *104*, 419-426. (http://dx.doi.org/10.1002/bip.22634)

2.1 Introduction

Azide-containing peptides have gained prominence in chemistry[1] due to the success of the copper-catalyzed azide-alkyne cycloaddition (CuAAC) reaction[2-4] for site-specifically modifying peptides and proteins. The bioorthogonal strain-promoted azide-alkyne cycloaddition (SPAAC) reaction[5] and the Staudinger ligation[6,7] also exploit the azide functional group to expand the range of non-natural functional groups that can be incorporated into amino acid sequences.[8-10] Several amino acids with azide groups in the side chain have been reported for use in solid-phase peptide synthesis (SPPS)[1] (e.g., N^{α}-Fmoc-protected derivatives of azidonorleucine,[11,12] azidonorvaline,[12] azidohomoalanine,[12] and azidoalanine[13]), and these have been routinely used to site-specifically introduce into peptides a single bioorthogonal reaction site. Peptides in which several azides have been site-specifically incorporated have also been reported, and these serve as key intermediates in the syntheses of tools for chemical biology[14,15,16-18,19-21] and of hybrid biomaterials.[22-26,27] Each of these examples relies upon suitably protected azide-containing amino acids in solid-phase peptide synthesis. A complementary strategy to incorporate high degrees of azide functional groups site-specifically into amino acid sequences should contribute to the continued growth of applications that exploit these peptides. Herein we present a general strategy for replacing polar residues with apolar, azide-containing residues (Figure 2.1). We demonstrate below that the diazotransfer reagent imidazole-1-sulfonyl azide[28] can achieve high degrees of conversion of amine to azide. In

combination with an orthogonal protecting group strategy, we exploit the reactivity of this diazotransfer reagent to site-specifically introduce azide groups on-resin while leaving some lysine residues unaffected.

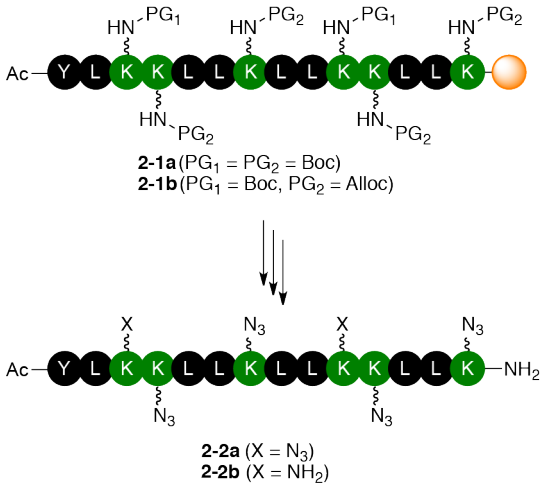

Figure 2.1 Peptides containing multiple azide functional groups are prepared in a site-specific manner (Y = tyrosine, L = leucine, K = lysine; side chain protecting group on tyrosine is not shown).

Solid-phase peptide synthesis provides rapid access to a broad spectrum of chemical structures.[29-31] While the technology is mature and robust, attention must still be paid to subtle factors that make the synthesis of some peptides especially challenging or even intractable. An abrupt decline in the efficiency of the N^{α}-protecting group elimination and/or amino acid coupling reactions during peptide chain assembly is the hallmark of these so-called "difficult sequences," and results in low product yield.[32-35] The causes of this poor reactivity include association of peptide chains while they are still attached to the solid support[36,37] and/or changes to the swelling properties of the resin as the peptide chain is assembled.[36,38] Guidelines for anticipating difficult sequences cite the number of or sequence of apolar residues as indicators of potential problems.[32-35] Polar residues with small side chain protecting groups help solubilize the

growing peptide chain in the reaction solvent so that the reactive chain end is accessible to reagents. Amino acid residues with apolar side chains or with polar side chains that have large, apolar protecting groups lower the solubility of the resin-bound peptide and strengthen hydrogen bonding. Nonetheless, difficult sequences are usually found by chance, and there is little reward for these discoveries. When we replaced Lys3 and Lys11 of peptide **2-1a** (Figure 2.1) with propargylglycine, we encountered problems during synthesis that are associated with "difficult sequences." We observed 1) a significant increase in deletion peptides (especially of peptides missing Leu5 or Leu6) which could be overcome by increasing the number of equivalents of amino acid in the coupling reactions and introducing double couplings, and 2) inefficient elimination of Fmoc protecting groups which necessitated repeated (up to five times) treatment with the deprotection solution. Figure 2.1 presents a strategy that is versatile enough that we can replace any number of the polar residues with amino acids that participate in azide-alkyne click reactions.

2.2 Results and Discussion

2.2.1 Solution-Phase Diazotransfer

Imidazole-1-sulfonyl azide hydrochloride salt (ISA•HCl)[28] has been shown to be an efficient diazotransfer reagent in a variety of contexts relevant to our objective. We are aware that the reagent is impact sensitive,[39] but we found it convenient to prepare and handle. In the presence of a Cu(II) salt and base, ISA•HCl has been used to convert amines into azides on various proteins,[40] polymers,[41] oligosaccharides,[42] and dendrimers;[43] this suggested to us that the diazotransfer reagent is capable of achieving high degrees of reaction on peptides with multiple exposed lysine side chains. The reagent has also been successfully applied to modify resin-bound amines.[44-46] Löwik and co-workers demonstrated that nearly quantitative conversion of the *N*-

terminus of resin-bound and side chain-protected peptides could be achieved in the presence of any natural amino acid except methionine and *S*-trityl cysteine.[44] We, therefore, focused our attention on ISA•HCl as a diazotransfer reagent.

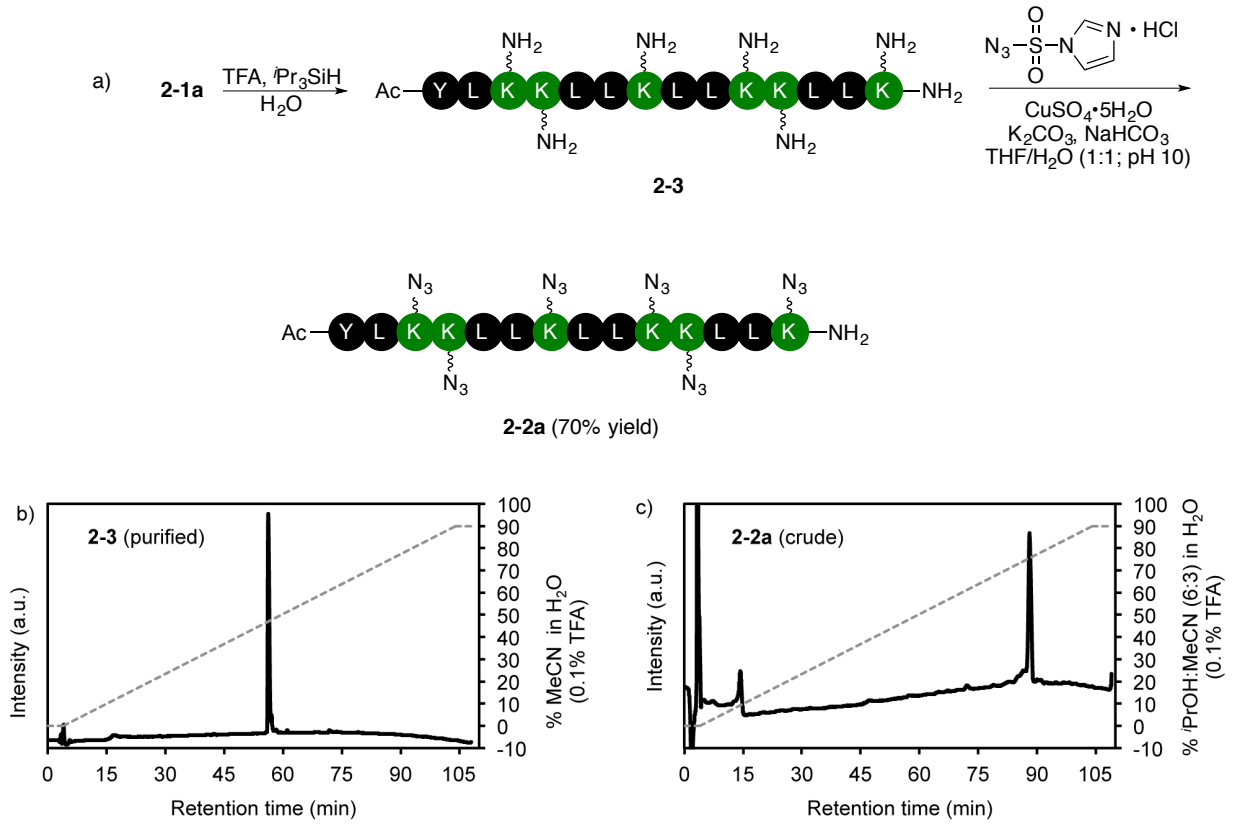

Figure 2.2 a) Solution-phase reaction in which ISA•HCl effects the transformation of multiple lysine residues to azidonorleucine residues. b) Chromatogram of the purified peptide **2-3** (solid line). The dashed line indicates the solvent composition during elution of the peptide at 1 mL/min from a C18 column (solvent A = H_2O + 0.1% TFA; solvent B = MeCN/H_2O (9:1 v/v) + 0.1% TFA). c) Chromatogram of the crude reaction product **2-2a** (solid line). The dashed line indicates the solvent composition during elution of the peptide at 1 mL/min from a C4 column (solvent A = H_2O + 0.1% TFA; solvent B = ^{i}PrOH/MeCN/H_2O (6:3:1 v/v/v) + 0.1% TFA).

To evaluate the potential for ISA•HCl to effect diazotransfer reactions at several lysine residues in a peptide, we first investigated the solution-phase reaction between peptide **2-3** and

ISA·HCl. Peptide **2-3** is a fourteen-residue peptide that contains six lysine residues arranged such that they are all on one face of an amphipathic α-helix.[47] Resin-bound peptide **2-1a** was manually synthesized by standard peptide synthesis protocols. The amino acid sequence was assembled on a polyethyleneglycol-based Rink amide resin with N^{α}-Fmoc-protected amino acid derivatives (i.e., Fmoc-Leu-OH, Fmoc-Lys(Boc)-OH, and Fmoc-Tyr(O^{t}Bu)-OH) activated with HBTU in the presence of HOBt and DIEA in DMF. Each coupling reaction was performed for 45 min. After each amino acid was coupled to the resin, the resin was treated with Ac_2O to cap any unreacted peptide chains. The Fmoc group was eliminated by treating the resin with 20% piperidine in DMF for 5 min followed by a second treatment with 20% piperidine in DMF for 5 min. The extent of elimination of the Fmoc group was monitored by UV absorbance at 300 nm following a modified literature procedure.[48] We observed no problems by this method during the assembly of the peptide on resin. Cleavage of the peptide from the resin and concomitant elimination of the side chain-protecting groups was accomplished in 2 h by treating the resin with TFA/^{i}Pr$_3$SiH/H_2O (Figure 2.2a). Peptide **2-3**, purified by preparative reversed-phase HPLC, was obtained as a colorless powder after lyophilization. The purity of the collected peptide was determined by analytical HPLC, (Figure 2.2b) and the identity of the peptide was confirmed by MALDI-TOF mass spectrometry.

All six lysine residues in peptide **2-3** were transformed to azidonorleucine residues to yield peptide **2-2a** (Figure 2.2). Diazotransfer reactions were performed in a 1:1 (v/v) mixture of THF and H_2O, because peptide **2-2a** is not soluble in H_2O. The reactions were monitored by reversed-phase HPLC, and were allowed to proceed until the desired product was the only observable peak. Aqueous solutions of **2-3** and $CuSO_4$·$5H_2O$ (0.02 eq/NH_2) were initially acidic, and so K_2CO_3 (3 eq/NH_2) was added to neutralize the solutions. Additional base is needed to

activate the diazotransfer reagent, ISA•HCl.[28] The reaction mixture pH was adjusted to 10 with saturated $NaHCO_3$ (aq). Under these conditions, we were able to obtain exclusively peptide **2-2a** using ISA•HCl (4 eq/NH_2) within 3 h. The analytical HPLC trace of the reaction mixture (Figure 2.2b) suggests that the reaction mixture is free of side products and intermediates. That the reaction is essentially quantitative supports conclusions drawn in prior reports of the reaction of ISA•HCl with polysaccharides[41] and dendrimers.[43] Peptide **2-2a** was obtained in 70% yield after purification by flash column chromatography.

2.2.2 On-Resin Diazotransfer

Solution-phase diazotransfer reactions are convenient for converting primary amines to azides, but an alternative strategy is needed to site-specifically transform only a fraction of the available amines. We envisaged that a pair of orthogonal protecting groups for the lysine side chains would allow us to site-specifically introduce azidonorleucine residues into amino acid sequences that contained lysine residues that we wanted to remain unaltered. Allyloxycarbonyl (Alloc) protecting groups can be selectively removed in the presence of *t*-butoxycarbonyl (Boc) protecting groups[49] and on-resin,[50,51] and so we used this orthogonal pair of protecting groups as a test-bed to investigate whether ISA•HCl could effect the transformation of multiple lysine residues into azidonorleucine residues on-resin.

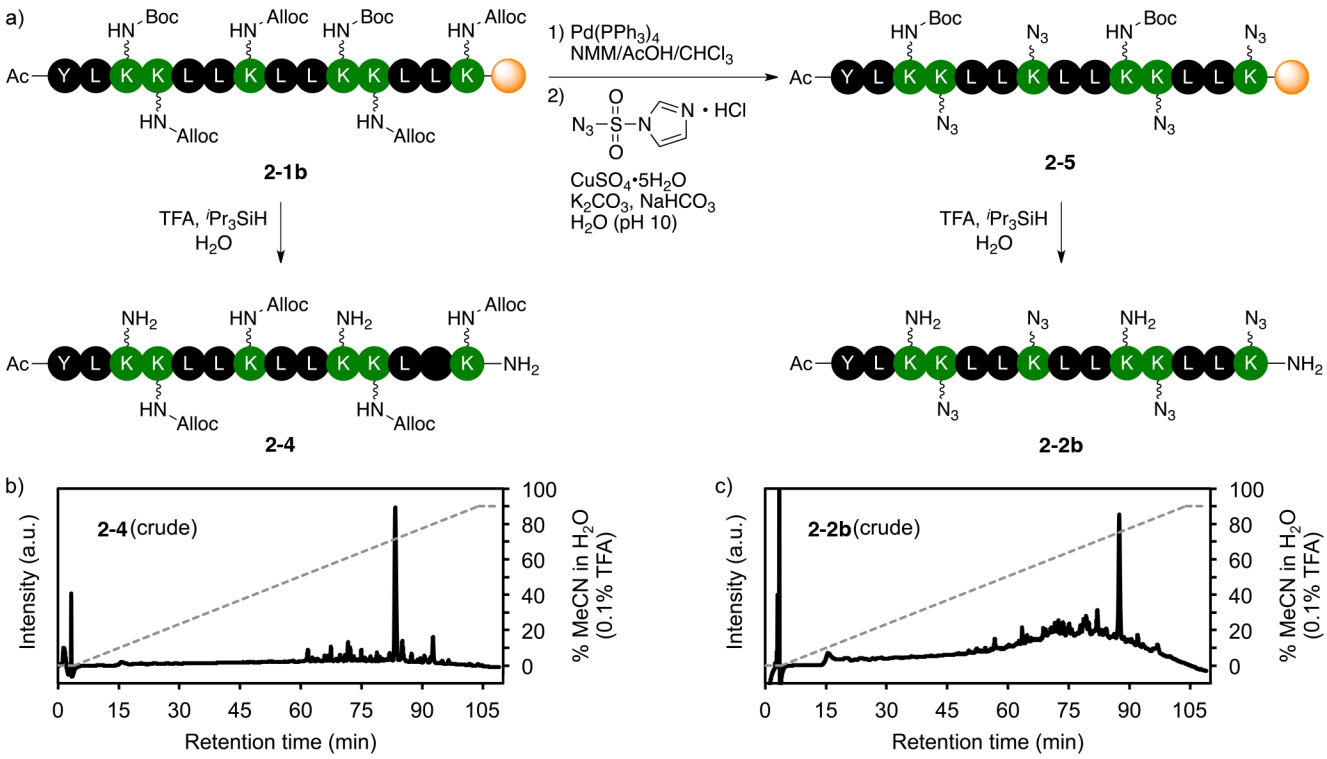

Figure 2.3 a) Reaction sequence for site-specific diazotransfer to multiple lysine residues on a polyethyleneglycol-based resin. b) Chromatogram of the crude product **2-4** (solid line) illustrates the purity of the resin-bound peptide before the deprotection-diazotransfer-cleavage/deprotection sequence. c) Chromatogram of the crude reaction product **2-2b** (solid line). The dashed line in panels (b) and (c) indicates the solvent composition during elution of the peptide at 1 mL/min from a C18 column (solvent A = H_2O + 0.1% TFA; solvent B = MeCN/H_2O (9:1 v/v) + 0.1% TFA).

Resin-bound peptide **2-1b** was assembled following the same protocol used to prepare peptide **2-1a**, except that Fmoc-Lys(Alloc)-OH was used in place of Fmoc-Lys(Boc)-OH at four positions in the amino acid sequence. Importantly, no difficulties were encountered when we replaced N^{ε}-Boc-protected lysine residues with N^{ε}-Alloc-protected lysine residues; the assembly of **2-1b** was as straightforward as the synthesis of peptide **2-1a**. The crude purity of **2-1b** was determined by characterization of peptide **2-4**. Treatment of **2-1b** with TFA/$^{i}Pr_3SiH/H_2O$ resulted

in cleavage of the peptide from the resin and elimination of the Boc and *t*-butyl ether protecting groups, but not the Alloc groups. The analytical HPLC trace of **2-4** in Figure 2.3b illustrates high crude purity of resin-bound peptide **2-1b**, which is desirable for assessing the overall efficiency of the planned deprotection-diazotransfer-cleavage/deprotection sequence.

Site-specific introduction of four azidonorleucine residues was accomplished through a three-step sequence (Figure 2.3). First, quantitative and selective elimination of the Alloc protecting groups from resin-bound peptide **2-1b** was effected by treating the resin with $Pd(PPh_3)_4$ in NMM/AcOH/$CHCl_3$.[52] Second, the ISA-mediated diazotransfer reaction was performed in H_2O under conditions that were otherwise identical to the solution-phase conditions described above. While the solution-phase transformation of **2-3** to **2-2a** required a co-solvent to keep **2-2a** in solution, the transformation of **2-4** to **2-5** required no organic co-solvent because the polyethyleneglycol-based support swells in H_2O. Finally, the peptide was cleaved from the resin and the remaining protecting groups were removed by treating the resin-bound peptide with TFA/$^{i}Pr_3SiH$/H_2O. The crude purity of the product was assessed by analytical HPLC (Figure 2.3c). We were pleased to see that **2-1b** was cleanly transformed into **2-2b**. Had the on-resin deprotection-diazotransfer reaction sequence been incomplete, then products more polar than the target peptide would be observed at lower retention times. The azidonorleucine-containing peptide **2-2b** was purified by reversed-phase HPLC.

2.2.3 CuAAC Reaction of an Azide-Rich Peptide

To demonstrate the suitability of azide-rich peptides for bioorthogonal transformations, we focused on the CuAAC reaction (Figure 2.4a).[2-4] Alkyne **2-6** is a second-generation

dendron[53] with peripheral hydroxy groups.* The combination of the highly branched structure of **2-6** and the close proximity of conjugation sites in **2-2a** should serve as a demanding test of how well the CuAAC reaction tolerates sterically encumbered substrates. Peptide **2-2a** is insoluble in H_2O, but could be solubilized in a mixed solvent of THF/H_2O (1:1 v/v). The CuAAC reaction of **2-2a** and **2-6** was, therefore, performed in THF/H_2O (1:1 v/v) with $CuSO_4 \bullet 5H_2O$ as the catalyst source and sodium ascorbate as an *in situ* reducing agent. The reaction was deemed complete after 16 h when **2-7** was the only species observed in the ESI–MS of an aliquot from the reaction mixture. Peptide-dendron conjugate **2-7** was obtained in 57% yield after purification by reversed-phase HPLC. The analytical HPLC and MALDI-TOF mass spectrum† of **2-7** (Figure 2.4b,c) demonstrate the purity of the isolated product. Furthermore, the observed isotope pattern and the simulated spectrum are in close agreement.

* Synthesis route for second generation dendrons with hydroxyl peripheral groups were developed by Shuang Song and Xiaoli Liang.

† The MALDI-TOF mass spectrum of **2-7** was acquired by Dr. Robert Rieger (Stony Brook University Proteomics Center)

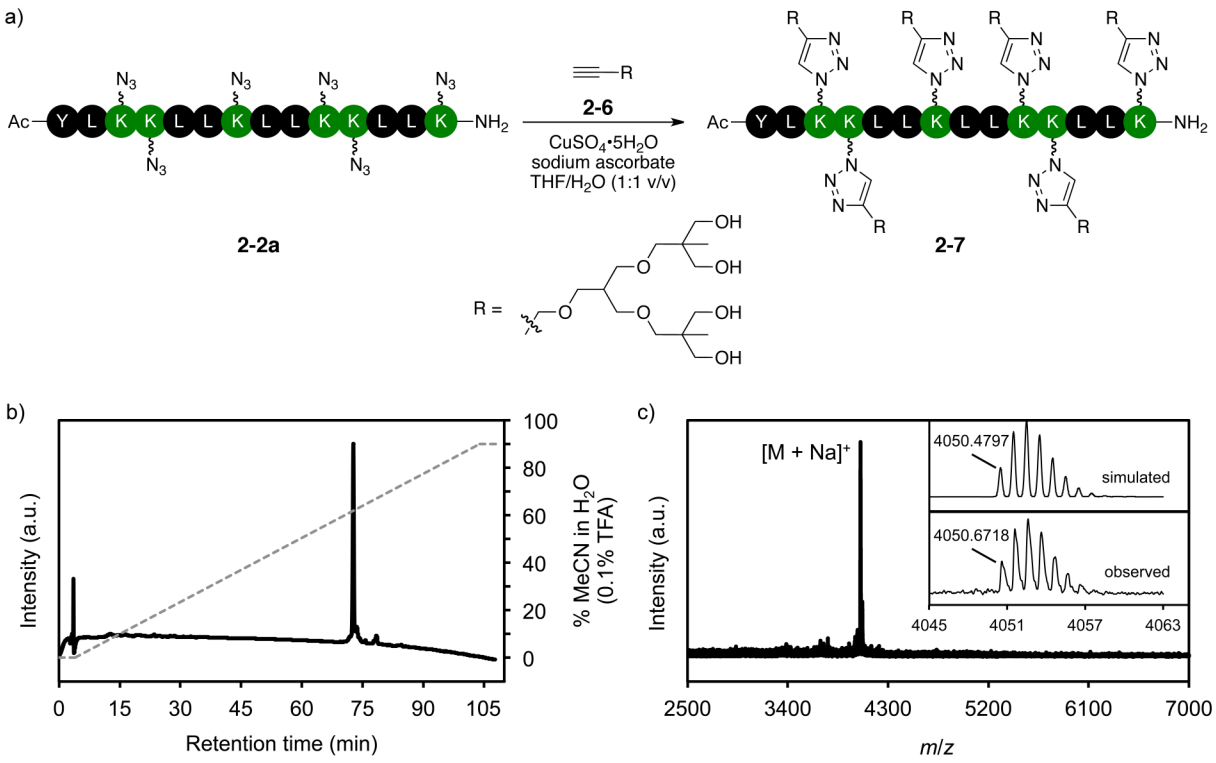

Figure 2.4 a) Scheme showing the CuAAC reaction of azide-rich peptide **2-2a**. b) Chromatogram of the product **2-7** (solid line). The dashed line indicates the solvent composition during elution of the peptide at 1 mL/min from a C18 column (solvent A = H_2O + 0.1% TFA; solvent B = MeCN/H_2O (9:1 v/v) + 0.1% TFA). c) MALDI-TOF Mass spectrum of **2-7**.‡ The inset compares the simulated[54,55] isotope pattern (upper) with the observed isotope envelope for the [**2-7** + Na]$^+$ ion ($C_{191}H_{343}N_{33}O_{58}Na$).

2.3 Conclusion

Peptides are attractive building blocks in bioorganic and supramolecular chemistry[56-59] because of the available diversity of amino acid sequences and their predictable conformational properties. Bioorthogonal reactions offer convenient methods to introduce non-native functionality into peptide sequences.[8-10] The standard approach to preparing azide-containing

‡ The MALDI-TOF mass spectrum of **2-7** was acquired by Dr. Robert Rieger (Stony Brook University Proteomics Center)

peptides by solid-phase peptide synthesis relies upon suitably protected amino acids with azide functional groups in the side chain.[1] We have described a complementary strategy wherein side-chain amine groups are converted to azide functional groups through the action of an imidazole-1-sulfonyl azide reagent after assembly of the peptide according to standardized protocols. The compatibility of this reagent with canonical amino acids[44] suggests that the approach can be extended to a wide range of peptides. We expect that this strategy will be advantageous for peptides in which multiple azide groups are to be introduced and for amino acid sequences that are prone to aggregation during solid-phase synthesis.

2.4 Experimental Procedures

2.4.1 Materials

Fmoc-Leu-OH, Fmoc-Lys(Boc)-OH, Fmoc-Lys(Alloc)-OH, Fmoc-Tyr(O^{t}Bu)-OH, *O*-(benzotriazol-1-yl)-*N*,*N*,*N*',*N*'-tetramethyluronium hexafluorophosphate (HBTU), hydroxybenzotriazole (HOBt), hydrochloric acid, *N*-methylmorpholine (NMM), sodium azide, dichloromethane, *N*,*N*-dimethylformamide (DMF), methanol (MeOH), diisopropylethylamine (DIEA), trifluoroacetic acid (TFA), piperidine, acetyl chloride (AcCl), tetrakis(triphenylphosphine)palladium(0), diethyl ether (Et_2O), ethylenediaminetetraacetic acid disodium salt dihydrate (EDTA), acetonitrile (MeCN), acetic anhydride (Ac_2O), imidazole, triisopropylsilane ($^i Pr_3SiH$), potassium carbonate (anhydrous), sulfuryl chloride, sodium diethyldithiocarbamate trihydrate, copper(II) sulfate pentahydrate, ethanol (EtOH), 5-nonanone, 1,1,1-tris(hydroxymethyl)ethane, anhydrous tetrahydrofuran (THF), boron trifluoride diethyl etherate, 3-chloro-2-(chloromethyl)prop-1-ene, dry sodium hydride, 15-crown-5, tetrahydrofuran (THF), ethyl acetate (EtOAc), sodium hydroxide, hexanes, sodium chloride, magnesium sulfate, hydrogen peroxide solution (30% w/w), 0.5 M solution of 9-borabicyclo[3.3.1]nonane (9-BBN)

in THF, 80 wt% solution of propargyl bromide in toluene, Dowex® 50WX2 hydrogen form (50-100 mesh), molecular sieve (4Å), and isopropanol (^{i}PrOH) were used as received. H-Rink Amide-ChemMatrix resin (0.51 mmol/g) was swelled in CH_2Cl_2 for 1 h prior to use.

2.4.2 Techniques

The MALDI-TOF data were recorded on a Bruker Autoflex II TOF/TOF workstation. MALDI-TOF samples (10 mg/mL) were prepared in MeCN/H_2O with α-cyano-4-hydroxycinnamic acid as the matrix. Equal volumes of the matrix and peptide solutions were mixed and 1 μL of the mixture was injected onto the target plate. Thin layer chromatography (TLC) was performed using Whatman silica gel 60 Å plates (250 μm) with fluorescent indicator and visualized using a UV lamp (254 nm) or $KMnO_4$ stain. Flash column chromatography was performed on a Teledyne Isco CombiFlash Rf with RedSep Rf Normal Phase disposable silica columns. High-performance liquid chromatography (HPLC) was performed on a Waters 1525 Binary pump equipped with a Waters 2489 UV/Visible Detector set at 210 nm and 280 nm. To determine the analytical purity of samples, the HPLC was equipped with a SunFire^{TM} C18 column (5 μm, 4.6 mm × 250 mm; Waters) or PROTO^{TM} 300 C4 column (5 μm, 4.6 mm × 250 mm, 300 Å; Higgins) operating at a flow rate of 1 mL/min and a solvent gradient of 1%/min. Purification of samples was done on the HPLC equipped with a SunFire^{TM} C18 (5 μm, 19 mm × 250 mm) column operating at a flow rate of 17 mL/min and a solvent gradient of 5%/min. Absorbance of peptide solutions in deionized water at 280 nm was recorded on an Evolution 201 spectrophotometer using a 1-cm quartz cuvette. The concentration of the peptide was calculated from the absorbance using Beer's Law and an extinction coefficient (ε) for tyrosine of 1490 L mol^{-1} cm^{-1}.

2.4.3 Synthesis

General Solid-Phase Peptide Synthesis Procedures. Single Coupling Protocol. To a solution of the Fmoc-protected amino acid (0.52 M), HBTU (0.51 M), and HOBt (0.52 M) in DMF, DIEA (2 eq/Fmoc-protected amino acid) was added. A sufficient volume of the solution to deliver 10 eq Fmoc-protected amino acid per reactive group on the resin was transferred to a peptide synthesis vessel containing the swelled resin. The reaction mixture was agitated for 45 min. Liquids were removed from the reaction vessel by vacuum filtration, and the resin was washed sequentially with DMF (10 mL/g) twice, CH_2Cl_2 (10 mL/g) twice, and DMF (10 mL/g) twice.

Double Coupling Protocol. To a solution of the Fmoc-protected amino acid (0.52 M), HBTU (0.51 M), and HOBt (0.52 M) in DMF, DIEA (2 eq/Fmoc-protected amino acid) was added. A sufficient volume of the solution to deliver 10 eq Fmoc-protected amino acid per reactive group on the resin was transferred to a peptide synthesis vessel containing the swelled resin. The reaction mixture was agitated for 45 min. Liquids were removed from the reaction vessel by vacuum filtration, and the resin was washed sequentially with DMF (10 mL/g) twice, CH_2Cl_2 (10 mL/g) twice, and DMF (10mL/g) twice. To a solution of the Fmoc-protected amino acid (0.52 M), HBTU (0.51 M), and HOBt (0.52 M) in DMF, DIEA (2 eq/Fmoc-protected amino acid) was added. A sufficient volume of the solution to deliver 10 eq Fmoc-protected amino acid per reactive group on the resin was transferred to a peptide synthesis vessel containing the swelled resin. The reaction mixture was agitated for 45 min. Liquids were removed from the reaction vessel by vacuum filtration, and the resin was washed sequentially with DMF (10 mL/g) twice, CH_2Cl_2 (10 mL/g) twice, and DMF (10 mL/g) twice.

Protocol for Capping and Acetylation of the *N*-Terminus. To the resin, a solution of DMF/DIEA/Ac_2O (9:0.5:0.5 v/v/v; 5 mL) was added. The reaction mixture was gently agitated for 5 min. Liquids were removed from the reaction vessel by vacuum filtration, and the resin was washed sequentially with DMF (10 mL/g) twice, CH_2Cl_2 (10 mL/g) twice, and DMF (10 mL/g) twice.

***N*$^{\alpha}$ -Fmoc Deprotection Protocol.** A stock solution of 20% (v/v) piperidine in DMF was prepared fresh each day. A portion of the stock solution (5 mL/g) was added to the resin, and the mixture was gently agitated for 5 min. An aliquot of the reaction mixture (250 mL) was removed for quantitation of the eliminated product, and the remaining liquids were removed by vacuum filtration. The resin was washed sequentially with DMF twice, CH_2Cl_2 twice, and DMF twice. A 20% (v/v) solution of piperidine in DMF (5 mL/g) was added to the resin, and the mixture was gently agitated for 5 min. An aliquot of the reaction mixture (250 mL) was removed for quantitation of the eliminated product, and the remaining liquids were removed by vacuum filtration. The resin was washed sequentially with DMF twice, CH_2Cl_2 twice, and DMF twice.

An aliquot (5 mL) from the reaction mixture was taken and diluted with MeCN (2 mL). The absorbance of the solution at 300 nm was measured in a 1-cm quartz cuvette. The concentration of the piperidine-dibenzofulvene adduct in the solution was calculated from the absorbance measurement using the reported molar absorptivity[48] of 6234 $M^{-1}cm^{-1}$ at 300 nm.

Cleavage and Side-Chain Deprotection. To the resin, a mixture of TFA/$^{i}Pr_3SiH/H_2O$ (95:2.5:2.5 v/v/v; 20 mL) was added. The reaction mixture was agitated for 1 h. The liquids were separated from the resin and collected by forcing the liquid phase through the peptide reaction vessel frit by positive pressure displacement with N_2. The resin was washed with TFA/$^{i}Pr_3SiH/H_2O$ (95:2.5:2.5 v/v/v; 2 mL) and the liquids were separated from the resin and

collected by positive pressure displacement with N_2. The volume of the collected liquids was reduced under a stream of N_2. The mixture was precipitated into cold Et_2O. The solids were separated from the liquids by centrifugation (Thermo Scientific CL10) at 3500 rpm for 5 min, and the solids were isolated by decanting the supernatant liquid. The crude peptide was precipitated from TFA into cold Et_2O two more times. The solid pellet was dissolved in H_2O (peptide **2-3**) or a mixture of H_2O/MeCN (9:1 v/v for peptide **2-2b**) and lyophilized. The peptide was purified by preparative HPLC on a C18 reversed-phase column.

Imidazole-1-sulfonyl-azide hydrochloride (ISA•HCl). The diazotransfer reagent was prepared according to a literature procedure.[28] Sulfuryl chloride (7.5 mL, 92 mmol) was added dropwise to an ice-water bath-cooled suspension of NaN_3 (6.00 g, 92.3 mmol) in MeCN (100 mL) and the mixture stirred overnight at room temperature. The reaction was cooled in an ice-water bath while imidazole (11.89 g, 174.7 mmol) was added to the reaction mixture and the resulting slurry stirred overnight. The mixture was diluted with EtOAc (200 mL), washed with H_2O (2 x 200 mL) then saturated aqueous $NaHCO_3$ (2 x 200 mL), dried over $MgSO_4$ and the solids were filtered in vacuo. The filtrate was cooled in an ice-water bath and a solution of HCl in EtOH[60] was added dropwise while stirring. The mixture was filtered and the filter cake was washed with EtOAc to yield ISA•HCl as colorless needles (10.30 g, 54 %). ^{1}H NMR (400 MHz, D_2O, δ, ppm): 9.10 (dd, $J_1 = J_2$ =1.3 Hz, 1H), 7.95 (dd, $J_1 = J_2$ = 1.5 Hz, 1H), 7.52 (dd, $J_1 = J_2$= 1.1 Hz, 1H) ^{13}C NMR (100 Hz, D_2O, δ, ppm): 137.8, 125.6, 119.6. Spectral data agree with those previously reported.[28]

Assembly of Ac-YLKKLLKLLKKLLK-NH_2 (2-3). Resin-bound peptide **2-1a** was assembled on ChemMatrix rink amide resin (0.50 mmol, 0.9628 g) in a glass-fritted peptide reaction vessel

and cleaved from the resin to yield peptide **2-3**. The sequence of operations is detailed in the table below:

Table 2-1 Protocol for the synthesis of Ac-YLKKLLKLLKKLLK-NH_2 (**2-3**).

		Mass of Reagents (g)		
Cycle		Fmoc-AA-OH	HBTU	HOBt
1	Single Coupling: Fmoc-Lys(Boc)-OH	2.3219	1.8593	0.7898
	Capping			
	N$^{\alpha}$-Fmoc Deprotection			
2	Single Coupling: Fmoc-Leu-OH	1.7894	1.8655	0.7696
	Capping			
	N$^{\alpha}$-Fmoc Deprotection			
3	Single Coupling: Fmoc-Leu-OH	1.7750	1.8643	0.7660
	Capping			
	N$^{\alpha}$-Fmoc Deprotection			
4	Single Coupling: Fmoc-Lys(Boc)-OH	2.3715	1.8803	0.7732
	Capping			
	N$^{\alpha}$-Fmoc Deprotection			
5	Single Coupling: Fmoc-Lys(Boc)-OH	2.3225	1.8678	0.7898
	Capping			
	N$^{\alpha}$-Fmoc Deprotection			
6	Double Coupling: Fmoc-Leu-OH	1.7639	1.8588	0.7863
		1.7748	1.8564	0.7522
	Capping			
	N$^{\alpha}$-Fmoc Deprotection			
7	Single Coupling: Fmoc-Leu-OH	1.17690	1.8614	0.7586
	Capping			
	N$^{\alpha}$-Fmoc Deprotection			
8	Single Coupling: Fmoc-Lys(Boc)-OH	2.3292	1.8778	0.77700
	Capping			
	N$^{\alpha}$-Fmoc Deprotection			
9	Single Coupling: Fmoc-Leu-OH	1.7471	1.8877	0.7810
	Capping			
	N$^{\alpha}$-Fmoc Deprotection			
10	Single Coupling: Fmoc-Leu-OH	1.7781	1.8548	0.7963
	Capping			
	N$^{\alpha}$-Fmoc Deprotection			
11	Single Coupling: Fmoc-Lys(Boc)-OH	2.3251	1.8457	0.7631
	Capping			
	N$^{\alpha}$-Fmoc Deprotection			
12	Single Coupling: Fmoc-Lys(Boc)-OH	2.3099	1.8425	0.7760
	Capping			
	N$^{\alpha}$-Fmoc Deprotection			

13	Single Coupling: Fmoc-Leu-OH	1.7792	1.8679	0.7799
	Capping			
	N^{α}-Fmoc Deprotection			
14	Single Coupling: Fmoc-Tyr(tBu)-OH	2.2917	1.8649	0.7877
	N^{α}-Fmoc Deprotection			
	Acetylation of the *N*-terminus			
	Cleavage and Side-Chain Deprotection			

Synthesis of Ac-YLAnlAnlLLAnlLLAnlAnlLLAnl-NH_2 (2-2a). To a solution of **2-3** (10 mg, 0.0056 mmol), ISA•HCl (30.6 mg, 0.135 mmol), K_2CO_3 (13.9 mg, 0.101 mmol) and $CuSO_4$•$5H_2O$ (8 mL, 0.25g/ mL solution, 0.0006 mmol) in THF/H_2O (1:1 v/v, 5.6 mL) the reaction was adjusted to pH 10 with sat. $NaHCO_3$ (aq) (430 mL) was stirred for 3 h at room temperature under a N_2 atmosphere. The reaction mixture was diluted with CH_2Cl_2 and washed three times with EDTA (0.03 M) solution. The CH_2Cl_2 layer was dried over $MgSO_4$ and the solids were removed by vacuum filtration. The resulting product was purified by flash chromatography (SiO_2, CH_2Cl_2 to 9:1 CH_2Cl_2/MeOH) to yield a colorless solid.

Assembly of Ac-Y(^{t}Bu)LK(Boc)K(Alloc)LLK(Alloc)LLK(Boc)K(Alloc)LLK(Alloc)-NH-Resin (2-1b). Resin-bound peptide **2-1b** was assembled on ChemMatrix rink amide resin (0.25 mmol, 0.5510 g) in a glass-fritted peptide reaction vessel. The sequence of operations is detailed in the table below:

Table 2-2 Protocol for the synthesis of

Ac-Y(^{t}Bu)LK(Boc)K(Alloc)LLK(Alloc)LLK(Boc)K(Alloc)LLK(Alloc)-NH-resin (**2-1b**).

		Mass of Reagents (g)		
Cycle		Fmoc-AA-OH	HBTU	HOBt
1	Single Coupling: Fmoc-Lys(Alloc)-OH	1.1272	0.9184	0.3845
	Capping			
	N^{α}-Fmoc Deprotection			
2	Single Coupling: Fmoc-Leu-OH	0.8831	0.9281	0.3840

	Capping			
	N$^{\alpha}$-Fmoc Deprotection			
3	Single Coupling: Fmoc-Leu-OH	0.8853	0.9263	0.3827
	Capping			
	N$^{\alpha}$-Fmoc Deprotection			
4	Single Coupling: Fmoc-Lys(Alloc)-OH	1.1290	0.9239	0.3868
	Capping			
	N$^{\alpha}$-Fmoc Deprotection			
5	Single Coupling: Fmoc-Lys(Boc)-OH	1.1739	0.9286	0.3876
	Capping			
	N$^{\alpha}$-Fmoc Deprotection			
6	Double Coupling: Fmoc-Leu-OH	0.8890	0.9198	0.3767
		0.8904	0.9174	0.3862
	Capping			
	N$^{\alpha}$-Fmoc Deprotection			
7	Single Coupling: Fmoc-Leu-OH	0.8906	0.9201	0.3835
	Capping			
	N$^{\alpha}$-Fmoc Deprotection			
8	Single Coupling: Fmoc-Lys(Alloc)-OH	1.1157	0.9211	0.3878
	Capping			
	N$^{\alpha}$-Fmoc Deprotection			
9	Single Coupling: Fmoc-Leu-OH	0.8857	0.9207	0.3831
	Capping			
	N$^{\alpha}$-Fmoc Deprotection			
10	Single Coupling: Fmoc-Leu-OH	0.8835	0.9188	0.3879
	Capping			
	N$^{\alpha}$-Fmoc Deprotection			
11	Single Coupling: Fmoc-Lys(Alloc)-OH	1.1220	0.9287	0.3802
	Capping			
	N$^{\alpha}$-Fmoc Deprotection			
12	Single Coupling: Fmoc-Lys(Boc)-OH	1.1192	0.9278	0.3811
	Capping			
	N$^{\alpha}$-Fmoc Deprotection			
13	Single Coupling: Fmoc-Leu-OH	0.8883	0.9250	0.3824
	Capping			
	N$^{\alpha}$-Fmoc Deprotection			
14	Single Coupling: Fmoc-Tyr(tBu)-OH	1.1482	0.9315	0.3844
	N$^{\alpha}$-Fmoc Deprotection			
	Acetylation of the *N*-terminus			

Removal of Alloc Groups. To the resin (0.1007 g), a solution of $Pd(PPh_3)_4$ (0.3001 g, 0.2592 mmol) in NMM/AcOH/$CHCl_3$ (2.5:5:92.5 v/v/v) was added. The reaction mixture was gently agitated for 3.5 h under N_2. Liquids were removed from the reaction vessel by vacuum filtration, and the resin was washed with $CHCl_3$ (3 mL). A solution of DMF/DIEA/sodium diethyldithiocarbamate trihydrate (9:0.5:0.5 w/w/w) was added to the reaction vessel and the reaction mixture was gently agitated for 5 min. The liquids were removed from the reaction vessel by vacuum filtration, and the resin was washed with DMF. A solution of DMF/DIEA/sodium diethyldithiocarbamate trihydrate (9:0.5:0.5 w/w/w) was added to the reaction vessel and the reaction mixture was gently agitated for 5 min. The liquids were removed from the reaction vessel by vacuum filtration, and the resin was washed sequentially with DMF (3 mL) and H_2O (3 mL).

On-Resin Diazotransfer Reaction Protocol. To the resin, a solution of K_2CO_3 (0.0580 g, 0.389 mmol) and ISA•HCl (0.1007 g, 0.5184 mmol) in of H_2O (2 mL) was added, followed by $CuSO_4$•$5H_2O$ (10 mL, 0.25 g/mL solution). The reaction mixture was gently agitated for 3 h under N_2. Liquids were removed from the reaction vessel by vacuum filtration, and the resin was washed sequentially with CH_2Cl_2 (3 mL) twice, MeOH (3 mL) twice, and Et_2O (3 mL) twice.

2.5 References

1. Johansson, H.; Pedersen, D. S., Azide- and Alkyne-Derivatised α-Amino Acids. *Eur. J. Org. Chem.* **2012**, 4267-4281.

2. Tornøe, C. W.; Christensen, C.; Meldal, M., Peptidotriazoles on solid phase: [1,2,3]-Triazoles by regiospecific copper(I)-catalyzed 1,3-dipolar cycloadditions of terminal alkynes to azide. *J. Org. Chem.* **2002,** *67*, 3057-3064.

3. Kolb, H. C.; Finn, M. G.; Sharpless, K. B., Click chemistry: Diverse chemical function from a few good reactions. *Angew. Chem., Int. Ed.* **2001,** *40*, 2004-2021.

4. Rostovtsev, V. V.; Green, L. G.; Fokin, V. V.; Sharpless, K. B., A Stepwise Huisgen Cycloaddition Process: Copper(I)-Catalyzed Regioselective "Ligation" of Azides and Terminal Alkynes. *Angew. Chem., Int. Ed.* **2002,** *41*, 2596-2599.

5. Agard, N. J.; Prescher, J. A.; Bertozzi, C. R., A Strain-Promoted [3 + 2] Azide−Alkyne Cycloaddition for Covalent Modification of Biomolecules in Living Systems. *J. Am. Chem. Soc.* **2004,** *126*, 15046-15047.

6. Saxon, E.; Bertozzi, C. R., Cell Surface Engineering by a Modified Staudinger Reaction. *Science* **2000,** *287*, 2007-2010.

7. Nilsson, B. L.; Kiessling, L. L.; Raines, R. T., Staudinger Ligation: A Peptide from a Thioester and Azide. *Org. Lett.* **2000,** *2*, 1939-1941.

8. Tang, W.; Becker, M. L., "Click" reactions: a versatile toolbox for the synthesis of peptide-conjugate. *Chem. Soc. Rev.* **2014,** *43*, 7013-7039.

9. Ramil, C. P.; Lin, Q., Bioorthogonal chemistry: Strategies and recent developments. *Chem. Commun.* **2013,** *49*, 11007-11022.

10. Sletten, E. M.; Bertozzi, C. R., Bioorthogonal chemistry: Fishing for selectivity in a sea of functionality. *Angew. Chem., Int. Ed.* **2009,** *48*, 6974-6998.

11. Canalle, L. A.; Vong, T.; Adams, P. H. H. M.; van Delft, F. L.; Raats, J. M. H.; Chirivi, R. G. S.; van Hest, J. C. M., Clickable Enzyme-Linked Immunosorbent Assay. *Biomacromolecules* **2011,** *12*, 3692-3697.

12. Le Chevalier Isaad, A.; Barbetti, F.; Rovero, P.; D'Ursi, A. M.; Chelli, M.; Chorev, M.; Papini, A. M., N^{α}-Fmoc-Protected ω-Azido- and ω-Alkynyl-L-amino Acids as Building Blocks for the Synthesis of "Clickable" Peptides. *Eur. J. Org. Chem.* **2008**, 5308-5314.

13. Torres, O.; Yüksel, D.; Bernardina, M.; Kumar, K.; Bong, D., Peptide tertiary structure nucleation by side-chain crosslinking with metal complexation and double "click" cycloaddition. *ChemBioChem* **2008,** *9*, 1701-1705.

14. Miller, N.; Williams, G. M.; Brimble, M. A., Synthesis of Fish Antifreeze Neoglycopeptides Using Microwave-Assisted "Click Chemistry". *Org. Lett.* **2009,** *11*, 2409-2412.

15. Oba, M.; Takazaki, H.; Kawabe, N.; Doi, M.; Demizu, Y.; Kurihara, M.; Kawakubo, H.; Nagano, M.; Suemune, H.; Tanaka, M., Helical Peptide-Foldamers Having a Chiral Five-Membered Ring Amino Acid with Two Azido Functional Groups. *J. Org. Chem.* **2014,** *79*, 9125-9140.

16. Bossu, I.; Berthet, N.; Dumy, P.; Renaudet, O., Synthesis of glycocyclopeptides by click chemistry and inhibition assays with lectins. *J. Carbohydr. Chem.* **2011,** *30*, 458-468.

17. Bonnet, R.; Murat, P.; Spinelli, N.; Defrancq, E., Click-click chemistry on a peptidic scaffold for easy access to tetrameric DNA structures. *Chem. Commun.* **2012,** *48*, 5992-5994.

18. Ghosh, P. S.; Hamilton, A. D., Noncovalent Template-Assisted Mimicry of Multiloop Protein Surfaces: Assembling Discontinuous and Functional Domains. *J. Am. Chem. Soc.* **2012,** *134*, 13208-13211.

19. Lau, Y. H.; de Andrade, P.; Quah, S.-T.; Rossman, M.; Laraia, L.; Sköld, N.; Sum, T. J.; Rowling, P. J. E.; Joseph, T. L.; Verma, C.; Hyvönen, M.; Itzhaki, L. S.; Venkitaraman, A. R.;

Brown, C. J.; Lane, D. P.; Spring, D. R., Functionalised staple linkages for modulating the cellular activity of stapled peptides. *Chem. Sci.* **2014,** *5*, 1804-1809.

20. Lau, Y. H.; de Andrade, P.; Sköld, N.; McKenzie, G. J.; Venkitaraman, A. R.; Verma, C.; Lane, D. P.; Spring, D. R., Investigating peptide sequence variations for 'double-click' stapled p53 peptides. *Organic and Biomolecular Chemistry* **2014,** *12*, 4074-4077.

21. Kawamoto, S. A.; Coleska, A.; Ran, X.; Yi, H.; Yang, C.-Y.; Wang, S., Design of Triazole-Stapled BCL9 α -Helical Peptides to Target the β -Catenin/B-Cell CLL/lymphoma 9 (BCL9) Protein–Protein Interaction. *J. Med. Chem.* **2012,** *55*, 1137-1146.

22. Blunden, B. M.; Chapman, R.; Danial, M.; Lu, H.; Jolliffe, K. A.; Perrier, S.; Stenzel, M. H., Drug Conjugation to Cyclic Peptide-Polymer Self-Assembling Nanotubes. *Chem.–Eur. J.* **2014,** *20*, 12745-12749.

23. Chapman, R.; Warr, G. G.; Perrier, S.; Jolliffe, K. A., Water-Soluble and pH-Responsive Polymeric Nanotubes from Cyclic Peptide Templates. *Chem.–Eur. J.* **2013,** *19*, 1955-1961.

24. Poon, C. K.; Chapman, R.; Jolliffe, K. A.; Perrier, S., Pushing the limits of copper mediated azide–alkyne cycloaddition (CuAAC) to conjugate polymeric chains to cyclic peptides. *Polym. Chem.* **2012,** *3*, 1820-1826.

25. Chapman, R.; Jolliffe, K. A.; Perrier, S., Modular design for the controlled production of polymeric nanotubes from polymer/peptide conjugates. *Polym. Chem.* **2011,** *2*, 1956-1963.

26. Chapman, R.; Jolliffe, K. A.; Perrier, S., Synthesis of Self-assembling Cyclic Peptide-polymer Conjugates using Click Chemistry. *Aust. J. Chem.* **2010,** *63*, 1169-1172.

27. Ma, D.; Bettis, S. E.; Hanson, K.; Minakova, M.; Alibabaei, L.; Fondrie, W.; Ryan, D. M.; Papoian, G. A.; Meyer, T. J.; Waters, M. L.; Papanikolas, J. M., Interfacial energy

conversion in Ru^{II} polypyridyl-derivatized oligoproline assemblies on TiO_2. *J. Am. Chem. Soc.* **2013,** *135*, 5250-5253.

28. Goddard-Borger, E. D.; Stick, R. V., An Efficient, Inexpensive, and Shelf-Stable Diazotransfer Reagent: Imidazole-1-sulfonyl Azide Hydrochloride. *Org. Lett.* **2007,** *9*, 3797-3800.

29. Palomo, J. M., Solid-phase peptide synthesis: an overview focused on the preparation of biologically relevant peptides. *RSC Adv.* **2014,** *4*, 32658-32672.

30. Chan, W. C.; White, P. D., *Fmoc Solid Phase Peptide Synthesis: A Practical Approach*. Oxford University Press: New York, NY, 2004.

31. Kates, S. A.; Albericio, F., *Solid-Phase Synthesis: A Practical Guide*. Marcel Dekker, Inc.: New York, NY, 2000.

32. Miranda, M. T. M.; Liria, C. W.; Remuzgo, C., Difficult Peptides. In *Amino Acids, Peptides and Proteins in Organic Chemisty: Building Blocks, Catalysis, and Coupling Chemistry*, Hughes, A. B., Ed.; Wiley-VCH, 2011; Vol. 3, pp 549-569.

33. Coin, I., The depsipeptide method for solid-phase synthesis of difficult peptides. *J. Pept. Sci.* **2010,** *16*, 223-230.

34. Tickler, A. K.; Wade, J. D., Overview of Solid Phase Synthesis of "Difficult Peptide" Sequences. In *Current Protocols in Protein Science*, 2007; Vol. 50, pp 18.8.1-18.8.6.

35. Kent, S. B. H., Chemical synthesis of peptides and proteins. *Annu. Rev. Biochem.* **1988,** *57*, 957-989.

36. Tam, J. P.; Lu, Y.-A., Coupling Difficulty Associated with Interchain Clustering and Phase Transition in Solid Phase Peptide Synthesis. *J. Am. Chem. Soc.* **1995,** *117*, 12058-12063.

37. Atherton, E.; Woolley, V.; Sheppard, R. C., Internal association in solid phase peptide synthesis. Synthesis of cytochrome C residues 66–104 on polyamide supports. *J. Chem. Soc., Chem. Commun.* **1980**, 970-971.

38. Fields, G. B.; Fields, C. G., Solvation effects in solid-phase peptide synthesis. *J. Am. Chem. Soc.* **1991,** *113*, 4202-4207.

39. Fischer, N.; Goddard-Borger, E. D.; Greiner, R.; Klapötke, T. M.; Skelton, B. W.; Stierstorfer, J., Sensitivities of Some Imidazole-1-sulfonyl Azide Salts. *J. Org. Chem.* **2012,** *77*, 1760-1764.

40. van Dongen, S. F. M.; Teeuwen, R. L. M.; Nallani, M.; van Berkel, S. S.; Cornelissen, J. J. L. M.; Nolte, R. J. M.; van Hest, J. C. M., Single-Step Azide Introduction in Proteins via an Aqueous Diazo Transfer. *Bioconjugate Chem.* **2009,** *20*, 20-23.

41. Kulbokaite, R.; Ciuta, G.; Netopilik, M.; Makuska, R., N-PEG'ylation of chitosan via ''click chemistry" reactions. *React. Funct. Polym.* **2009,** *69*, 771-778.

42. Huang, H.; Jin, Y.; Xue, M.; Yu, L.; Fu, Q.; Ke, Y.; Chu, C.; Liang, X., A novel click chitooligosaccharide for hydrophilic interaction liquid chromatography. *Chem. Commun.* **2009**, 6973-6975.

43. Tosh, D. K.; Yoo, L. S.; Chinn, M.; Hong, K.; Kilbey, S. M., II; Barrett, M. O.; Fricks, I. P.; Harden, T. K.; Gao, Z.-G.; Jacobson, K. A., Polyamidoamine (PAMAM) Dendrimer Conjugates of "Clickable" Agonists of the A3 Adenosine Receptor and Coactivation of the P2Y14 Receptor by a Tethered Nucleotide. *Bioconjugate Chem.* **2010,** *21*, 372-384.

44. Hansen, M.; van Gurp, T. H. M.; van Hest, J. C. M.; Löwik, D. W. P. M., Simple and Efficient Solid-Phase Preparation of Azido-peptides. *Org. Lett.* **2012,** *14*, 2330-2333.

45. Castro, V.; Blanco-Canosa, J. B.; Rodriguez, H.; Albericio, F., Imidazole-1-sulfonyl Azide-Based Diazo-Transfer Reaction for the Preparation of Azido Solid Supports for Solid-Phase Synthesis. *ACS Comb. Sci.* **2013,** *15*, 331-334.

46. Hansen, M. B.; Verdurmen, W. P. R.; Leunissen, E. H. P.; Minten, I.; van Hest, J. C. M.; Brock, R.; Löwik, D. W. P. M., A Modular and Noncovalent Transduction System for Leucine-Zipper-Tagged Proteins. *ChemBioChem* **2011,** *12*, 2294-2297.

47. DeGrado, W. F.; Lear, J. D., Induction of peptide conformation at apolar/water interfaces. 1. A study with model peptides of defined hydrophobic periodicity. *J. Am. Chem. Soc.* **1985,** *107*, 7684-7689.

48. Gude, M.; Ryf, J.; White, P. D., An accurate method for the quantification of Fmoc-derivatized solid phase supports. *Lett. Pept. Sci.* **2002,** *9*, 203-206.

49. Dangles, O.; Guibé, F.; Balavoine, G., Selective cleavage of the allyl and (allyloxy)carbonyl groups through palladium-catalyzed hydrostannolysis with tributyltin hydride. Application to the selective protection-deprotection of amino acid derivatives and in peptide synthesis. *J. Org. Chem.* **1987,** *52*, 4984-4993.

50. Trzeciak, A.; Bannwarth, W., Synthesis of 'head-to-tail' cyclized peptides on solid support by Fmoc chemistry. *Tetrahedron Lett.* **1992,** *33*, 4557-4560.

51. Kates, S. A.; Solé, N. A.; Johnson, C. R.; Hudson, D.; Barany, G.; Albericio, F., A novel, convenient, three-dimensional orthogonal strategy for solid-phase synthesis of cyclic peptides. *Tetrahedron Lett.* **1993,** *34*, 1549-1552.

52. Kates, S. A.; Daniels, S. B.; Albericio, F., Automated Allyl Cleavage for Continuous-Flow Synthesis of Cyclic and Branched Peptides. *Anal. Biochem.* **1993,** *212*, 303-310.

53. Grayson, S. M.; Fréchet, J. M. J., Synthesis and surface functionalization of aliphatic polyether dendrons. *J. Am. Chem. Soc.* **2000,** *122*, 10335-10344.

54. Strohalm, M.; Kavan, D.; Novák, P.; Volný, M.; Havlíček, V., *mMass* 3: A cross-platform software environment for precise analysis of mass spectrometric data. *Analytical Chemistry* **2010,** *82*, 4648-4651.

55. Strohalm, M. *mMass*, 5.5.0. Available at: http://www.mmass.org/.

56. Cavalli, S.; Albericio, F.; Kros, A., Amphiphilic peptides and their cross-disciplinary role as building blocks for nanoscience. *Chem. Soc. Rev.* **2010,** *39*, 241-263.

57. Woolfson, D. N., Building fibrous biomaterials from α-helical and collagen-like coiled-coil peptides. *Biopolymers* **2010,** *94*, 118-127.

58. Bromley, E. H. C.; Channon, K. J., Alpha-helical peptide assemblies giving new function to designed structures. *Prog. Mol. Biol. Transl. Sci.* **2011,** *103*, 231-275.

59. Branco, M. C.; Sigano, D. M.; Schneider, J. P., Materials from peptide assembly: Towards the treatment of cancer and transmittable disease. *Curr. Opin. Chem. Biol.* **2011,** *15*, 427-434.

60. The solution of HCl in EtOH was prepared by dropwise addition of AcCl (17 mL, 240 mmol) ethanol (60 mL); the reaction vessel was cooled with an ice-water bath.

Chapter 3

3. Bundle-Forming α-Helical Peptide–Dendron Hybrid

Marine, J. E.; Song S.; Liang, X.; Watson, M. D.; Rudick, J.G. *Chem. Commun.* **2015**, *51*, 14314-14317. Adapted with permission from the Royal Society of Chemistry (RSC). http://dx.doi.org/10.1039/C5CC05468K

3.1 Introduction

Hybrid materials that harness the properties of peptides constitute a broad class of functional supramolecular materials.[1-3] α-Helical bundles are especially attractive building blocks for materials because the helix bundle motif is found in the functional domain of diverse proteins (e.g., metalloenzymes, heme proteins, and transmembrane channel proteins).[4-6] Motivated by the goal of creating tractable models for understanding complex proteins, rules for designing peptides that self-assemble into helix bundle mimetics have been developed and leveraged to create proteins with functions that are not found in nature.[6] Bundle-forming α-helical peptides can be programmed to assemble into discrete aggregates or into one-dimensional assemblies.[4-6] The supramolecular and functional properties of these designed helix bundles can be retained when a polymer chain is conjugated to the peptide.[2,3] We therefore hypothesized that bundle-forming α-helical peptides could direct the assembly of dendrons. Our long-term goal is to make the helix bundle motif compatible with non-biological environments by varying the structure of the peripheral end groups of the dendrons. While there has been significant interest in peptide-dendron hybrids,[7-25] there are no examples of dendronized α-helix bundle-forming peptides. Herein, we demonstrate that folding and assembly properties encoded

in the amino acid sequence will direct the assembly of dendrons attached to solvent-exposed, exterior residues of an α-helical bundle (Figure 3.1a).

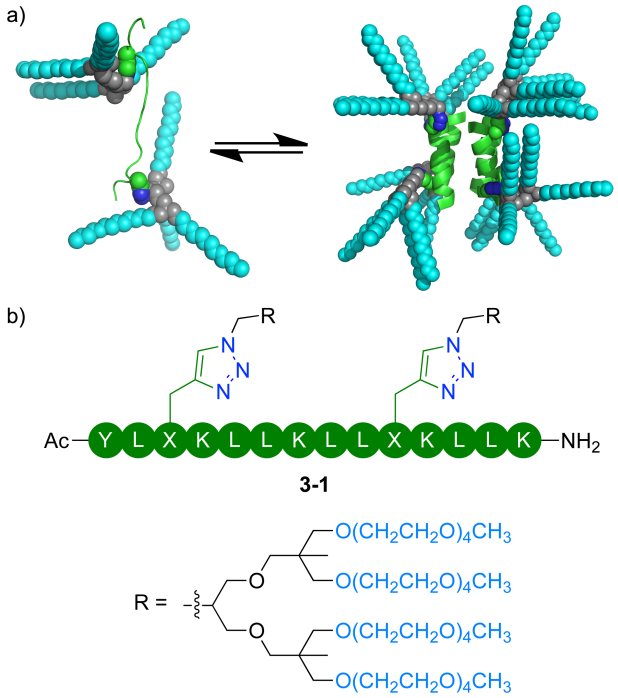

Figure 3.1 (a) The folding and assembly of a peptide (green ribbon) with two dendritic side-chains (spheres) to form a dendronized bundle of α-helices, and (b) the structure of peptide-dendron hybrid **3-1**.

3.2 Results and Discussion

Peptide-dendron hybrid **3-1** (Figure 3.1b) was designed by arranging polar and non-polar amino acid residues such that in the folded state an amphipathic α-helix would form. DeGrado and Lear demonstrated that, following this design principle, peptides as short as fourteen residues and composed of only polar lysine and non-polar leucine residues cooperatively fold and self-assemble into a tetrameric bundle of α-helices.[26] Because of the simplicity of the design and compact size of the peptides, a family of α-helical "LK" peptides has been developed as self-assembling modules for biomaterials.[27-31] Starting from an amino acid sequence similar to these α-helical "LK" peptides,[32] we

replaced two surface lysine residues with residues bearing water-soluble poly(alkyl ether) dendrons in the side chain.

Hybrid **3-1** reflects several design elements that are specific to α-helical peptide-dendron conjugates. The spacing between the dendrons (i, i + 7) was chosen to match the seven-residue periodicity of the α-helix. The density (one dendron/heptad) at which the dendrons are grafted to the peptide was intentionally kept low to accommodate the large volume that the dendrons occupy. The hydrophilic peripheral groups contribute a great deal of steric bulk to the second-generation dendron. Lee and Fréchet showed that, when grafted to each repeat unit of poly(L-lysine), sufficiently large dendrons induce a conformational transition from an α-helix to a β-sheet.[33] Furthermore, the poly(alkyl ether) dendrons were chosen for their dense branching pattern and non-planar structure. Shao and Parquette encountered an unanticipated transformation of a monomeric α-helical peptide to a self-assembling β-sheet peptide-dendron hybrid due, in part, to π-stacking interactions between dendrons.[20] The poly(alkyl ether) dendrons were expected to minimize favorable dendron-dendron interactions that might promote misfolding of the conjugate.

Peptide-dendron hybrid **3-1** was prepared by conjugating pre-formed second-generation dendrons to the unprotected peptide (a.k.a., graft-to approach). Both the peptide and dendron fragments are prepared through iterative chemical synthesis. Removing impurities that have small structural defects introduced during iterative syntheses can be especially challenging when dealing with large molecules. The graft-to approach employs monodisperse starting materials to avoid structural defects in the product. The graft-to approach has been adopted for the synthesis of most peptide-

dendron conjugates,[7-19,23-25,33,34] however the chemistries employed in those examples were not amenable to site-specific conjugation of dendrons to unprotected peptides. Several groups have successfully conjugated unprotected peptides to the peripheral groups of dendrons using copper-catalyzed azide-alkyne cycloaddition (CuAAC) reactions.[35-38] That approach appeared promising for our objective because CuAAC reactions have also proven to be suitable for grafting dendrons[39] or polymers[40] to linear polymers. We recently showed that a high density of dendrons can be grafted to a peptide via CuAAC.[32]

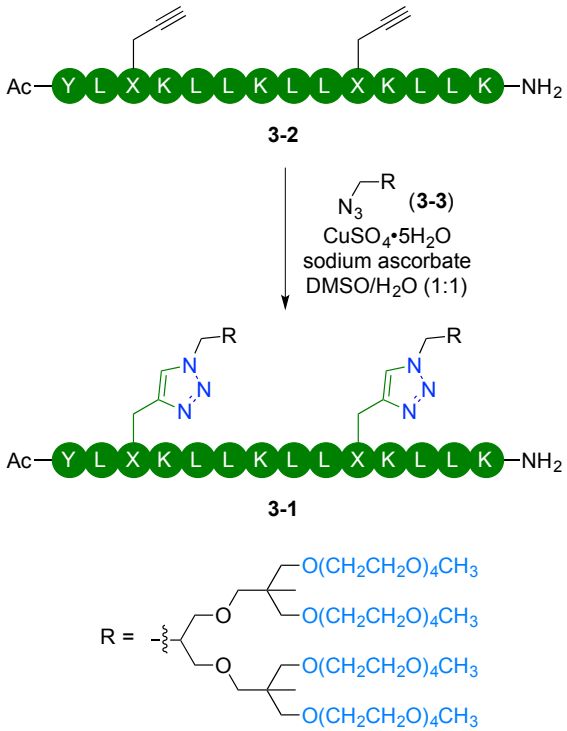

Figure 3.2 Graft-to synthesis of peptide-dendron hybrid **3-1**.

Azide **3-3** was conjugated to peptide **3-2** under ligand-free CuAAC reaction conditions[41] in DMSO/H_2O (Figure 3.2). Peptide **3-2** is soluble in the reaction solvent at concentrations >1 mM, and does not contain residues that are prone to side reactions.[42,43]

We were therefore able to execute the CuAAC reaction in the presence of substoichiometric amounts of $CuSO_4 \cdot 5H_2O$ and sodium ascorbate. The reaction was performed under an N_2 atmosphere, but no further effort was made to deoxygenate the reaction mixture. An excess of azide (1.3 eq./alkyne) was used to help drive the reaction to completion. The reaction was judged complete when the target conjugate was the only observable species in MALDI-TOF mass spectra of the reaction mixture. The conjugate was purified by preparative reversed-phase HPLC. The identity and purity of the conjugate were confirmed by MALDI-TOF mass spectrometry (Figure 3.3a) and analytical reversed-phase HPLC (Figure 3.3b), respectively. The MALDI-TOF mass spectrum shown in Figure 3.3[§] supports that we have successfully isolated peptide-dendron hybrid **3-1** from any residual dendron, starting peptide, or singly dendronized intermediates. We observe three different ionized forms of the conjugate ($[M + X]^+$, X = H, Na, and K). The remaining low-intensity peaks could not be assigned to any reasonable side-reaction products or fragmentations of the conjugate. We see excellent agreement between the observed isotope pattern for the peak assigned as the $[M + H]^+$ ion to the expected isotope pattern for the same ion (Figure 3.3a inset). The attributes of the MALDI-TOF mass spectrum emphasize that we have synthesized the desired peptide-dendron hybrid as a monodisperse macromolecule with a completely defined chemical structure. Peptide-dendron hybrid **3-1** was also characterized by NMR spectroscopy.

[§] The MALDI-TOF mass spectrum of **3-1** shown in Figure 3.3 was acquired by Dr. Robert Rieger (Stony Brook University Proteomics Center)

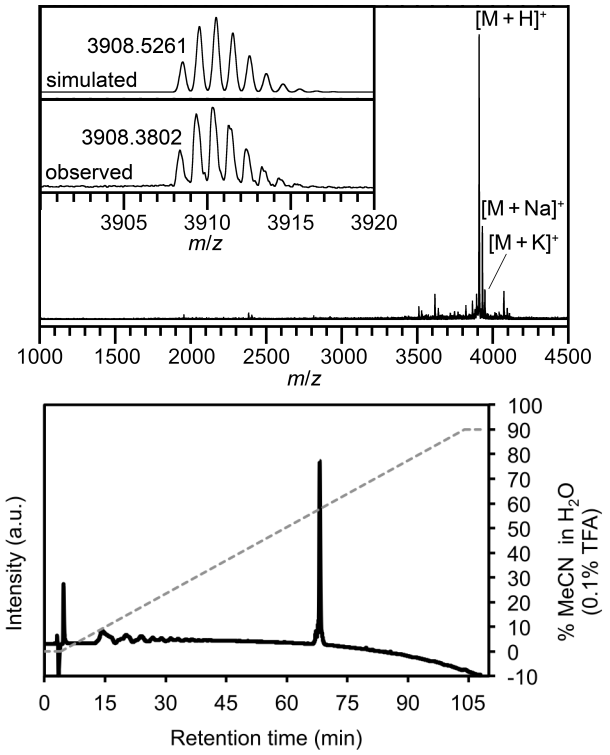

Figure 3.3 a) MALDI-TOF Mass spectrum** of **3-1**. The inset compares the simulated isotope pattern[44] (upper) with the observed isotope envelope (lower) for the [**3-1** + H]$^+$ ion ($C_{187}H_{352}N_{25}O_{60}$). b) HPLC chromatogram of peptide-dendron conjugate **3-1** (solid line) eluted with solvent A = H_2O + 0.1% TFA and solvent B = MeCN/H_2O (9:1 v/v) + 0.1% TFA.

Amides in the peptide backbone give rise to circular dichroism (CD) spectra that are characteristic for different secondary structures. In particular, negative bands are observed at 208 and 222 nm in the CD spectrum when the peptide adopts an α-helical conformation.[45] The poly(alkyl ether) dendrons are optically transparent in this region of the UV spectrum, so CD spectroscopy reports the conformation of **3-1**. The measured CD spectrum of **3-1** in tris(hydroxymethyl)aminomethane (Tris) buffer (pH 7.3) is shown in

** The MALDI-TOF mass spectrum of **3-1** was acquired by Dr. Robert Rieger (Stony Brook University Proteomics Center)

Figure 3.4 The spectrum confirms that the peptide is α-helical, and validates the design considerations described above.

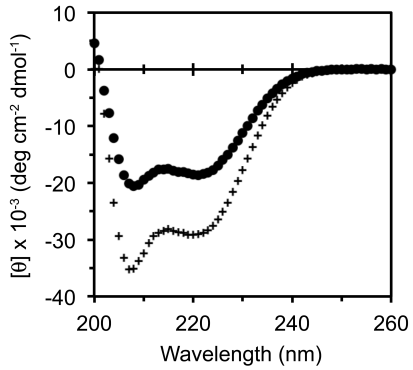

Figure 3.4 Circular dichroism (CD) spectra of peptide-dendron hybrid **3-1** (500 μM, ●) and Ac-YLKKLLKLLKKLLK-NH_2 (500 μM, +) in 20 mM Tris buffer (pH 7.3) with 285 mM KCl (total [Cl^-] = 300 mM) at 25 ºC.

The CD spectrum of a bundle-forming peptide without the dendrons (i.e., Ac-YLKKLLKLLKKLLK-NH_2) is shown in Figure 3.4 for comparison with peptide-dendron hybrid **3-1**. The peptide composed entirely of natural amino acids produces a more intense CD spectrum, which suggests that some fraying of the helix is caused by the introduction of the dendrons. The mean residue ellipticity at 222 nm ([θ_{222}]) is proportional to the amount of folded, α-helical peptide for both **3-1** and Ac-YLKKLLKLLKKLLK-NH_2. We can compare [θ_{222}] for the dendronized and conventional peptides to estimate the extent to which dendronization disrupts folding of the peptides. From this analysis we estimate that **3-1** is approximately 76% as helical as Ac-YLKKLLKLLKKLLK-NH_2.

In the α-helical conformation, peptide-dendron hybrid **3-1** has a globally amphipathic structure that is the driving force for assembly of **3-1** into bundles of α-helices. Hydrophobic leucine residues lie on one face of the α-helix, and the lysine

residues and hydrophilic dendrons reside on the opposite face. To investigate whether the α-helical peptide-dendron hybrid self-associates to form a dendronized helix bundle, we measured CD spectra at various concentrations of **3-1**. If folding into an α-helical conformation and association of the conjugates into bundles are coupled equilibria, then $[\theta_{222}]$ will depend on the concentration of **3-1**. Figure 3.5a plots $[\theta_{222}]$ for various concentrations of **3-1**, and shows that the α-helical peptide-dendron conjugate self-assembles as a bundle. Additionally, the sharp change of $[\theta_{222}]$ at concentrations below 125 μM suggests that the assembly process is cooperative. DeGrado and Lear demonstrated similar behavior for their α-helical "LK" peptide.[26] The folding and assembly behavior that is apparent from Figure 3.5a distinguishes **3-1** from previous examples of α-helical peptide-dendron hybrids,[20,33,34] which were monomeric, and from hybrids that rely upon an extended peptide conformation for self-assembly.[7-21,23-25]

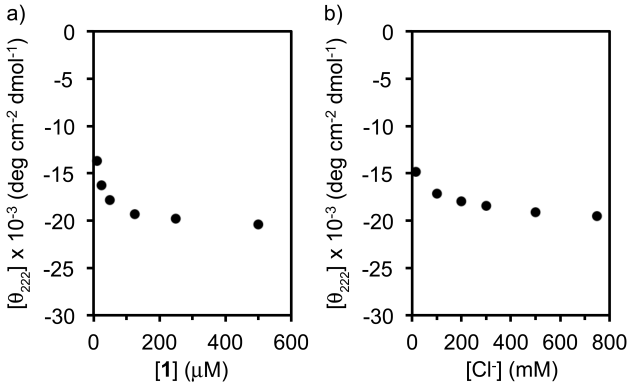

Figure 3.5 Plots of the mean residue ellipticity at 222 nm versus (a) the concentration of peptide-dendron hybrid **3-1** (285 mM KCl; total $[Cl^-]$ = 300 mM), and (b) the total concentration of chloride ion ([**3-1**] = 500 μM). All spectra were recorded in 20 mM Tris buffer (pH 7.3) at 25 ºC.

Combining rationally designed peptides with dendrons provides a modular platform for creating peptide-dendron hybrid materials with predictable structure and

function. The "LK" peptide upon which hybrid **3-1** is based is sensitive to the concentration of chloride anions.[26] Increasing chloride concentration shields electrostatic repulsions between the positively charged lysine residues on the polar face of the amphipathic helix. Figure 3.5b plots [θ_{222}] at various concentrations of chloride anion ([Cl^-]). The Tris buffer is a mixture of Tris and Tris·HCl, which contains 15 mM chloride, and the concentration of chloride was increased by adding KCl. The data plotted in Figure 3.5b indicate a transition from an unfolded state at low chloride concentration to a dendronized bundle of α-helices at higher concentrations of chloride. While other self-assembling peptide-dendron hybrids were found to be responsive to environmental cues (e.g., solvent, temperature, ionic strength, and pH),[7-21,23-25] the response of peptide-dendron hybrid **3-1** to chloride anions exemplifies how rationally designed properties in helix bundle-forming peptides can be transplanted into hybrid materials.

3.3 Conclusion

Helix bundle motifs in natural proteins provide the framework to support diverse functions by precisely positioning functional groups from the side-chains of different amino acids. Motivated by the rich functionality embedded in helix bundles, peptides that emulate the structure and function of helix bundle motifs have been developed as simpler models of biological macromolecules. These studies have also lead to the development of principles for designing helix bundles de novo and the creation of proteins with non-biological (or non-natural functions). Utilizing these design principles to program the assembly of dendrons into larger supramolecular structures provides a pathway to create supramolecular dendrimers with a folded, protein-like core. In addition to the structural precision gained through this strategy, it is intriguing to consider whether dendron-

peptide hybrids can support additional functions (e.g., catalytic activity) that have been successfully designed into model helix-bundle proteins. Several groups have explored how designed helix bundle-forming peptides conjugated to polymers program assembly and impart functionality to peptide-polymer conjugates.[2,3] Dendron-peptide conjugates offer additional insight by virtue of being monodisperse.

3.4 Experimental Procedures

3.4.1 Materials

Dowex-50W2X hydrogen form (50-100 mesh), sodium hydride, anhydrous dichloromethane, anhydrous tetrahydrofuran (THF), trifluoroacetic acid (TFA), and piperdine were used as received from Aldrich. Anhydrous dimethylformamide (DMF), sodium azide, and Fmoc-Tyr(*t*-Bu)-OH were used as received from EMD. Fmoc-Lys(Boc)-OH, Fmoc-Leu-OH, Fmoc-Pra-OH, *N*-methylmorpholine, and *O*-(benzotriazol-1-yl)-*N*,*N*,*N*',*N*'-tetramethyluroniumhexafluorophosphate (HBTU) were used as received from Chem-Impex International. Ethyl acetate (EtOAc), diethyl ether (Et_2O), sodium hydroxide, sodium bicarbonate, acetonitrile (MeCN), and pyridine were used as received from Fisher. Triisopropylsilane ($^{i}Pr_3SiH$) and copper(II) sulfate pentahydrate ($CuSO_4 \bullet 5H_2O$) were used as received from Acros. Sodium chloride and anhydrous magnesium sulfate were used as received from J. T. Baker. Methanesulfonyl chloride (MsCl), tetraethyleneglycol monomethyl ether, *p*-toluenesulfonyl chloride (*p*-TsCl), L-ascorbic acid sodium salt, and acetic anhydride (Ac_2O) were used as received from Alfa-Aesar. Hexanes (hex), methanol (MeOH), dichloromethane, dimethylsulfoxide (DMSO), and silica gel 60 (60-200 microns) were used as received from BDH. Chloroform-*d* with 0.03% v/v tetramethylsilane ($CDCl_3$) and Dimethylsulfoxide-d_6 (DMSO-d_6) were used as

received from Cambridge Isotope Laboratories. H-Rink amide-ChemMatrix resin (0.51 mmol/g) was used as received from PCAS BioMatrix Inc. Isopropyl alcohol was used as received from Pharmaco-Aaper. Potassium chloride was used as received from G-Biosciences. Tris-(hydroxymethyl) aminomethane hydrochloride (Tris•HCl) and were 2-Amino-2-(hydroxymethyl)-1,3-propanediol were used as received from Ameresco. Compound Ac-YLKKLLKLLKKLLK-NH_2 were prepared according to literature procedures.[46,32]

3.4.2 Techniques

^{1}H NMR (400 MHz, 500 MHz, 700 MHz) and ^{13}C NMR (100 MHz, 125 MHz, 175 MHz) spectra were recorded on a Bruker Avance III (400, 500, and 700) NMR spectrometer. Peak multiplicities are denoted as follows: s = singlet, d = doublet, t = triplet, q = quartet, pent = pentet, hept = heptet, sept = septet, and m = multiplet. The MALDI-TOF data were recorded on a Bruker Autoflex II TOF/TOF workstation. MALDI-TOF samples (10 mg/mL) were prepared in MeCN/H_2O with α-cyano-4-hydroxycinnamic acid as the matrix. Equal volumes of the matrix and peptide solutions were mixed and 1 μL of the mixture was injected onto the target plate. Gel permeation chromatography (GPC) in THF (1 mL/min) was performed using a Shimadzu LC-20AD liquid chromatography pump equipped with a DGU-20A5 degasser, CBM-20A controller, RID-10A RI detector, CTO-20A column oven (all from Shimadzu), and three American Polymer Standards AM GPC gel columns of 100 Å (5 μm), 500 Å (5 μm), and 10,000 Å (5 μm). Relative molecular weights and molecular weight distributions were determined according to a calibration with narrow polydispersity polystyrene standards (American Polymer Standards). Thin layer chromatography (TLC) was performed using Whatman

silica gel 60 Å plates (250 μm) with fluorescent indicator and visualized using a UV lamp (254 nm) or $KMnO_4$ stain. Flash column chromatography was performed on a Teledyne Isco CombiFlash Rf with RedSep Rf Normal Phase disposable silica columns. Low-resolution electrospray mass spectrometry (ESI–MS) were acquired in positive polarity mode on an Agilent LC-MSD with an 1100 HPLC and a G1956A single-quadrupole mass spectrometer (accuracy ±0.1 amu). High-resolution electrospray ionization mass spectra (HRMS–ESI) were acquired by the Mass Spectrometry Laboratory at the University of Illinois at Urbana-Champaign on a Micromass Q-Tof Ultima. Peptides were synthesized using 9-fluorenylmethoxycarbonyl (Fmoc) chemistry on a Protein Technologies PS3 peptide synthesizer. Peptides were cleaved from the resin using a TFA/$^{i}Pr_3SiH/H_2O$ (95:2.5:2.5 v/v/v; 10 mL). High-performance liquid chromatography (HPLC) was performed on a Waters 1525 Binary pump equipped with a Waters 2489 UV/Visible Detector set at 210 nm and 280 nm. To determine the analytical purity of samples, the HPLC was equipped with a SunFire^{TM} C18 column (5 μm, 4.6 mm × 250 mm; Waters) operating at a flow rate of 1 mL/min and a solvent gradient of 1%/min. Purification of samples was done on the HPLC equipped with a SunFire^{TM} C18 (5 μm, 19 mm × 250 mm) column operating at a flow rate of 17 mL/min and a solvent gradient of 5%/min. Absorbance of peptide solutions in deionized water at 280 nm was recorded on an Evolution 201 spectrophotometer using a 1-cm quartz cuvette. The concentration of the peptide was calculated from the absorbance using Beer's Law and an extinction coefficient (ε) for tyrosine of 1490 L mol^{-1} cm^{-1}.[47] Circular dichroism (CD) spectra were performed on an Applied Photophysics Chirascan instrument.

Peptide Concentration CD Experiments. The samples for the peptide concentration CD experiments were made by serial dilution of peptide-dendron hybrid **3-1** (500 μM) with 20 mM Tris buffer (pH 7.3) were vortexed to allow for mixing. The 500 μM, 250 μM, 125 μM were measured in a 10-mm quartz cuvette and the 50 μM, 25 μM, 10 μM, 5 μM, 2.5 μM were measured in a 1-mm quartz cuvette.

Salt Titration CD Experiments. The salt titration CD experiments were performed using a 1-mm quartz cuvette to aquire CD spectra with Cl^- concentrations of: 1 M, 0.75 M, 0.5 M, 0.3 M, 0.2 M, and 0.1 M solutions after they had been vortexed to allow appropriate mixing. Two equimolar (500 μM) peptide solutions with initial concentrations of 1M Cl^- and 0.015 M Cl^- were mixed together using a vortex to form solution with a final concentration of 0.75 M and 0.1 M Cl^-. The 0.75 M solution and 0.1 M solution were mixed together using a vortex to form solution with a final concentration of 0.50 M and 0.2 M. The 0.5 M and 0.2 M solutions were mixed together using a vortex to form a final concentration of 0.3M Cl^-.

3.4.3 Synthesis

General Solid-Phase Peptide Synthesis Procedures. Single Coupling Protocol. The resin was washed three times for 30 seconds with DMF (15 mL/g). The N-terminus was deprotected using a 8:2 DMF/piperdine solution (15 mL/g) two times for 5 minutes. The resin was then washed six times using DMF (15 mL/g) for 30 seconds each time. The Fmoc-protected amino acid and HBTU was dissolved in a 0.2 M NMM. The solution was then transferred to the peptide reaction vessel containing the swelled resin and was further diluted with DMF to a concentration achieve a final concentration of Fmoc-

protected amino acid (0.22 M) and HBTU (0.21 M). The coupling was done for 20 minutes. The resin was then washed three times for 30 seconds each time

General Solid-Phase Peptide Synthesis Procedures. Double Coupling Protocol. The resin was washed three times for 30 seconds with DMF. The N-terminus was deprotected using a 8:2 DMF/piperdine solution two times for 5 minutes. The resin was then washed six times using DMF for 30 seconds each time. The Fmoc-protected amino acid (0.50 M) and HBTU (0.48 M) was dissolved in 0.2 M NMM. The solution was then transferred to the peptide reaction vessel containing the swelled resin and was further diluted with DMF to a concentration achieve a final concentration of Fmoc-protected amino acid (0.22 M) and HBTU (0.21 M). The coupling was done for 20 minutes. The resin was drained and Fmoc-protected amino acid (0.52 M) and HBTU (0.48 M) was dissolved in 0.2 M NMM. The solution was then transferred to the peptide reaction vessel and was further diluted with DMF to a concentration achieve a final concentration of Fmoc-protected amino acid (0.22 M) and HBTU (0.21 M). The coupling was done for 20 minutes after which the resin was then washed three times with DMF (3 mL) for 30 seconds each time.

***N*$^{\alpha}$-Fmoc Deprotection Protocol.** The resin was washed three times for 30 seconds using DMF (15 mL/g). The N-terminus was then deprotected using a stock solution of 20% (v/v) piperdine in DMF two times for five minutes each time. The resin was then washed six times for 30 seconds each time.

Protocol for Capping and Acetylation of the *N*-Terminus. The resin was washed six times for 30 seconds using DMF. A vial containing acetic anhydride (2 mL) was diluted with a 0.2 M NMM solution (2 mL) the solution was then transferred to the reaction vessel and further diluted with DMF (2.5 mL). The solution in the reaction vessel was

mixed for 5 minutes. The resin was then washed three times with DMF (15 mL/g) for 30 seconds each time.

Cleavage and Side-Chain Deprotection. To the resin, a mixture of TFA/^{i}Pr$_3$SiH/H_2O (95:2.5:2.5 v/v/v; 10 mL) was added. The reaction mixture was agitated for 1 h. The liquids were separated from the resin and collected by forcing the liquid phase through the peptide reaction vessel frit by positive pressure displacement with N_2. The resin was washed with TFA/^{i}Pr$_3$SiH/H_2O (95:2.5:2.5 v/v/v; 2 mL) and the liquids were separated from the resin and collected by positive pressure displacement with N_2. The volume of the collected liquids was reduced under a stream of N_2. The mixture was precipitated into cold Et_2O. The solids were separated from the liquids by centrifugation (Thermo Scientific CL10) at 3500 rpm for 5 min, and the solids were isolated by decanting the supernatant liquid. The crude peptide was precipitated from TFA into cold Et_2O two more times. The solid pellet was dissolved in H_2O and lyophilized. The peptide was purified by preparative HPLC on a C18 reversed-phase column.

Assembly of Ac-YLXKLLKLLXKLLK-NH_2 X = propargyl glycine (3-2). Peptide **3-2** was assembled on ChemMatrix Rink amide resin (0.10 mmol, 0.2288 g) in a glass-fritted peptide reaction vessel using a PS3 synthesizer and cleaved from the resin to yield peptide **3-2**. The sequence of operations is detailed in the table below:

Table 3-1. Protocol for the synthesis of Ac-YLXKLLKLLXKLLK-NH_2 X = propargyl glycine(**3-2**).

		Mass of Reagents (g)	
Cycle		Fmoc-AA-OH	HBTU
1	Single Coupling: Fmoc-Lys(Boc)-OH	0.4714	0.3596
	Capping		
	N^{α}-Fmoc Deprotection		

2	Single Coupling: Fmoc-Leu-OH	0.3531	0.3543
	Capping		
	N^{α}-Fmoc Deprotection		
3	Single Coupling: Fmoc-Leu-OH	0.3531	0.3513
	Capping		
	N^{α}-Fmoc Deprotection		
4	Single Coupling: Fmoc-Lys(Boc)-OH	0.4634	0.3578
	Capping		
	N^{α}-Fmoc Deprotection		
5	Single Coupling: Fmoc-Pra-OH	0.3380	0.3556
	Capping		
	N^{α}-Fmoc Deprotection		
6	Singe Coupling: Fmoc-Leu-OH	0.3566	0.3543
	Capping		
	N^{α}-Fmoc Deprotection		
7	Single Coupling: Fmoc-Leu-OH	0.3542	0.3539
	Capping		
	N^{α}-Fmoc Deprotection		
8	Single Coupling: Fmoc-Lys(Boc)-OH	0.4735	0.3552
	Capping		
	N^{α}-Fmoc Deprotection		
9	Single Coupling: Fmoc-Leu-OH	0.3552	0.3545
	Capping		
	N^{α}-Fmoc Deprotection		
10	Double Coupling: Fmoc-Leu-OH	0.3526	0.3530
		0.3567	0.3518
	Capping		
	N^{α}-Fmoc Deprotection		
11	Single Coupling: Fmoc-Lys(Boc)-OH	0.4699	0.3538
	Capping		
	N^{α}-Fmoc Deprotection		
12	Single Coupling: Fmoc-Pra-OH	0.3394	0.3551
	Capping		
	N^{α}-Fmoc Deprotection		
13	Single Coupling: Fmoc-Leu-OH	0.3567	0.3508
	Capping		
	N^{α}-Fmoc Deprotection		
14	Single Coupling: Fmoc-Tyr(t-Bu)-OH	0.4598	0.3543
	N^{α}-Fmoc Deprotection		
	Acetylation of the *N*-terminus		
	Cleavage and Side-Chain Deprotection		

Peptide-Dendron Hybrid (3-1)

Dendritic azide **3-3** (33.1 mg, 0.0302 mmol) was dissolved in 600 μL H_2O and transferred to a vial containing peptide **3-2** (20.0 mg, 0.012 mmol), $CuSO_4 \cdot 5H_2O$ (1.2 mg, 0.0048 mmol), sodium ascorbate (4.1 mg, 0.021 mmol) in 600 μL of DMSO. The reaction mixture was agitated at room temperature under a N_2 atmosphere for 22 h. The reaction mixture was purified by preparative HPLC on a C18 reversed-phase column by gradient elution using a H_2O/MeCN mobile phase containing 0.1% TFA. The resulting oil yielded peptide dendron hybrid **3-1** (12.5 mg, 27 %). ^{1}H NMR (700 MHz, DMSO-d_6, δ): 8.43 (s, 1H), 8.16 (s, 1 H), 8.09 (s, 1H), 7.98 (s, 1 H), 7.92 (s, 1H), 7.87 (s, 2H), 7.85 (s, 1H), 7.78 (s, 1H), 7.70 (s, 7H), 7.65 (s, 3H), 7.62 (s, 1H), 7.47 (m, 1 H), 7.38 (m, 1 H), 7.29 (m, 1 H), 7.21 (m, 1 H), 7.05 (s, 1 H), 6.99 (d, 2H), 6.65 (d, 2H), 4.34 (m, 2 H), 4.20 (s, 2 H), 4.10-3.87 (m, 6 H), 3.47-3.44 (m, 105 H), 3.39 (m, 15 H), 3.20 (m, 38 H), 3.15 (m, 9 H), 2.85 (m, 1 H), 2.73 (m, 6 H), 2.60 (m, 1 H), 2.34 (m, 1 H), 2.04 (m, 1 H), 1.94 (s, 2 H), 1.72-1.27 (m, 34 H), 0.83 (m, 48 H). ^{13}C NMR (175 MHz, $CDCl_3$, δ): 173.4, 173.0, 173.0, 172.6, 172.6, 172.5, 172.9, 172.2, 171.9, 171.8, 171.74, 171.74, 171.7, 171.2, 170.3, 158.3, 158.1, 157.9, 157.8, 155.9, 142.9, 130.0, 127.9, 125.4, 123.5, 118.2, 116.5, 114.9, 73.3, 73.1, 71.3, 70.5, 69.9, 69.85, 69.84, 69.82, 69.6, 68.7, 68.6, 58.1, 52.2, 48.3, 40.6, 36.2, 31.2, 30.6, 30.6, 26.8, 26.8, 26.72, 26.66, 24.1, 24.09, 24.1, 23.96, 23.19, 23.04, 23.02, 22.98, 22.9, 22.8, 22.7, 22.5, 22.3, 22.25, 22.2, 21.7, 21.6, 21.4, 21.3, 21.3, 21.2, 17.3.

3.5 References

1. Aida, T.; Meijer, E. W.; Stupp, S. I., Functional Supramolecular Polymers. *Science* **2012,** *335*, 813-817.

2. Shu, J. Y.; Panganiban, B.; Xu, T., Peptide-polymer conjugates: from fundamental science to application. *Annu. Rev. Phys. Chem.* **2013,** *64*, 631-657.

3. Klok, H.-A., Peptide/protein-synthetic polymer conjugates: Quo vadis. *Macromolecules* **2009,** *42*, 7990-8000.

4. Marsden, H. R.; Kros, A., Self-assembly of coiled coils in synthetic biology: inspiration and progress. *Angew. Chem., Int. Ed.* **2010,** *49*, 2988-3005.

5. Cavalli, S.; Albericio, F.; Kros, A., Amphiphilic peptides and their cross-disciplinary role as building blocks for nanoscience. *Chem. Soc. Rev.* **2010,** *39*, 241-263.

6. Apostolovic, B.; Danial, M.; Klok, H.-A., Coiled coils: attractive protein folding motifs for the fabrication of self-assembled, responsive and bioactive materials. *Chem. Soc. Rev.* **2010,** *39*, 3541-3575.

7. Jang, W.-D.; Jiang, D.-L.; Aida, T., Dendritic physical gel: Hierarchical self-organization of a peptide-core dendrimer to form a micrometer-scale fibrous assembly. *J. Am. Chem. Soc.* **2000,** *122*, 3232-3233.

8. Jang, W.-D.; Aida, T., Dendritic Physical Gels: Structural Parameters for Gelation with Peptide-Core Dendrimers. *Macromolecules* **2003,** *36*, 8461-8469.

9. Percec, V.; Dulcey, A. E.; Balagurusamy, V. S. K.; Miura, Y.; Smidrkal, J.; Peterca, M.; Nummelin, S.; Edlund, U.; Hudson, S. D.; Heiney, P. A.; Duan, H.; Magonov, S. N.; Vinogradov, S. A., Self-Assembly of Amphiphilic Dendritic Dipeptides into Helical Pores. *Nature* **2004,** *430*, 764-768.

10. Percec, V.; Dulcey, A.; Peterca, M.; Ilies, M.; Miura, Y.; Edlund, U.; Heiney, P. A., Helical Porous Protein Mimics Self-Assembled from Amphiphilic Dendritic Dipeptides. *Aust. J. Chem.* **2005,** *58*, 472-482.

11. Percec, V.; Dulcey, A. E.; Peterca, M.; Ilies, M.; Ladislaw, J.; Rosen, B. M.; Edlund, U.; Heiney, P. A., The internal structure of helical pores self-assembled from dendritic dipeptides is stereochemically programmed and allosterically regulated. *Angew. Chem., Int. Ed.* **2005,** *44*, 6516-6521.

12. Percec, V.; Dulcey, A. E.; Peterca, M.; Ilies, M.; Sienkowska, M. J.; Heiney, P. A., Programming the internal structure and stability of helical pores self-assembled from dendritic dipeptides via the protective groups of the peptide. *J. Am. Chem. Soc.* **2005,** *127*, 17902-17909.

13. Percec, V.; Dulcey, A. E.; Peterca, M.; Ilies, M.; Nummelin, S.; Sienkowska, M. J.; Heiney, P. A., Principles of self-assembly of helical pores from dendritic dipeptides. *Proc. Natl. Acad. Sci. U. S. A.* **2006,** *103*, 2518-2523.

14. Peterca, M.; Percec, V.; Dulcey, A. E.; Nummelin, S.; Korey, S.; Ilies, M.; Heiney, P. A., Self-assembly, structural, and retrostructural analysis of dendritic dipeptide pores undergoing reversible circular to elliptical shape change. *J. Am. Chem. Soc.* **2006,** *128*, 6713-6720.

15. Kaucher, M. S.; Peterca, M.; Dulcey, A. E.; Kim, A. J.; Vinogradov, S. A.; Hammer, D. A.; Heiney, P. A.; Percec, V., Selective transport of water mediated by porous dendritic dipeptides. *J. Am. Chem. Soc.* **2007,** *129*, 11698-11699.

16. Percec, V.; Dulcey, A. E.; Peterca, M.; Adelman, P.; Samant, R.; Balagurusamy, V. S. K.; Heiney, P. A., Helical pores self-assembled from homochiral dendritic

dipeptides based on L-Tyr and nonpolar alpha-amino acids. *J. Am. Chem. Soc.* **2007,** *129*, 5992-6002.

17. Kim, A. J.; Kaucher, M. S.; Davis, K. P.; Peterca, M.; Imam, M. R.; Christian, N. A.; Levine, D. H.; Bates, F. S.; Percec, V.; Hammer, D. A., Proton Transport from Dendritic Helical-Pore-Incorporated Polymersomes. *Adv. Funct. Mater.* **2009,** *19*, 2930-2936.

18. Rosen, B. M.; Peterca, M.; Morimitsu, K.; Dulcey, A. E.; Leowanawat, P.; Resmerita, A.-M.; Imam, M. R.; Percec, V., Programming the supramolecular helical polymerization of dendritic dipeptides via the stereochemical information of the dipeptide. *J. Am. Chem. Soc.* **2011,** *133*, 5135-5151.

19. Lee, J.; Kim, J. M.; Yun, M.; Park, C.; Park, J.; Lee, K. H.; Kim, C., Self-organization of amide dendrons with focal dipeptide units. *Soft Matter* **2011,** *7*, 9021-9026.

20. Shao, H.; Lockman, J. W.; Parquette, J. R., Coupled Conformational Equilibria in β -Sheet Peptide−Dendron Conjugates. *J. Am. Chem. Soc.* **2007,** *129*, 1884-1885.

21. Shao, H.; Parquette, J. R., Controllable Peptide–Dendron Self-Assembly: Interconversion of Nanotubes and Fibrillar Nanostructures. *Angew. Chem., Int. Ed.* **2009,** *48*, 2525-2528.

22. Shao, H.; Bewick, N. A.; Parquette, J. R., Intramolecular chiral communication in peptide-dendron hybrids. *Org. Biomol. Chem.* **2012,** *10*, 2377-2379.

23. Sato, K.; Itoh, Y.; Aida, T., Columnarly Assembled Liquid-Crystalline Peptidic Macrocycles Unidirectionally Orientable over a Large Area by an Electric Field. *J. Am. Chem. Soc.* **2011,** *133*, 13767-13769.

24. Sato, K.; Itoh, Y.; Aida, T., Homochiral supramolecular polymerization of bowl-shaped chiral macrocycles in solution. *Chem. Sci.* **2014,** *5*, 136-140.

25. Amorín, M.; Pérez, A.; Barberá, J.; Ozores, H. L.; Serrano, J. L.; Granja, J. R.; Sierra, T., Liquid crystal organization of self-assembling cyclic peptides. *Chem. Commun.* **2013,** *50*, 688-690.

26. DeGrado, W. F.; Lear, J. D., Induction of peptide conformation at apolar/water interfaces. 1. A study with model peptides of defined hydrophobic periodicity. *J. Am. Chem. Soc.* **1985,** *107*, 7684-7689.

27. Jain, A.; Buchko, G. W.; Reback, M. L.; O'Hagan, M.; Ginovska-Pangovska, B.; Linehan, J. C.; Shaw, W. J., Active Hydrogenation Catalyst with a Structured, Peptide-Based Outer-Coordination Sphere. *ACS Catal.* **2012,** *2*, 2114-2118.

28. Fu, L.; Liu, J.; Yan, E. C. Y., Chiral sum frequency generation spectroscopy for characterizing protein secondary structures at interfaces. *J. Am. Chem. Soc.* **2011,** *133*, 8094-8097.

29. Mermut, O.; Phillips, D. C.; York, R. L.; McCrea, K. R.; Ward, R. S.; Somorjai, G. A., In situ adsorption studies of a 14-amino acid leucine-lysine peptide onto hydrophobic polystyrene and hydrophilic silica surfaces using quartz crystal microbalance, atomic force microscopy, and sum frequency generation vibrational spectroscopy. *J. Am. Chem. Soc.* **2006,** *128*, 3598-3607.

30. Long, J. R.; Oyler, N.; Drobny, G. P.; Stayton, P. S., Assembly of α-helical Peptide Coatings on Hydrophobic Surfaces. *J. Am. Chem. Soc.* **2002,** *124*, 6297-6303.

31. Kiyota, T.; Lee, S.; Sugihara, G., Design and Synthesis of Amphiphilic α-Helical Model Peptides with Systematically Varied Hydrophobic−Hydrophilic Balance and Their Interaction with Lipid- and Bio-Membranes. *Biochemistry* **1996,** *35*, 13196-13204.

32. Marine, J. E.; Liang, X.; Song, S.; Rudick, J. G., Azide-Rich Peptides Via an On-Resin Diazotransfer Reaction. *Biopolymers* **2015,** *104*, 419-426.

33. Lee, C. C.; Fréchet, J. M. J., Synthesis and Conformations of Dendronized Poly(l-lysine). *Macromolecules* **2006,** *39*, 476-481.

34. Zhuravel, M. A.; Davis, N. E.; Nguyen, S. T.; Koltover, I., Dendronized protein polymers: synthesis and self-assembly of monodisperse cylindrical macromolecules. *J. Am. Chem. Soc.* **2004,** *126*, 9882-9883.

35. Wan, J.; Huang, J. X.; Vetter, I.; Mobli, M.; Lawson, J.; Tae, H.-S.; Abraham, N.; Paul, B.; Cooper, M. A.; Adams, D. J.; Lewis, R. J.; Alewood, P. F., α-Conotoxin Dendrimers Have Enhanced Potency and Selectivity for Homomeric Nicotinic Acetylcholine Receptors. *J. Am. Chem. Soc.* **2015,** *137*, 3209-3212.

36. Tang, W.; Ma, Y.; Xie, S.; Guo, K.; Katzenmeyer, B.; Wesdemiotis, C.; Becker, M. L., Valency-Dependent Affinity of Bioactive Hydroxyapatite-Binding Dendrons. *Biomacromolecules* **2013,** *14*, 3304-3313.

37. Schellinger, J. G.; Danan-Leon, L. M.; Hoch, J. A.; Kassa, A.; Srivastava, I.; Davis, D.; Gervay-Hague, J., Synthesis of a Trimeric gp120 Epitope Mimic Conjugated to a T-Helper Peptide To Improve Antigenicity. *J. Am. Chem. Soc.* **2011,** *133*, 3230-3233.

38. Rijkers, D. T.; van Esse, G. W.; Merkx, R.; Brouwer, A. J.; Jacobs, H. J. F.; Pieters, R. J.; Liskamp, R. M. J., Efficient microwave-assisted synthesis of multivalent

dendrimeric peptides using cycloaddition reaction (click) chemistry. *Chem. Commun.* **2005**, 4581-4583.

39. Helms, B.; Mynar, J. L.; Hawker, C. J.; Fréchet, J. M. J., Dendronized linear polymers via "click chemistry". *J. Am. Chem. Soc.* **2004,** *126*, 15020-15021.

40. Engler, A. C.; Lee, H.-i.; Hammond, P. T., Highly efficient "grafting onto" a polypeptide backbone using click chemistry. *Angew. Chem., Int. Ed.* **2009,** *48*, 9334-9338.

41. Rostovtsev, V. V.; Green, L. G.; Fokin, V. V.; Sharpless, K. B., A Stepwise Huisgen Cycloaddition Process: Copper(I)-Catalyzed Regioselective "Ligation" of Azides and Terminal Alkynes. *Angew. Chem., Int. Ed.* **2002,** *41*, 2596-2599.

42. Hong, V.; Presolski, S. I.; Ma, C.; Finn, M. G., Analysis and Optimization of Copper-Catalyzed Azide- "Alkyne Cycloaddition for Bioconjugation. *Angew. Chem., Int. Ed.* **2009,** *48*, 9879-9883.

43. Kumar, A.; Li, K.; Cai, C., Anaerobic conditions to reduce oxidation of proteins and to accelerate the copper-catalyzed "Click" reaction with a water-soluble bis(triazole) ligand. *Chem. Commun.* **2011,** *47*, 3186-3188.

44. Strohalm, M. *mMass*, 5.5.0. Available at: http://www.mmass.org/.

45. Greenfield, N. J., Using circular dichroism spectra to estimate protein secondary structure. *Nat. Protoc.* **2006,** *1*, 2876-2890.

46. Grayson, S. M.; Fréchet, J. M. J., Synthesis and surface functionalization of aliphatic polyether dendrons. *J. Am. Chem. Soc.* **2000,** *122*, 10335-10344.

47. Pace, C. N.; Vajdos, F.; Fee, L.; Grimsley, G.; Gray, T., How to measure and predict the molar absorption coefficient of a protein. *Protein Sci.* **1995,** *4*, 2411-2423.

Chapter 4

4. Synthesis and Self-Assembly of Bundle-Forming α-Helical Peptide–Dendron Hybrids

Marine, J. E.; Liang, X.; Song, S.; Rudick, J. G. *Biomacromolecules* **2016**, *17,* 336-344. Adapted with permission from the American Chemical Society (ACS). http://dx.doi.org/10.1021/acs.biomac.5b01452

4.1 Introduction

Control over polymer chain length, monomer sequence, and chain folding are essential to the functionality of natural biopolymers (e.g., proteins, DNA, RNA). Dendrimers[1-6] and β-peptide foldamers[7-12] are among the best examples of synthetic macromolecules to rival natural biopolymers. These materials, however, highlight the challenges to bridging the gap between controlled structure and function.[13] De novo protein design and protein engineering strategies, on the other hand, exploit natural building blocks to create protein mimetics that perform natural and non-natural functions.[14,15] Considering the limited range of properties available to natural protein materials, hybrid materials are a promising route to combine desirable properties of both natural and synthetic materials.[16,17]

Peptide-dendron conjugates[18-40] are hybrid materials in which synthetic chemistry provides complete control over macromolecular structure and chain folding can be regulated through self-assembly. A variety of morphologies have been observed from peptide-dendron hybrids that self-assemble due to backbone-backbone hydrogen bonding interactions.[18,19,38-40] It is possible to interconvert between some of these morphologies in response to external stimuli,[19,38,39] and to program their polymerization and depolymerization.[24] Functional supramolecular materials such as organogels,[21,22] porous channel protein mimetics,[25-33] and switchable channels[23] illustrate the advantages of hybrid materials to address long-standing challenges in supramolecular materials. These abiotic materials can perform biological functions in biologically relevant environments,[25,34,35] and have inspired curiosity about the origins of homochirality in nature.[33,41-46]

We recently described a helix bundle-forming peptide-dendron hybrid (**4-1a**, Scheme 4.1).[47] Helix bundle motifs in proteins support diverse functions such a catalysis in water-soluble enzymes[15] and ion/small-molecule transport among transmembrane proteins[48] due, in part, to the well defined arrangement of amino acid side chains in the core of the bundle. Our long-term goal is to encapsulate helix bundles in a dendritic sheath that will allow us to deploy functional helix bundle nanostructures in non-biological environments. Here we provide a detailed account of our efforts to design, synthesize, and characterize helix bundle-forming peptide-dendron hybrids **4-1a**,**b** and **4-2** (Scheme 4.1).

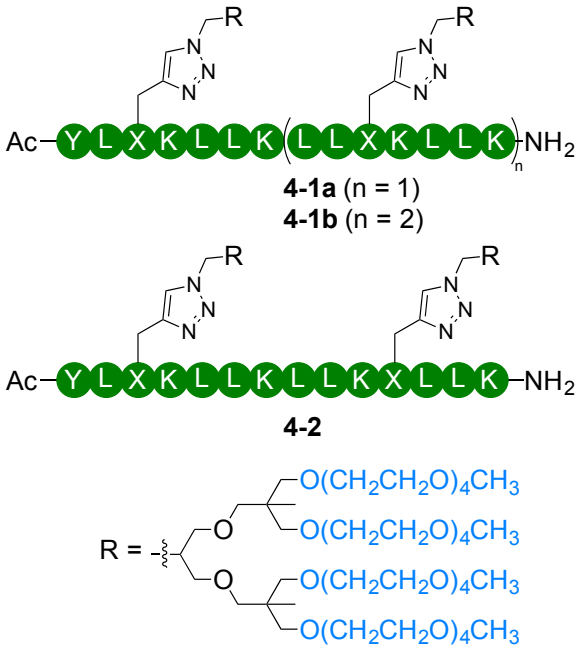

Scheme 4.1. Structures of α-helical bundle-forming peptide-dendron hybrids **4-1** and **4-2**. Adapted from ref. 47 with permission from the Royal Society of Chemistry.

4.2 Results and Discussion

4.2.1 Design Rationale

Bundle-forming α-helical peptide-dendron hybrids were designed by site-specifically introducing water-soluble dendrons at solvent-exposed, surface residues of the helix bundle assembly. A design principle that is common to all water-soluble helix bundle-forming peptides is that polar and non-polar

amino acid residues are clustered on opposite sides of the α-helix so that an amphipathic structure is produced upon folding of the peptide.[49,50] Sequestration of the hydrophobic residues at the core of the bundle provides the driving force for assembly of the α-helical peptides. Further design considerations such as the choice of residues that form the core of the bundle, the types of interactions at the interface between helices, and placement of molecular recognition motifs within the core of the bundle improve the specificity of the design.[49,50] Nonetheless, patterning of polar and non-polar residues in the amino acid sequence to match the periodicity of the α-helical fold in a bundle (Scheme 4.2) can be sufficient to design a bundle-forming peptide.[51,52] Residues on the exterior of the bundle minimally contribute to the folding and assembly of helix bundle-forming peptides, which makes these residues convenient sites to which prosthetic groups can be conjugated. Indeed, polymers,[53-58] catalysts,[59] and other groups[60,61] have been appended to exterior positions of helical bundles.

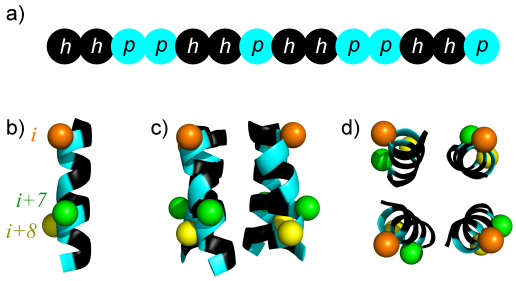

Scheme 4.2. (a) Pattern of hydrophobic (h, black color) and polar (p, cyan color) amino acids employed in the design of α-helical bundle-forming peptide-dendron hybrids **4-1a** and **4-2**. (b) Amphipathic α-helical structure that results from folding of the linear amino acid sequence from (a). Positions *i* (orange), *i* + *7* (green), and *i* + *8* (yellow) designate the positions to which dendrons have been attached. (c) Side and (d) top views of a parallel four-helix bundle assembled from the designed peptides.

Leucine and lysine were chosen as the hydrophobic (h) and polar (p) amino acids, respectively. Several leucine-lysine (a.k.a., "LK") peptides that form α-helical bundles have been designed by following the pattern $(hpphhph)_2$.[51,52,62-65] Notably, the groups of DeGrado and Lear[51] and Shaw[52] have

independently shown that "LK" peptides as short as fourteen residues form α-helical bundles made up of only four or five helices. Our designed peptide[66] follows a similar pattern $(hhpphhp)_2$ with the polar residues more central to the heptad (Scheme 4.2a). The *N*-terminus was acetylated and the *C*-terminus was amidated to maximize α-helix propensity of the peptide by replacing ionizable groups with hydrogen bonding groups.[67,68] The *N*-terminal hydrophobic residue was assigned as tyrosine rather than leucine in order to have a spectroscopic probe with which we could determine the concentration of the peptide-dendron hybrid in solution.[69] Two of the polar residues were selected as sites for conjugating hydrophilic dendrons to the peptide.

A single hydrophilic dendron was positioned in each heptad of the bundle-forming peptide-dendron hybrid. A seven-residue repeat encodes the helix bundle motif, and three of these residues are polar, surface residues in our designed α-helical bundle. We chose residue-3 in the first heptad of the amino acid sequence as the position for the first dendron. Positioning the dendrons at surface residues following an *i*, *i* + 7 periodicity matches the natural periodicity of the α-helix. Residues at positions *i* and *i* + 7 are in register with each other when viewed along the long axis of the α-helix (Scheme 4.2d), so we placed the second dendron at residue-10 in peptide-dendron hybrid **4-1a**. This arrangement was anticipated to minimize contact between the dendrons on one helix with the other α-helical peptide-dendron hybrids in the bundle. On the other hand, having the dendrons in register along the α-helix increases the likelihood for intramolecular interactions between the dendrons that could destabilize the α-helical folded state of the hybrid. We, therefore, designed a second peptide-dendron hybrid **4-2** wherein the dendrons are spaced *i*, *i* + 8 (Scheme 4.2d).

Water-soluble poly(alkyl ether) dendrons were chosen to conjugate to the helix bundle because these dendrons would facilitate circular dichroism (CD) spectroscopy experiments to characterize the folding and self-assembly of the peptide-dendron hybrids. Chromophores in a chiral environment

differentially absorb left- and right-handed circularly polarized light. The chromophores of interest in peptides are the backbone amide groups, which can be obscured by other amide or aromatic chromophores in the molecule.[70] While several groups have circumvented this complication through combinations of spectroscopies,[18-33] we preferred to identify dendrons that would not interfere with our interpretation of the CD spectra. Furthermore, it was important that the water-soluble dendrons be achiral so that the dendrons do not contribute to the asymmetric environment of the amide chromophores. The dendrons in hybrids **4-1a** and **4-2** are composed of symmetrically branched alkyl ether units that do not absorb UV light in the same region as the amides.

The dendrons are linked to the peptide through 1,4-triazole groups that are introduced in copper-catalyzed azide-alkyne cycloaddition (CuAAC) reactions. While the diversity of amino acids in peptide-dendron hybrids **4-1** and **4-2** is intentionally limited, we sought a synthesis strategy that would be compatible with a wide range of amino acids. The CuAAC reaction is bioorthogonal,[71] and introduces a relatively small side-chain functionality. Because the CuAAC reaction can be performed in mixed aqueous/organic solvent and is compatible with the functional groups of most natural amino acids, the 1,4-triazole linkages make it feasible to attach the dendrons to the peptides in a graft-to manner. That is to say that the dendrons and peptide can be synthesized and purified to homogeneity using standard techniques before attempting the synthesis of the hybrids. This represents a highly convergent synthesis strategy and ensures that the products of the CuAAC reaction are free of any structurally defective impurities.

4.2.2 Synthesis of the Alkyne-Containing Peptides

Alkyne-containing peptides **4-3a** and **4-4** were prepared following manual[66] or automated[47] solid-phase peptide synthesis protocols. Commercially available Fmoc-Pra-OH (Pra = propargylglycine) was coupled to the peptide at positions in the amino acid sequence where the hydrophilic dendrons were

to be conjugated. The assembled peptides were cleaved from the resin and purified to homogeneity by HPLC. The suitability of **4-3** and **4-4** to preparation and purification by standard peptide chemistry protocols illustrates the versatility of peptides as sequence defined macromolecular building blocks.

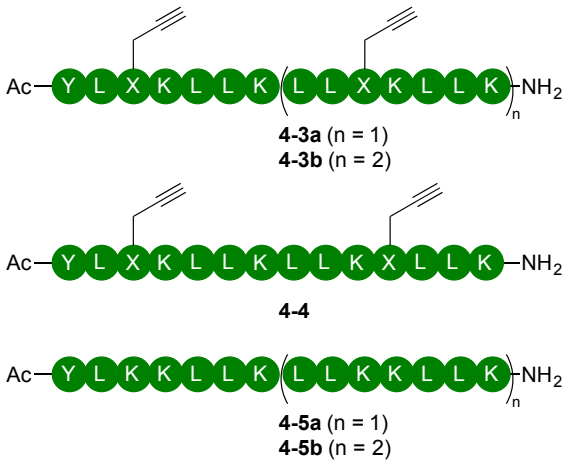

Scheme 4.3. Amino acid sequences of peptides **4-4**, **4-5**, and **4-6.** Amino acids are identified by single-letter codes: Y = tyrosine; L = leucine; K = lysine; X = propargylglycine.

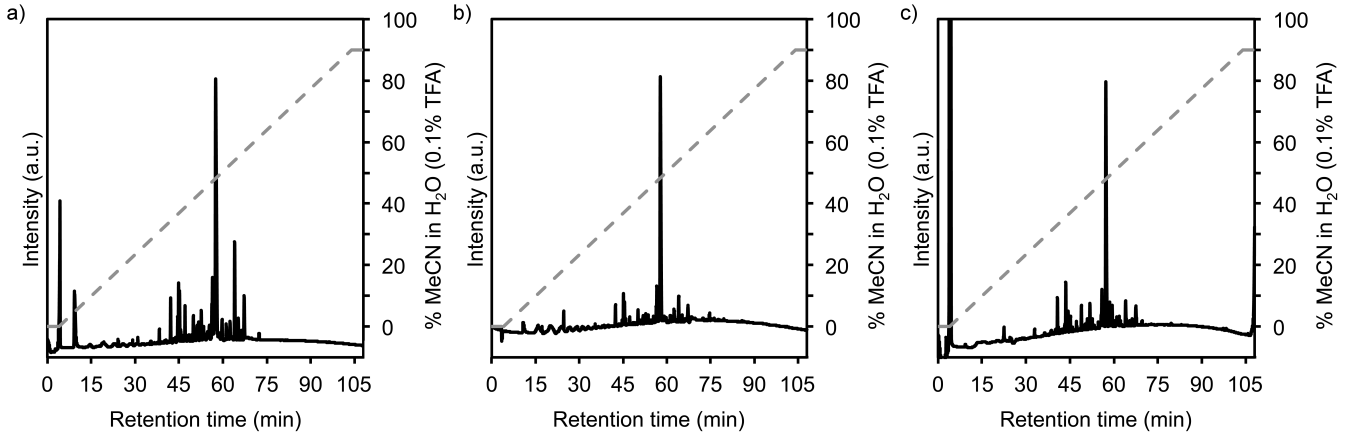

Figure 4.1. Chromatograms of the crude reaction product **4-5a** (solid line) obtained from syntheses on (a) high-loading PS resin, (b) low-loading PS resin, and (c) PEG resin. The dashed line indicates the solvent composition during elution of the peptide at 1 mL/min from a C18 column (solvent A = H_2O + 0.1% TFA; solvent B = MeCN/H_2O (9:1 v/v) + 0.1% TFA).

An optimized protocol for the manual synthesis of peptide **4-5a** was developed. Peptide **4-5a** is a control peptide in which all of the surface residues are lysines. Manual solid-phase peptide synthesis allows us to monitor the deprotection of each amino acid coupled to the resin, which indirectly reports on the efficiency of each coupling reaction. We judged the overall success of the synthesis from analytical HPLC traces of the crude products. Figure 4.1 shows representative HPLC data for syntheses on three different solid-phase resins: a high-loading polystyrene (PS) resin (0.71 mmol/g), a low-loading PS resin (0.38 mmol/g), and a polyethylene glycol (PEG) resin (0.51 mmol/g). Low purity of crude peptides can be attributed, in part, to collapse of the growing peptide chain due to hydrophobic effects and/or hydrogen bonding between growing chains during peptide assembly. Hydrophobic resins like PS can exacerbate aggregation of growing peptides. Reducing the loading of the resin and the effective concentration of growing chains has been reported to increase the crude purity of peptides.[72-74] The polar PEG resin has gained attention for yielding very clean crude peptides compared to high-loading PS resins.[74,75] Because the PEG resin swells much more than PS resin in the reaction solvent (i.e., DMF), we included the low-loading PS resin to assess the extent to which the effective concentration of growing peptide chains effects the purity of the crude peptide products. The data in Figure 4.1 show that the crude product from the high-loading PS resin is significantly less pure than the crude products from the low-loading PS and PEG resins. The effective concentration of growing chains on the resin appears to be the major determinant of the purity of crude peptide **4-5a**, and similar results were later obtained for peptide **4-4**. Because more peptide is obtained per mass of resin from the PEG resin than the low-loading PS resin, we prefer the PEG resin rather than the low-loading PS resin.

Manual synthesis of peptide **4-4** presented challenges that were not encountered in the synthesis of **4-5a**. When we synthesized **4-4** on high-loading PS resin, we found that several amino acids required multiple iterations of the deprotection protocol to completely remove the *N*-terminal protecting group

and observed a steep decline of the coupling efficiencies for residues 1-7 of the amino acid sequence. These symptoms are associated with so-called "difficult sequences,"[76-78] and can be attributed to the added hydrophobicity of the amino acid sequence when lysine residues are replace with propargylglycine residues. One defect structure was especially troubling. Poor coupling of Leu5 resulted in a truncated peptide that co-elutes with **4-4** from the HPLC column. The structure of the co-eluting peptide was identified from a tandem mass spectrometry experiment.[79] Changing the resin to the PEG resin alleviated most of the difficulties in the synthesis of **4-4**, however we continued to double couple Leu5 to avoid any contamination from the co-eluting impurity.

Adaptation of the manual solid-phase synthesis protocol to an automated system was straightforward, and worked equally well for peptides **4-3a** and **4-4**. A single coupling reaction was required to introduce each amino acid to the resin except for Leu5; a double coupling was used to introduce Leu5. The protocol was also extended to the synthesis of the 21-residue peptides **4-3b** and **4-5b**. Peptide **4-3b** required double couplings at Leu5 and Leu12, and peptide **4-5b** required double couplings at Leu6 and Leu13. The key differences between the manual[66] and automated syntheses[47] have to do with the coupling reaction conditions. In the manual synthesis the N^{α}-Fmoc-protected amino acids are activated with HBTU/HOBt and diisopropylethylamine as the base ($[HBTU]_0/[HOBt]_0/[DIEA]_0/[Fmoc\text{-}AA\text{-}OH]_0$ = 0.9/1/2/1; $[Fmoc\text{-}AA\text{-}OH]_0$ = 0.5 M). The automated synthesis employs HBTU with *N*-methylmorpholine as the base ($[HBTU]_0/[HOBt]_0/[NMM]_0/[Fmoc\text{-}AA\text{-}OH]_0$ = 0.9/0/0.8/1; $[Fmoc\text{-}AA\text{-}OH]_0$ = 0.2 M). The coupling reaction times were shorter for the automated synthesis than the manual synthesis (20 min vs. 40 min). Capping with Ac_2O was performed after each amino acid was coupled to the resin to prevent chain extension of any defective peptides. The conditions for removing the *N*-terminal protecting group and for cleaving the peptide from the resin with simultaneous side-chain deprotection were identical for the manual and automated syntheses. After

purification by reversed-phase HPLC, the identity and purity of the peptides were confirmed by MALDI-TOF mass spectrometry and analytical HPLC, respectively.

4.2.3 Synthesis of the Dendritic Azide

A water-soluble, second-generation dendron **4-11** was prepared by surface functionalization[80,81] of poly(alkyl ether) dendron **4-10** (Scheme 4.4). As demonstrated by Fréchet and co-workers,[80,81] the surface functionalization strategy combines the precision of convergent dendron syntheses with the structural diversity of end groups that is usually reserved for dendrimers prepared in the divergent manner. A single intermediate dendron can be transformed into materials with diverse physical properties.[80,81]

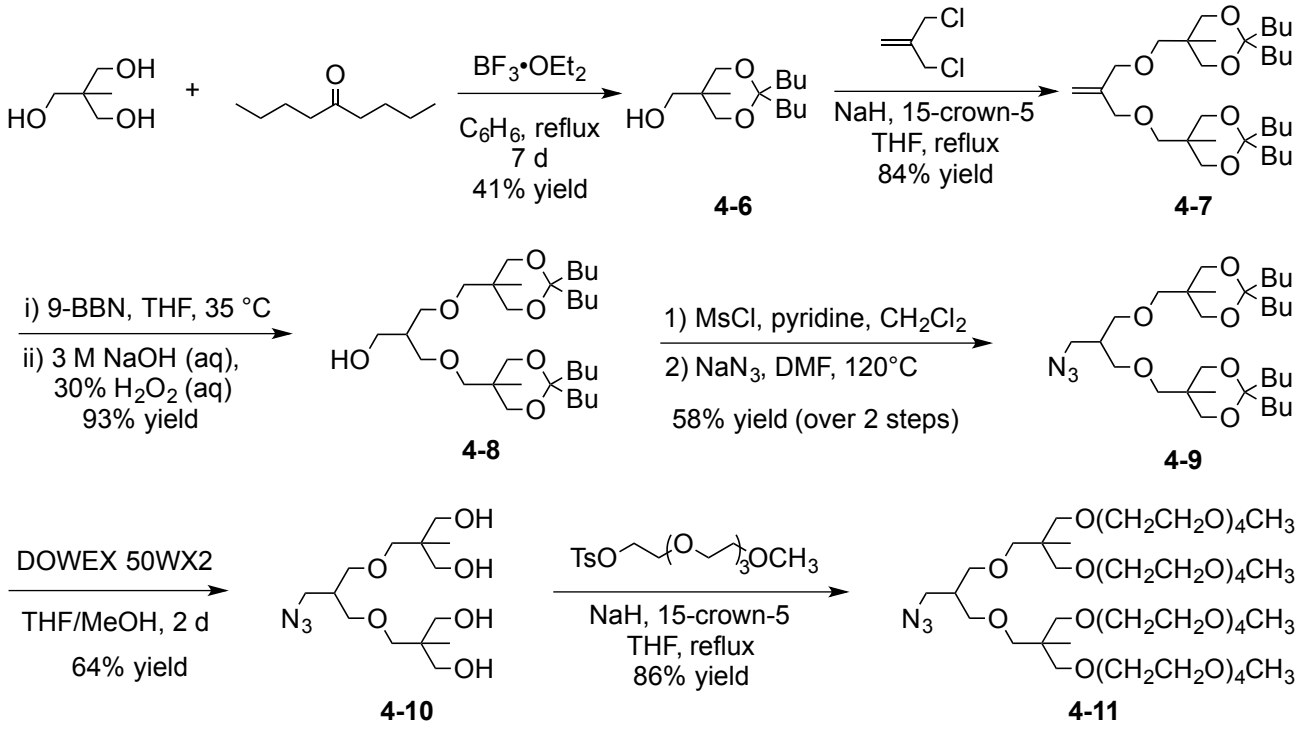

Scheme 4.4 Synthesis of the dendritic azide **4-11**.

The second-generation poly(alkyl ether) dendron **4-8** was prepared in the convergent manner developed by Fréchet and co-workers.[80-82] Acid-catalyzed condensation of tris(hydroxymethyl)ethane with 5-nonanone in refluxing benzene provided the ketal-protected, first-generation dendron **4-6**.

Dietherification of methallyl dichloride with **4-6** under Williamson conditions afforded the second-generation alkene **4-7**. We have previously noted that 15-crown-5 improves the efficiency of the generational growth step in the synthesis of poly(alkyl ether) dendrons,[83,84] and this modification was employed in the synthesis of **4-7**. Dendritic alcohol **4-8** was obtained from hydroboration-oxidation of **4-7**. As mentioned by Grayson and Fréchet,[81] the solubility and polarity of the ketal-protected dendrons **4-6**, **4-7**, and **4-8** facilitate the synthesis and purification of these dendrons on a multigram (>10-g) scale.

Dendron **4-10** with orthogonally reactive apex and peripheral groups was prepared in three steps from alcohol **4-8**. Treatment of **4-8** with mesyl chloride and pyridine in CH_2Cl_2 affords a mesylate intermediate that was isolated and used without further purification. Nucleophilic substitution of the mesylate with sodium azide introduced the desired azide group at the apex of the dendron for CuAAC reactions. A solid-supported acid catalyst was employed to effect hydrolysis of the ketal groups[80,81] in **4-9**, and which made it possible to isolate **4-10** by filtration to remove the resin and evaporation of the solvent.

Exhaustive surface functionalization of the peripheral hydroxyl groups of poly(alkyl ether) dendrons such as **4-10** can be achieved with a range of electrophiles. Fréchet and co-workers have shown that acyl chlorides, *O*-acylisoureas, allylic and benzylic halides, and alkyl tosylates are all sufficiently good electrophiles to effect quantitative reaction with each of 16 surface hydroxyl groups on a fourth-generation dendron with alkene apex functionality.[80,81] Etherification of **4-10** with the tosylate of tetraethylene glycol monomethyl ether was quantitative, which highlights the orthogonality of the azide and hydroxyl groups. Dendritic azide **4-11** was obtained in 86% yield after chromatographic purification.

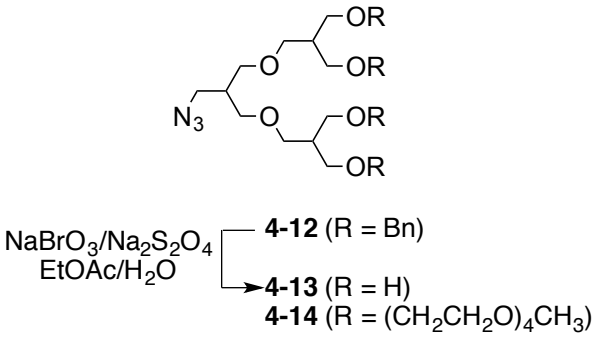

Scheme 4.5. Alternative hydrophilic dendrons.[††]

The surface functionalization approach proved especially valuable in the synthesis of a water-soluble dendritic azide for conjugation to peptides. Dendron **4-10** efficiently undergoes CuAAC reactions with dipeptides and peptide **4-4** to yield peptide-dendron hybrids that were soluble in aqueous/organic solvent mixtures but not in aqueous buffer. Surface functionalization of dendron **4-10** with tetraethylene glycol units was required to obtain a peptide-dendron hybrid that is soluble in aqueous buffer. We also investigated syntheses of **4-13** and **4-14** (Scheme 4.5).[††] Chemoselective debenzylation of **4-12**[83] under oxidative conditions[85,86] yielded **4-13** but the product was difficult to isolate from the reaction mixture. An attempt to synthesize **4-14** in a fully convergent manner similar to that described by Cho and co-workers[87] was abandoned because tedious chromatographic purifications were needed to obtain dendrons of acceptable purity. Dendron **4-11**, on the other hand, was readily prepared in good overall yield.

4.2.4 Grafting Dendrons to Peptides

A graft-to strategy for synthesizing the α-helical bundle-forming peptide-dendron hybrids should minimize the number of impurities that need to be removed during purification. Conjugating the dendrons to a deprotected peptide avoids having to perform additional chemical reactions and purification operations on the hybrid materials. The hydrophilicity of the dendrons made it convenient to

[††] Experiments performed by Shuang Song, Yue Wu, and Jonathan G. Rudick.

purify the peptide-dendron hybrids by reversed-phase HPLC. Defect-free hybrids, such as those obtained through this strategy, enable a detailed understanding of the structure-property relationships in architecturally complex macromolecules

Ligand-free copper-catalyzed azide-alkyne cycloaddition (CuAAC) of dendron **4-11** with peptides **4-3** and **4-4** yielded peptide-dendron hybrids **4-1** and **4-2**, respectively (Scheme 4.6). Ligands are usually employed for bioconjugation by CuAAC to compensate for slow reaction kinetics at low substrate concentrations,[71,88,89] to stabilize the catalytically active Cu(I)-species against oxidation,[89-92] and to suppress side reactions with certain amino acids (e.g., histidine).[90,92] High concentrations (>1 mM) of **4-3**, **4-4**, and **4-11** were achieved in DMSO/H_2O mixtures (1:1 v/v). Substoichiometric amounts of Cu(I) (0.2 eq. per alkyne) with the high concentrations of the substrates afforded fast reactions. Although the reaction mixtures were not degased, the reactions were performed under an N_2 atmosphere and sodium ascorbate (4 eq. per Cu) was used as an *in situ* reducing agent to prevent accumulation of Cu(I) before the reactions were complete. CuAAC Reactions with **4-3b** required deoxygenated solvents to achieve complete conversion. The reactions were monitored by MALDI-TOF mass spectrometry. We observed complete disappearance of the starting peptide and monodendritic peptide-dendron hybrid intermediate without any evidence for copper-mediated macrocyclization or oligomerization of the peptides.

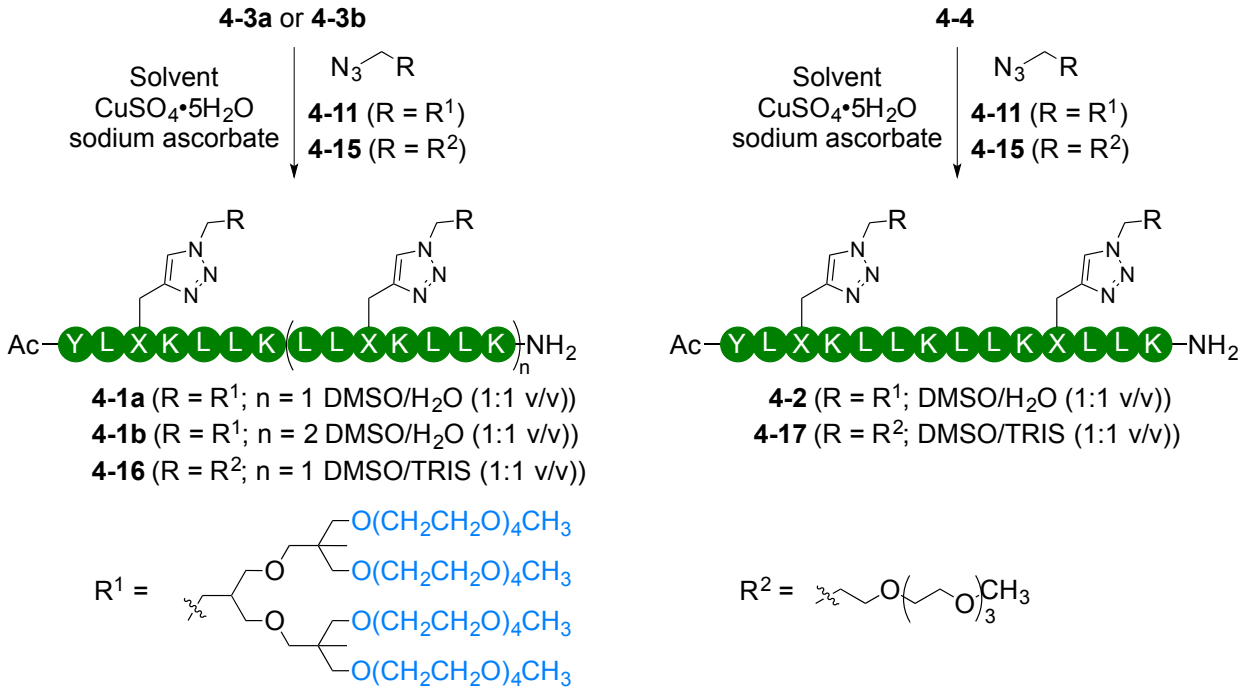

Scheme 4.6. Grafting to peptides via CuAAC.

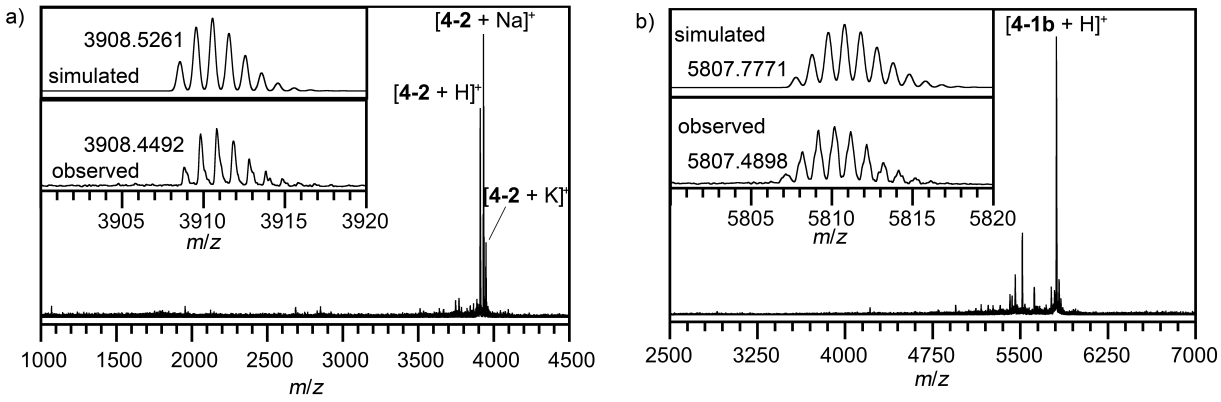

Figure 4.2. MALDI-TOF Mass spectra of (a) **4-2** and (b) **4-1b**.‡‡ The inset in each panel compares the simulated isotope pattern[93] (upper) with the observed isotope envelope (lower) for the $[M + H]^+$ ions (**4-2**: $C_{187}H_{352}N_{25}O_{60}$; **4-1b**: $C_{278}H_{525}N_{37}O_{89}$).

MALDI-TOF Mass spectrometry and analytical reversed-phase HPLC experiments confirmed the identity and purity of the peptide-dendron hybrids. The MALDI-TOF mass spectra‡‡ shown in Figure

‡‡ The MALDI-TOF mass spectra of **4-2** and **4-1b** were acquired by Dr. Robert Rieger (Stony Brook University Proteomics Center)

4.2 support that we have successfully isolated peptide-dendron hybrids **4-2** and **4-1b** from any residual dendron, starting peptide, or partially dendronized intermediates. We observe three different ionized forms of **4-2** ($[M + X]^+$, X = H, Na, and K). We see excellent agreement between the observed isotope pattern for the peak assigned as the $[M + H]^+$ ion to the expected isotope pattern for the same ion (Figure 4-2 insets). The attributes of the MALDI-TOF mass spectrum emphasize that we have synthesized the desired peptide-dendron hybrid as a monodisperse macromolecule with a completely defined chemical structure. Similar results for peptide-dendron hybrid **4-1a** were reported previously.[47]

Azides **4-11** and **4-15** revealed a stark dependence on solvent in their CuAAC reactions. When the reaction of peptide **4-4** with linear azide **4-15** was attempted in DMSO/H_2O (1:1 v/v), we obtained a mixture of starting peptide, monotriazole intermediates, and ditriazole product. We speculated that trifluoroacetic acid bound to peptide **4-4** might interfere with the CuAAC reaction as some ligand-assisted CuAAC reactions are sensitive to pH.[94] Typical conditions for preparing bioconjugates via the CuAAC reaction employ buffered aqueous solvent (or co-solvent) rather than H_2O.[71,88-92] Because concentrated solutions of peptide **4-5** (i.e., 0.5 M) are stable in TRIS buffer, we attempted CuAAC reactions in DMSO/TRIS (pH 8) (1:1 v/v). Linear azide **4-15** reacts cleanly with both peptides **4-3** and **4-4** in buffered solvent mixture whereas the dendritic azide **4-11** yields a mixture of starting peptide, monotriazole intermediates, and ditriazole product. We further note that the same batch of peptide **4-4** that reacted incompletely with **4-15** underwent a clean reaction with **4-11** in DMSO/H_2O (1:1 v/v). These results demonstrate that residual trifluoroacetic acid is not the source of observed slow reaction kinetics. While the different reactivity of azides **4-11** and **4-15** is hard to reconcile, these experiments highlight the benefit of CuAAC reactions being "wide in scope"[95] with respect to the range of solvent conditions under which the reaction exhibits high fidelity.

4.2.5 Folding and Self-Assembly

Circular dichroism (CD) spectra used to characterize the secondary structure of the peptides were found to depend on the peptide concentration and ionic strength of the solutions. The unfolded–folded and monomer–*n*-mer equilibria are coupled (Figure 4.3a) so we measure the extent to which bundles have formed on the basis of the intensity of the α-helix signature in the CD spectrum. CD Spectra of α-helical peptides are characterized by minima at 208 and 222 nm. We used the mean residue ellipticity at 222 nm ($[\theta]_{222}$) to monitor the formation of α-helical bundles of peptide-dendron hybrids **4-1a** and **4-2** as well as peptide **4-5a** and conjugates **4-16** and **4-17**. From a series of titration experiments in which the peptide concentration or chloride concentration were varied, we identified conditions under which peptide **4-5a**, peptide-dendron hybrids **4-1a** and **4-2**, and conjugates **4-16** and **4-17** were maximally folded and assembled as α-helical bundles (Figure 4.3).

Plots of $[\theta]_{222}$ versus the concentration of peptide demonstrate that each compound cooperatively self-assembles into a bundle of α-helices. The CD spectra for monomeric α-helical structures would be independent of the concentration of compound. The observed dependences confirm that our designed, α-helical "LK" peptide (**4-5a**) creates an amphipathic structure upon folding. Furthermore, the dramatic change in $[\theta]_{222}$ at concentrations of **4-5a** below 50 μM is indicative of a cooperative folding process. Similar features are observed in the titrations of **4-1a**, **4-2**, **4-16**, and **4-17** (Figure 4.3b,c). Replacing polar surface residues with hydrophilic dendrons (**4-1a** and **4-2**) or linear tetraethylene glycol moieties (**4-16** and **4-17**) does not interfere with the folding and self-assembly program encoded in the primary structure (i.e., amino acid sequence) of the peptide.

The high density of cationic residues makes α-helical "LK" peptides sensitive to chloride ion concentration.[51] Increasing ionic strength shields the cationic charges. Because the cationic residues are clustered together on one face of the amphipathic α-helix formed by these peptides, increasing ionic

strength stabilizes the helix bundle assembly. Peptide **4-5a** exhibits the strongest dependence on chloride ion concentration among the compounds in Figure 4.3d,e. Peptides **4-3a** and **4-4** have two fewer lysine residues on the surface compared to **4-5a**. Because we conjugated non-ionic, hydrophilic groups to these surface positions, the overall number of charged sites on **4-1a**, **4-2**, **4-16**, and **4-17** are fewer than the number of cationic charges on **4-5a**. We reason that the larger number of cationic surface groups makes **4-5a** more sensitive to chloride concentration than the other compounds.

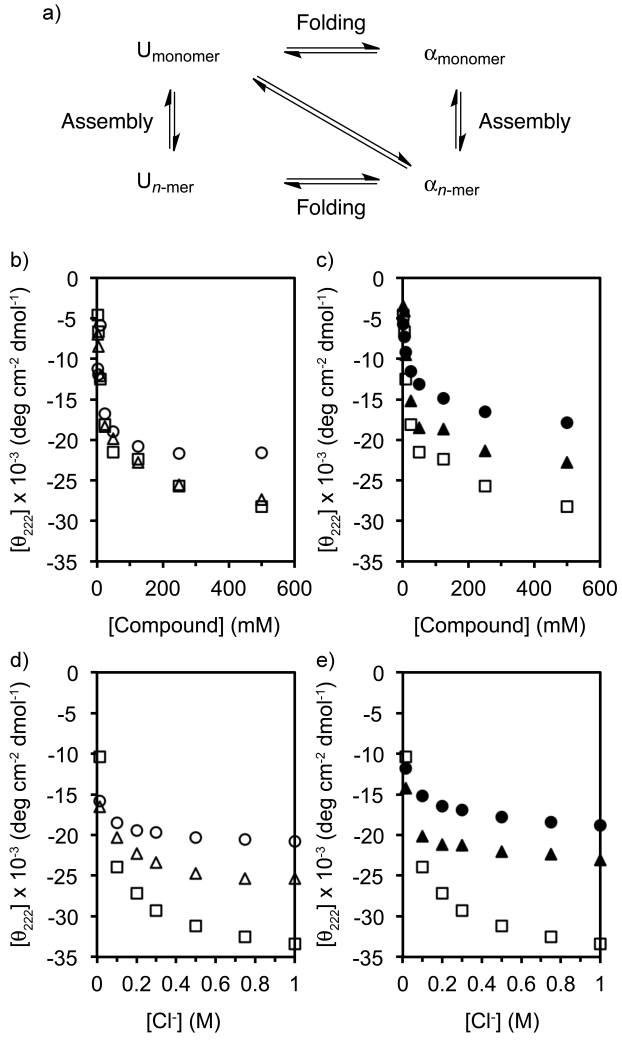

Figure 4.3. (a) Schematic showing that folding and self-assembly are coupled equilibria. (b and c) Plots of $[\theta]_{222}$ versus the concentration of **4-1a** (○),**4-16** (△),**4-5a** (□),**4-2** (●), and **4-17** (▲). (d and e) Plots of $[\theta]_{222}$ versus chloride concentration for **4-1a** (○),**4-16** (△),**4-5a** (□),**4-2** (●), and **4-17** (▲).

4.2.6 Spacing of Dendrons Along the α-Helix

Comparison of the CD spectra of peptide-dendron hybrids **4-1a** and **4-2** with that of peptide **4-5a** reveals that the hybrids are significantly less α-helical. The CD spectra in Figure 4.4 were recorded under conditions where each of the compounds is maximally folded, so the intensity of each spectrum directly reports on the effect of the changes to the surface residues. We calculated from $[\theta]_{222}$ values in each spectrum that hybrid **4-1a** is 76% as α-helical as **4-5a**[47] and hybrid **4-2** is 63% as helical as **4-5a**. A significant contribution to the decreased helicity comes from steric interactions between the dendrons, especially between the peripheral groups.

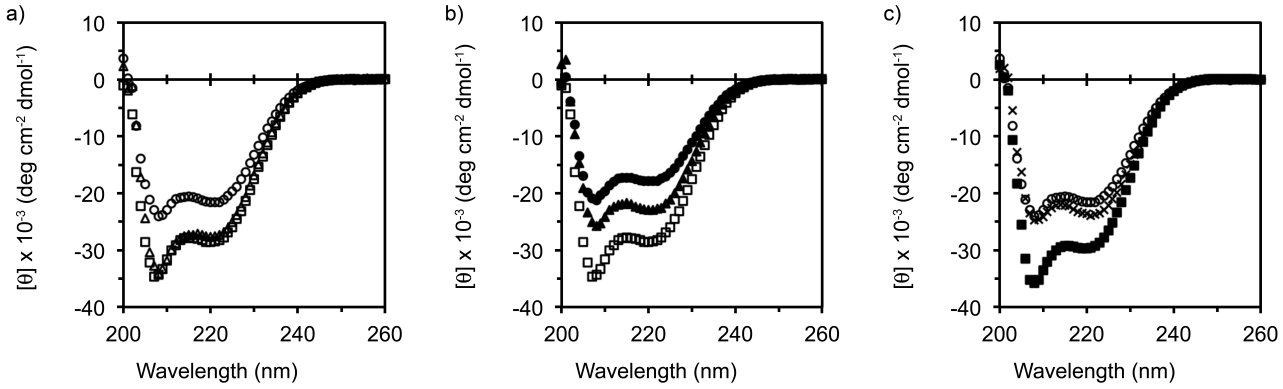

Figure 4.4. Circular dichroism (CD) spectra from 500 μM solutions of (a) **4-1a** (○),**4-16** (△), and **4-5a** (□), (b) **4-2** (●),**4-17** (▲), and **4-5a** (□), and (c) **4-1a** (○),**4-1b** (×), and **4-5b** (■). Spectra were recorded in 20 mM TRIS buffer (pH 7.3) with 285 mM KCl (total $[Cl^-]$ = 300 mM) at 25 ºC.

The CD spectra of **4-1a** and **4-16** clearly show that the size of the dendron destabilizes the α-helical bundle (Figure 4.4a). In conjugate **4-16** a linear tetraethylene glycol chain replaces the dendron in **4-1a**. Conjugate **4-16** is as well folded as peptide **4-5a** which shows that the 1,4-triazolyl linkage introduced by the CuAAC reaction does not dramatically decrease the helicity of the conjugate. The decreased intensity of the CD spectrum of **4-1a** compared to peptide **4-5a** and conjugate **4-16** is directly attributable to the structure of the dendron. Considering the large distance between the dendrons on each helix, we attribute the decreased helicity to the water-solubilizing peripheral groups on the dendron.

Each of the hybrids (**4-1a** and **4-2**) and conjugates (**4-16** and **4-17**) self-assemble into α-helical bundles, and those observations suggest that the self-assembled α-helical bundle is a resilient framework for building larger hybrid macromolecular assemblies. Comparing the CD spectra of **4-5a**, **4-16**, and **4-17** reveals that there are sequence-dependent factors that determine how well folded is each conjugate. Conjugates **4-16** and **4-17** have relatively small tetraethylene glycol groups conjugated at surface positions on the bundle that are spaced *i,i* + 7 and *i,i* + 8, respectively. Such a small change in sequence reduces the observed helicity by 17%. Compounding the observed sequence-dependent effect with the steric effect from large dendrons conjugated to the surface positions of the α-helical bundle would be expected to greatly reduce the helicity of **4-2** compared to **4-1a**. Indeed, hybrid **4-2** is less helical than **4-1a**.

4.2.7 Length of the Peptide

Increasing the length of the peptide has been shown to stabilize self-assembled α-helical bundles.[96] The *i*, *i* + 7 spacing in **4-1** places the dendrons in register with each other along the length of the α-helix, and *i*, *i* + 7 periodicity can be propagated over longer peptides without interfering with the bundling of the α-helices. Increasing the length of the peptides from 14 residues (**4-1a**) to 21 residues (**4-1b**) did not improve α-helical structure on the basis of CD spectra (Figure 4.4c). It is important to note that the CD spectra from peptides **4-5a** and **4-5b** were essentially identical under these conditions.

4.3 Conclusion

α-Helical bundles are a privileged motif in natural proteins that provide a defined three-dimensional arrangement of side-chain functional groups necessary to achieve highly efficient and selective functionality. Transplanting α-helical bundle motifs into hybrid macromolecules offers a pathway for transplanting protein-like structure and function into non-biological environments. Dendronized α-helical bundles encapsulate the protein-like structure in a dendritic sheath that insulates

the delicate structure of the folded, protein-like core. The peripheral groups of the dendrons can be varied in a modular fashion to tailor the compatibility of the dendronized helix bundle to different environments. We have described a convergent bioorthogonal strategy for conjugating dendrons site-specifically to peptides. Grafting dendrons at a density of one dendron per heptad along the hydrophilic face of an amphipathic α-helical peptide yields α-helical bundle-forming peptide-dendron hybrids. These new peptide-dendron hybrids are of fundamental interest to investigate the role of polymer architecture on folding of peptide-polymer conjugates, and may exhibit advantages over polydisperse polymer-peptide conjugates in applications such as drug delivery.[97] With a folded, protein-like core, the dendronized α-helical bundles described herein set a precedent for integrating other protein functions (e.g., catalysis) into supramolecular dendrimers.

4.4 Experimental Procedures

4.4.1 Materials

Trifluoroacetic acid (TFA) was used as received from Aldrich. Anhydrous *N*,*N*-dimethylformamide (DMF), sodium azide, and Fmoc-Tyr(*t*-Bu)-OH were used as received from EMD. Fmoc-Lys(Boc)-OH, Fmoc-Leu-OH, Fmoc-Pra-OH, *N*-methylmorpholine (NMM), and *O*-(benzotriazol-1-yl)-*N*,*N*,*N*',*N*'-tetramethyluroniumhexafluorophosphate (HBTU) were used as received from Chem-Impex International. Acetonitrile (MeCN) was used as received from Fisher. Triisopropylsilane and copper(II) sulfate pentahydrate were used as received from Acros. L-Ascorbic acid sodium salt and acetic anhydride (Ac_2O) were used as received from Alfa-Aesar. Methanol (MeOH) and dimethylsulfoxide (DMSO) were used as received from BDH. H-Rink amide-ChemMatrix resin (0.51 mmol/g) was used as received from PCAS BioMatrix Inc. Isopropyl alcohol was used as received from Pharmaco-Aaper. Potassium chloride was used as received from G-Biosciences. Tris(hydroxymethyl)aminomethane hydrochloride (TRIS•HCl) and 2-amino-2-(hydroxymethyl)-1,3-

propanediol were used as received from Amresco. Compounds **4-6**, **4-7**, **4-8**, **4-9**, **4-10**, **4-11**, peptide-dendron hybrid **4-1a**, peptide **4-3a** and Ac-YLKKLLKLLKKLLK-NH_2 (**4-5a**) were prepared according to literature procedures.[66,81] Peptides were assembled by manual[66] or automated[47] solid-phase peptide synthesis according to general protocols. Peptide concentration and salt titration CD experiments were done according to previously described general protocols.[47]

4.4.2 Techniques

Peptides were synthesized using 9-fluorenylmethoxycarbonyl (Fmoc) chemistry on a Protein Technologies PS3 peptide synthesizer. High-performance liquid chromatography (HPLC) was performed on a Waters 1525 Binary pump equipped with a Waters 2489 UV/Visible Detector set at 210 nm and 280 nm. To determine the analytical purity of samples, the HPLC was equipped with a SunFire^{TM} C18 column (5 μm, 4.6 mm × 250 mm; Waters) operating at a flow rate of 1 mL/min and a solvent gradient of 1%/min. Purification of samples was done on the HPLC equipped with a SunFire^{TM} C18 (5 μm, 19 mm × 250 mm) column operating at a flow rate of 17 mL/min and a solvent gradient of 5%/min. Samples for MALDI-TOF MS were prepared using α-cyano-4-hydroxycinnamic acid as the matrix. Equal volumes of solutions (10 mg/mL) of matrix and peptide in MeCN/H_2O (1:1 v/v) were mixed. The mixture of matrix and analyte (1 μL) was deposited on the target plate and allowed to dry before measurements were taken. Absorbance of peptide solutions in deionized water at 280 nm was recorded on an Evolution 201 spectrophotometer using a 1-cm quartz cuvette. The concentration of the peptide was calculated from the absorbance using Beer's Law and an extinction coefficient (ε) for tyrosine of 1490 L mol^{-1} cm^{-1}.[69] Circular dichroism (CD) spectra were recorded on an Applied Photophysics Chirascan instrument.

4.4.3 Synthesis

Assembly of Ac-YLPraKLLKLLPraKLLKLLPraKLLK-NH_2 (4-3b). Peptide **4-3b** was assembled on ChemMatrix Rink amide resin (0.2096 g, 0.1069 mmol) in a glass-fritted peptide reaction vessel using a PS3 synthesizer and cleaved from the resin to yield peptide **4-3b**. The sequence of operations is detailed in Table 4-1.

Table 4-1. Protocol for synthesis of Ac-YLXKLLKLLXKLLKLLXKLLK-NH_2

X= propargyl glycine (**4-3b**).

		Mass of Reagents (g)	
Cycle		Fmoc-AA-OH	HBTU
1	Single Coupling: Fmoc-Lys(Boc)-OH	0.4703	0.3581
	Capping		
	N^{α}-Fmoc Deprotection		
2	Single Coupling: Fmoc-Leu-OH	0.3575	0.3592
	Capping		
	N^{α}-Fmoc Deprotection		
3	Single Coupling: Fmoc-Leu-OH	0.3529	0.3560
	Capping		
	N^{α}-Fmoc Deprotection		
4	Single Coupling: Fmoc-Lys(Boc)-OH	0.4959	0.3573
	Capping		
	N^{α}-Fmoc Deprotection		
5	Single Coupling: Fmoc-Pra-OH	0.3171	0.3596
	Capping		
	N^{α}-Fmoc Deprotection		
6	Singe Coupling: Fmoc-Leu-OH	0.3583	0.3583
	Capping		
	N^{α}-Fmoc Deprotection		
7	Single Coupling: Fmoc-Leu-OH	0.3631	0.3509
	Capping		
	N^{α}-Fmoc Deprotection		
8	Single Coupling: Fmoc-Lys(Boc)-OH	0.4713	0.3501
	Capping		
	N^{α}-Fmoc Deprotection		
9	Single Coupling: Fmoc-Leu-OH	0.3615	0.3550
	Capping		
	N^{α}-Fmoc Deprotection		
10	Double Coupling: Fmoc-Leu-OH	0.3596	0.3538
		0.3556	0.3583

	Capping		
	N^{α}-Fmoc Deprotection		
11	Single Coupling: Fmoc-Lys(Boc)-OH	0.4738	0.3542
	Capping		
	N^{α}-Fmoc Deprotection		
12	Single Coupling: Fmoc-Pra-OH	0.3191	0.3527
	Capping		
	N^{α}-Fmoc Deprotection		
13	Single Coupling: Fmoc-Leu-OH	0.3715	0.3527
	Capping		
	N^{α}-Fmoc Deprotection		
14	Single Coupling: Fmoc-Leu-OH	0.3614	0.3539
	Capping		
	N^{α}-Fmoc Deprotection		
15	Single Coupling: Fmoc-Lys(Boc)-OH	0.4784	0.3584
	Capping		
	N^{α}-Fmoc Deprotection		
16	Single Coupling: Fmoc-Leu-OH	0.3502	0.3512
	Capping		
	N^{α}-Fmoc Deprotection		
17	Double Coupling: Fmoc-Leu-OH	0.3552	0.3492
		0.3590	0.3584
	Capping		
	N^{α}-Fmoc Deprotection		
18	Single Coupling: Fmoc-Lys(Boc)-OH	0.4791	0.3538
	Capping		
	N^{α}-Fmoc Deprotection		
19	Single Coupling: Fmoc-Pra-OH	0.3354	0.3581
	Capping		
	N^{α}-Fmoc Deprotection		
20	Single Coupling: Fmoc-Leu-OH	0.3636	0.3600
	Capping		
	N^{α}-Fmoc Deprotection		
21	Single Coupling: Fmoc-Tyr(t-Bu)-OH	0.4524	0.3547
	N^{α}-Fmoc Deprotection		
	Acetylation of the *N*-terminus		
	Cleavage and Side-Chain Deprotection		

Assembly of Ac-YLPraKLLKLLKPraLLK-NH_2 (4-4). Peptide **4-4** was assembled using a PS3 automated synthesizer on ChemMatrix Rink amide resin (0.1937 g, 0.09879 mmol) in a glass-fritted

peptide reaction vessel and cleaved from the resin to yield peptide **4-4**. The sequence of operations is detailed in Table 4-2.

Table 4-2. Protocol for the synthesis of Ac-YLXKLLKLLKXLLK-NH_2 X = propargyl glycine(**4-4**).

		Mass of Reagents (g)	
Cycle		Fmoc-AA-OH	HBTU
1	Single Coupling: Fmoc-Lys(Boc)-OH	0.4654	0.3770
	Capping		
	N^{α}-Fmoc Deprotection		
2	Single Coupling: Fmoc-Leu-OH	0.3528	0.3779
	Capping		
	N^{α}-Fmoc Deprotection		
3	Single Coupling: Fmoc-Leu-OH	0.3528	0.3702
	Capping		
	N^{α}-Fmoc Deprotection		
4	Single Coupling: Fmoc-Pra-OH	0.3311	0.3726
	Capping		
	N^{α}-Fmoc Deprotection		
5	Single Coupling: Fmoc-Lys(Boc)-OH	0.4684	0.3754
	Capping		
	N^{α}-Fmoc Deprotection		
6	Singe Coupling: Fmoc-Leu-OH	0.3529	0.3715
	Capping		
	N^{α}-Fmoc Deprotection		
7	Single Coupling: Fmoc-Leu-OH	0.3454	0.3695
	Capping		
	N^{α}-Fmoc Deprotection		
8	Single Coupling: Fmoc-Lys(Boc)-OH	0.4595	0.3721
	Capping		
	N^{α}-Fmoc Deprotection		
9	Single Coupling: Fmoc-Leu-OH	0.3500	0.3743
	Capping		
	N^{α}-Fmoc Deprotection		
10	Double Coupling: Fmoc-Leu-OH	0.3520	0.3743
		0.3563	0.3757
	Capping		
	N^{α}-Fmoc Deprotection		
11	Single Coupling: Fmoc-Lys(Boc)-OH	0.4687	0.3722
	Capping		
	N^{α}-Fmoc Deprotection		
12	Single Coupling: Fmoc-Pra-OH	0.3296	0.3734
	Capping		
	N^{a}-Fmoc Deprotection		

13	Single Coupling: Fmoc-Leu-OH	0.3508	0.3773
	Capping		
	N^{α}-Fmoc Deprotection		
14	Single Coupling: Fmoc-Tyr(t-Bu)-OH	0.4587	0.3764
	N^{α}-Fmoc Deprotection		
	Acetylation of the *N*-terminus		
	Cleavage and Side-Chain Deprotection		

Assembly of Ac-YLPraKLLKLLKPraLLK-NH_2 (4-4). Peptide **4-4** was assembled manually on ChemMatrix Rink amide resin (0.2511 g, 0.1280 mmol) in a glass-fritted peptide reaction vessel and cleaved from the resin to yield peptide **4-4**. The sequence of operations is detailed in Table 4-3.

Table 4-3. Protocol for the synthesis of Ac-YLXKLLKLLKXLLK-NH_2 X = propargyl glycine(**4-4**).

		Mass of Reagents (g)		
Cycle		Fmoc-AA-OH	HBTU	HoBT
1	Single Coupling: Fmoc-Lys(Boc)-OH	0.5854	0.4571	0.1973
	Capping			
	N^{α}-Fmoc Deprotection			
2	Single Coupling: Fmoc-Leu-OH	0.4374	0.4573	0.1942
	Capping			
	N^{α}-Fmoc Deprotection			
3	Single Coupling: Fmoc-Leu-OH	0.4452	0.4658	0.1900
	Capping			
	N^{α}-Fmoc Deprotection			
4	Single Coupling: Fmoc-Pra-OH	0.4182	0.4548	0.1976
	Capping			
	N^{α}-Fmoc Deprotection			
5	Single Coupling: Fmoc-Lys(Boc)-OH	0.5880	0.4544	0.1915
	Capping			
	N^{α}-Fmoc Deprotection			
6	Singe Coupling: Fmoc-Leu-OH	0.4431	0.4605	0.1980
	Capping			
	N^{α}-Fmoc Deprotection			
7	Single Coupling: Fmoc-Leu-OH	0.4402	0.4601	0.1902
	Capping			
	N^{α}-Fmoc Deprotection			
8	Single Coupling: Fmoc-Lys(Boc)-OH	0.5834	0.4642	0.1931
	Capping			
	N^{α}-Fmoc Deprotection			
9	Single Coupling: Fmoc-Leu-OH	0.4451	0.4638	0.1892

	Capping			
	N^{α}-Fmoc Deprotection			
10	Double Coupling: Fmoc-Leu-OH	0.4412	0.4612	0.1914
		0.4402	0.4430	0.1942
	Capping			
	N^{α}-Fmoc Deprotection			
11	Single Coupling: Fmoc-Lys(Boc)-OH	0.5811	0.4639	0.1911
	Capping			
	N^{α}-Fmoc Deprotection			
12	Single Coupling: Fmoc-Pra-OH	0.4183	0.4607	0.1932
	Capping			
	N^{α}-Fmoc Deprotection			
13	Single Coupling: Fmoc-Leu-OH	0.4420	0.4608	0.1938
	Capping			
	N^{α}-Fmoc Deprotection			
14	Single Coupling: Fmoc-Tyr(t-Bu)-OH	0.5713	0.4660	0.1920
	N^{α}-Fmoc Deprotection			
	Acetylation of the *N*-terminus			
	Cleavage and Side-Chain Deprotection			

Assembly of Ac-YLKKLLKLLKKLLKLLKKLLK-NH_2 (4-5b). Peptide **4-5b** was assembled using a PS3 automated synthesizer on ChemMatrix Rink amide resin (0.2567 g, 0.1309 mmol) in a glass-fritted peptide reaction vessel and cleaved from the resin to yield peptide **4-5b**. The sequence of operations is detailed in Supporting Information (Table 4-4).

Table 4-4. Protocol for the synthesis of Ac-YLKKLLKLLKKLLKLLKKLLK-NH_2 (**4-5b**).

		Mass of Reagents (g)	
Cycle		Fmoc-AA-OH	HBTU
1	Single Coupling: Fmoc-Lys(Boc)-OH	0.4679	0.3644
	Capping		
	N^{α}-Fmoc Deprotection		
2	Single Coupling: Fmoc-Leu-OH	0.3644	0.3625
	Capping		
	N^{α}-Fmoc Deprotection		
3	Single Coupling: Fmoc-Leu-OH	0.3630	0.3633
	Capping		
	N^{α}-Fmoc Deprotection		
4	Single Coupling: Fmoc-Lys(Boc)-OH	0.4723	0.3701
	Capping		

	N^{α}-Fmoc Deprotection		
5	Single Coupling: Fmoc-Lys(Boc)-OH	0.4814	0.3637
	Capping		
	N^{α}-Fmoc Deprotection		
6	Singe Coupling: Fmoc-Leu-OH	0.3634	0.3625
	Capping		
	N^{α}-Fmoc Deprotection		
7	Single Coupling: Fmoc-Leu-OH	0.3767	0.3591
	Capping		
	N^{α}-Fmoc Deprotection		
8	Single Coupling: Fmoc-Lys(Boc)-OH	0.4646	0.3661
	Capping		
	N^{α}-Fmoc Deprotection		
9	Double Coupling: Fmoc-Leu-OH	0.3594	0.3678
		0.3593	0.3593
	Capping		
	N^{α}-Fmoc Deprotection		
10	Single Coupling: Fmoc-Leu-OH	0.3543	0.3691
	Capping		
	N^{α}-Fmoc Deprotection		
11	Single Coupling: Fmoc-Lys(Boc)-OH	0.4775	0.3554
	Capping		
	N^{α}-Fmoc Deprotection		
12	Single Coupling: Fmoc-Lys(Boc)-OH	0.4682	0.3585
	Capping		
	N^{α}-Fmoc Deprotection		
13	Single Coupling: Fmoc-Leu-OH	0.3572	0.3567
	Capping		
	N^{α}-Fmoc Deprotection		
14	Single Coupling: Fmoc-Leu-OH	0.3528	0.3581
	Capping		
	N^{α}-Fmoc Deprotection		
15	Single Coupling: Fmoc-Lys(Boc)-OH	0.4836	0.3582
	Capping		
	N^{α}-Fmoc Deprotection		
16	Double Coupling: Fmoc-Leu-OH	0.3612	0.3563
		0.3711	0.3513
	Capping		
	N^{α}-Fmoc Deprotection		
17	Single Coupling: Fmoc-Leu-OH	0.3580	0.3570
	Capping		
	N^{α}-Fmoc Deprotection		
18	Single Coupling: Fmoc-Lys(Boc)-OH	0.4872	0.3522
	Capping		
	N^{α}-Fmoc Deprotection		

19	Single Coupling: Fmoc-Lys(Boc)-OH	0.4859	0.3513
	Capping		
	N^{α}-Fmoc Deprotection		
20	Single Coupling: Fmoc-Leu-OH	0.3589	0.3543
	Capping		
	N^{α}-Fmoc Deprotection		
21	Single Coupling: Fmoc-Tyr(t-Bu)-OH	0.4628	0.3576
	N^{α}-Fmoc Deprotection		
	Acetylation of the *N*-terminus		
	Cleavage and Side-Chain Deprotection		

(2,2-Dibutyl-5-methyl-1,3-dioxan-5-yl)methanol (4-6). Compound **4-6** was prepared according to a previously reported procedure.[81] The reaction was performed in a 250-mL, one-neck flask equipped with a magnetic stir bar and Soxhlet extractor containing molecular sieves. To an ice-water bath-cooled suspension of 1,1,1-tris(hydroxymethyl)ethane (36.01 g, 0.2996 mol) in anhydrous C_6H_6 (300 mL) and 5-nonanone (51.0 mL, 0.3296 mol), $BF_3{\cdot}Et_2O$ (1.5 mL) was added slowly. The suspension was stirred for 30 min, and then heated at reflux for 7 d. The reaction was cooled to room temperature, the residual solids were removed by filtration, and the crude product was obtained by rotary evaporation of volatiles from the filtrate. The product was purified by flash column chromatography (SiO_2, hex/EtOAc 4:1 to 3:2) to give **4-6** as slightly yellow oil (29.94 g, 41%). TLC (SiO_2, 7:3 hex/EtOAc): $R_f = 0.37$. ^{1}H NMR (400 MHz, $CDCl_3$, δ, ppm): 3.70 (d, $J = 5.7$ Hz, 2H), 3.64 (d, $^2J = 11.7$ Hz, 1H), 3.62 (d, $^2J = 11.0$ Hz, 1H), 3.58 (d, $^2J = 11.7$ Hz, 1H), 1.76 (m, 2H), 1.60 (m, 3H), 1.33 (m, 8H), 0.92 (t, $J = 7.1$ Hz, 3H), 0.90 (t, $J = 7.0$ Hz, 3H), 0.82 (s, 3H). ^{13}C NMR (100 MHz, $CDCl_3$, δ, ppm): 100.9, 66.6, 66.0, 36.9, 34.8, 30.1, 26.0, 25.3, 23.3, 23.2, 17.9. ESI–MS (*m/z*): $[M + H]^+$ calcd for $C_{14}H_{28}O_3$, 245.2; found 245.1. GPC: $M_n = 190$, $M_w/M_n = 1.06$. The spectral data agree with literature.[81]

2,2-Bis[(2,2-dibutyl-5-methyl-1,3-dioxan-5-yl)methoxymethyl]ethene (4-7). Compound **4-7** was prepared according to a literature procedure.[81] A solution of **4-6** (10.01 g, 0.04096 mol) in anhydrous THF (9 mL) was added dropwise to an ice-water bath-cooled suspension of dry NaH (1.31 g, 54.6

mmol) in anhydrous THF (8 mL), methallyl dichloride (1.9 mL, 16 mmol) and 15-crown-5 (0.8 mL, 4 mmol). The reaction mixture was heated at reflux for 12 h under a N_2 atmosphere while stirring. The reaction mixture was quenched with deionized water. The product was extracted with EtOAc. The organic washings were combined, washed once with saturated NaCl (aq) solution and dried over anhydrous $MgSO_4$. The solids were removed by filtration. The volatiles were removed by rotary evaporation. The resulting product was purified by flash chromatography (SiO_2, hex to 7:3 hex/EtOAc) to yield **4-7** as a colorless liquid (7.51 g, 84%). TLC (SiO_2, 7:3 hex/EtOAc): R_f = 0.67. ^{1}H NMR (500 MHz, $CDCl_3$, δ, ppm): 5.13 (s, 2H), 3.97 (s, 4H), 3.66 (d, ^2J = 11.7 Hz, 4H), 3.50 (d, ^2J = 11.7 Hz, 4H), 3.39 (s, 4H), 1.72 (m, 2H), 1.60 (m, 2H), 1.32 (m, 16H), 0.90 (t, J = 6.9 Hz, 6H), 0.89 (t, J = 7.0 Hz, 6H), 0.85 (s, 6H). ^{13}C NMR (125 MHz, $CDCl_3$, δ): 143.2, 113.3, 100.7, 73.4, 72.3, 66.1, 36.0, 34.3, 31.1, 25.8, 25.3, 23.3, 23.2, 18.6, 14.3. ESI–MS (*m/z*): $[M + H]^+$ calcd for $C_{32}H_{61}O_6$, 541.4; found, 541.5. GPC: M_n = 480, M_w/M_n = 1.05. The spectral data agree with literature.[81]

2,2-Bis[(2,2-dibutyl-5-methyl-1,3-dioxan-5-yl)methoxymethyl]ethanol (4-8). Compound **4-8** was prepared according to a literature procedure.[81] To a solution of **4-7** (5.00 g, 9.25 mmol) in anhydrous THF (3 mL), a 0.5 M 9-BBN in THF solution (28 mL, 14 mmol) was added dropwise under a N_2 atmosphere. The reaction mixture was stirred under a N_2 atmosphere for 20 h. The reaction was cooled in an ice-water bath while 3 M NaOH (aq) solution (12.5 mL, 37.0 mmol) was added dropwise to the reaction mixture. After the addition was complete, the reaction mixture was stirred under a N_2 atmosphere at room temperature for 15 min. The reaction vessel was cooled in an ice-water bath and 30 wt% H_2O_2 (aq) solution (12.5 mL) was added dropwise to the reaction mixture. After the addition was complete, the reaction mixture was stirred under a N_2 atmosphere at room temperature for 3 h. The reaction mixture was saturated with K_2CO_3. The product was extracted with EtOAc. The organic washings were combined and dried over anhydrous $MgSO_4$. The solids were removed by filtration. The

volatiles were removed from the filtrate by rotary evaporation. The resulting product was purified by flash chromatography (SiO_2, hex to 7:3 hex/EtOAc) to yield **4-8** as a colorless liquid (4.80 g, 93%). TLC (SiO_2, hex/EtOAc = 7:3): R_f = 0.42. ^{1}H NMR (500 MHz, $CDCl_3$, δ): 3.75 (dd, J = 5.4 Hz, J = 5.5 Hz, 2H), 3.62 (dd, ^2J = 11.7 Hz, ^4J = 2.6 Hz, 4H), 3.57 (dd, ^2J = 11.8 Hz, ^3J = 6.3 Hz, 1H), 3.56 (dd, ^2J = 9.3 Hz, ^3J = 5.4 Hz, 1H), 3.54 (dd, ^2J = 11.1 Hz, ^3J = 5.4 Hz, 1H), 3.53 (dd, ^2J = 9.2 Hz, ^3J = 6.2 Hz, 1H), 3.51 (d, ^2J = 10.0 Hz, 4H), 3.44 (d, ^2J = 8.9 Hz, 1H), 3.42 (d, ^2J = 9.2 Hz, 2H), 3.40 (d, ^2J = 9.0 Hz, 1H), 2.57 (t, J = 5.7 Hz, 1H), 2.15 (m, 1H), 1.72 (m, 4H), 1.60 (m, 4H), 1.32 (m, 16H), 0.91 (t, J = 6.8 Hz, 6H), 0.90 (t, J = 7.0 Hz, 6H), 0.88 (s, 6H). ^{13}C NMR (125 MHz, $CDCl_3$, δ): 100.9, 74.7, 71.7, 66.1, 64.5, 41.6, 36.2, 34.4, 30.8, 25.9, 25.3, 23.3, 23.2, 18.5, 14.3. ESI–MS (*m/z*): $[M + H]^+$ calcd for $C_{32}H_{63}O_7$, 559.5; found, 559.5. GPC: M_n = 620, M_w/M_n = 1.04. The spectral data agree with literature.[81]

2,2-Bis[(2,2-dibutyl-5-methyl-1,3-dioxan-5-yl)methoxy]ethyl azide (4-9)

A solution of **4-8** (4.00 g, 7.16 mmol), MsCl (1.66 mL, 21.5 mmol), and pyridine (1.71 mL, 21.5 mmol) in anhydrous CH_2Cl_2 (29 mL) was stirred for 21 h at room temperature under a N_2 atmosphere. The reaction mixture was washed with saturated $NaHCO_3$ (aq) solution. The organic layer was washed once with saturated NaCl (aq) solution, and dried over $MgSO_4$. The solids were removed by filtration and the solvent was removed from the filtrate *in vacuo*. To a solution of crude oil in anhydrous DMF (28 mL), and NaN_3 (2.33 g, 35.8 mmol) were added to the mixture. The mixture was heated at 120 °C in an oil bath under N_2 atmosphere for 41 h. The mixture was cooled to room temperature. The solids were removed by filtration and the solvent was removed from the filtrate *in vacuo*. The resulting oil was purified by flash column chromatography (SiO_2, hex to 9:1 hex:EtOAc) to yield **4-9** as a colorless oil (2.44 g, 58 %). TLC (SiO_2, hex/EtOAc = 9:1): R_f = 0.44. ^{1}H NMR (400 MHz, $CDCl_3$, δ): 3.63 (m, 4H; $CH_3CC\mathit{H}_2O$), 3.50 (d, J = 11.5 Hz, 4H; $CC\mathit{H}_2OC$), 3.45 (overlapping m, 4H; CCH_2OC), 3.39 (m, 6H; $CHC\mathit{H}_2O$, $C\mathit{H}_2N_3$), 2.14 (m, 1H; $C\mathit{H}CH_2O$), 1.73 (m, 4H; $CC\mathit{H}_2$), 1.62 (m, 4H; $CC\mathit{H}_2$), 1.33 (m, 16H;

$CCH_2CH_2CH_2CH_3$), 0.93 (t, J = 3.4 Hz, 6H, $CCH_2CH_2CH_2CH_3$), 0.90 (t, J = 3.4 Hz, 6H, $CCH_2CH_2CH_2CH_3$), 0.88 (s, 6H; CCH_3). ^{13}C NMR (100 MHz, $CDCl_3$, δ): 100.8 (CO_2), 74.4 (CH_3CCH_2OC), 69.9 ($CHCH_2$), 66.1 ($CH_3CCH_2OCH_2$), 50.7 (CH_2N_3), 40.3 (CCH_3), 36.1 ($CHCH_2$), 34.5 ($CCH_2CH_2CH_2CH_3$), 31.1 ($CCH_2CH_2CH_2CH_3$), 25.9 ($CCH_2CH_2CH_2CH_3$), 25.3 ($CCH_2CH_2CH_2CH_3$), 23.3 ($CCH_2CH_2CH_2CH_3$), 23.3 ($CCH_2CH_2CH_2CH_3$), 18.6 (CCH_3), 14.3 (CH_2CH_3). HRMS–ESI (*m/z*): [M + H]+ calcd for $C_{32}H_{62}N_3O_6$, 584.4639; found, 584.4644. GPC: M_n = 570, M_w/M_n= 1.06.

2,2-Bis[2,2-di(hydroxymethyl)propyloxymethyl]ethyl azide (4-10)

To a solution of **4-9** (2.44 g, 4.18 mmol) in 1:1 (v/v) THF/MeOH (20 mL), Dowex-50W acidic resin beads (42.01 g) were added. The mixture was stirred at room temperature under a N_2 atmosphere for 3 days. The resin was removed by filtration and the solvent was removed from the filtrate *in vacuo*. The resulting product was purified by flash column chromatorgraphy (SiO_2, CH_2Cl_2 to 9:1 CH_2Cl_2/MeOH) to yield **4-10** as a colorless soild (0.89 g, 64 %). TLC (SiO_2, CH_2Cl_2/MeOH = 9:1): R_f = 0.23. ^{1}H NMR (500 MHz, DMSO-d_6, δ): 4.28 (t, J = 5.3 Hz, 4H, CH_2CCH_3), 3.38 (d, J = 5.9 Hz, 2H; CH_2N_3), 3.32 (m, 4H; O*H*), 3.24 (d, 8H; CH_2OH), 3.18 (q, J = 8.1 Hz, 4H; $CHCH_2$), 2.05 (m, 1H; $CHCH_2O$), 0.76 (s, 6H; CCH_3). ^{13}C NMR (125 MHz, DMSO-d_6, δ): 73.4 ($CH_3CCH_2OCH_2$), 69.2 ($CHCH_2O$), 63.9 (CH_2OH), 50.0 (CH_2N_3), 41.5 (CCH_3), 16.8 (CCH_3). HRMS–ESI (*m/z*): [M + H]+ calcd for $C_{14}H_{30}N_3O_6$, 336.2135; found, 336.2131. GPC: M_n = 300, M_w/M_n = 1.08.

2-(2-[2-(2-Methoxyethoxy)ethoxy]ethoxy)ethyl tosylate (4-12) [66,81]

To an ice-water bath-cooled solution of tetraethylene glycol monomethyl ether (1.61 mL, 8.28 mmol) in THF (2.9 mL), 6 M NaOH (aq) solution (2.6 mL) was added dropwise. To this mixture *p*-TsCl (2.93 g, 15.4 mmol) was added. The mixture was stirred at room temperature under N_2 atmosphere for 20 h. The reaction mixture was diluted with H_2O (10 mL) and the product was extracted three times with CH_2Cl_2

(10 mL). The organic layer was washed once with saturated NaCl (aq) solution, and dried over $MgSO_4$. The solids were removed by filtration and the solvent was removed from the filtrate *in vacuo*. The resulting oil was purified by flash column chromatography (SiO_2, CH_2Cl_2 to 19:1 CH_2Cl_2/MeOH) to yield **4-12** as a colorless oil (2.64 g, 88 %). TLC (SiO_2, hex/EtOAc = 9:1): R_f = 0.32. ^{1}H NMR (500 MHz, $CDCl_3$, δ): 7.78 (d, *J* = 8.3 Hz, 2H; SCC*H*), 7.33 (d, *J* = 8.0 Hz, 2H; CH_3CCH), 4.15 (t, *J* = 5.0 Hz, 2H; SOCH_2), 3.68 (t, *J* = 4.9 Hz, 2H; $SOCH_2CH_2$), 3.63 (t, *J* = 4.6 Hz, 6H; $SOCH_2CH_2OCH_2CH_2OCH_2$), 3.58 (apparent s, 4H; $CH_2OCH_2CH_2OCH_3$), 3.54 (m, 2H; CH_2OCH_3), 3.37 (s, 3H; CH_3CCH), 2.44 (s, 3H; CH_2OCH_3). ^{13}C NMR (125 MHz, $CDCl_3$, δ): 144.8 (S*C*CH), 133.0 (CH_3CCH), 129.8 (SC*C*H), 128.0 (CH_3CCH), 71.9 ($SOCH_2$), 70.7 ($SOCH_2CH_2$), 70.6 ($SOCH_2CH_2OCH_2$), 70.6 ($SOCH_2CH_2OCH_2CH_2$), 70.5 ($CH_2CH_2OCH_2CH_2OCH_3$), 70.5 ($CH_2CH_2OCH_2CH_2OCH_3$), 69.2 ($CH_2CH_2OCH_3$), 68.7 ($CH_2CH_2OCH_3$), 59.0 (OCH_3), 21.7 (CH_3CCH). ESI–MS (*m/z*): $[M + NH_4]^+$ calcd for $C_{16}H_{30}O_7NS$, 380.2; found, 380.1. Spectral data agree with those previously reported.[98,99]

2,2-Bis(2,2-di[2-(2-[2-(2-methoxyethoxy)ethoxy]ethoxy)ethoxymethyl]-propyloxymethyl)ethyl azide (4-11) To an ice-water bath-cooled solution of **4-10** (0.20 g, 0.60 mmol) in anhydrous THF (6 mL), NaH (0.10 g, 4.2 mmol) (Caution! The addition of NaH to solutions of alcohol is exothermic) and **4-12** (1.09 g, 3.01 mmol) were added. The mixture was heated to reflux in an oil bath under N_2 atmosphere for 18 h. The mixture was cooled in an ice-water bath. The reaction mixture was quenched with deionized water. The product was extracted three times with CH_2Cl_2 (10 mL). The organic washings were combined, washed once with saturated NaCl (aq) solution and dried over anhydrous $MgSO_4$. The solid was removed by filtration and the solvent was removed from the filtrate *in vacuo*. The resulting oil was purified by flash chromatography (SiO_2, CH_2Cl_2 to 9:1 CH_2Cl_2/MeOH) to yield **4-11** as a colorless liquid (0.58 g, 86 %). TLC (SiO_2, CH_2Cl_2/MeOH = 9:1): R_f = 0.51. ^{1}H NMR (400 MHz, $CDCl_3$, δ): 3.65-3.69 (m, 48H; $CH_2O(CH_2CH_2O)_3CH_2CH_2OCH_3$), 3.54 (m, 16H;

$CH_2O(CH_2CH_2O)_3CH_2CH_2OCH_3$), 3.37 (s, 12H; $CH_2CH_2OCH_3$), 3.34-3.29 (m, 14H, CH_3CCH_2, CH_2N_3), 3.23 (t, J = 9.3 Hz, 4H; $CHCH_2$), 2.10 (m, 1H; $CHCH_2O$), 0.91 (s, 6H; CCH_3). ^{13}C NMR (100 MHz, $CDCl_3$, δ): 74.1 ($CH_3CCH_2OCH_2CH$), 72.1 ($CH_3CCH_2OCH_2CH_2$), 71.2 ($CCH_2O(CH_2CH_2O)_4CH_3$), 70.86 ($CCH_2O(CH_2CH_2O)_4CH_3$), 70.82 ($CCH_2O(CH_2CH_2O)_4CH_3$), 70.79 ($CCH_2O(CH_2CH_2O)_4CH_3$), 70.73 ($CCH_2O(CH_2CH_2O)_4CH_3$), 70.6 ($CCH_2O(CH_2CH_2O)_4CH_3$), 69.8 ($CHCH_2O$), 59.3 (OCH_3), 50.6 (CH_2N_3), 41.2 (CCH_3), 40.2 ($CHCH_2O$), 17.6 (CCH_3). HRMS–ESI (m/z): [M + H]+ calcd for $C_{50}H_{102}N_3O_{22}$, 1096.6955; found, 1096.6965. GPC: M_n =1,100, M_w/M_n=1.08.

Peptide-Dendron Hybrid 4-1b. Dendritic azide **4-11** (16.4 mg, 0.0150 mmol) was dissolved in 200 μL H_2O and transferred to a vial containing peptide **4-3b** (7.6 mg, 0.0030 mmol) in 300 μL of DMSO. The reaction mixture was purged with N_2 for one hour prior to adding $CuSO_4{\cdot}5H_2O$ (0.6 mg, 0.002 mmol) and sodium ascorbate (1.2 mg, 0.0061 mmol) in 100 μL H_2O. The reaction mixture was stirred at room temperature under a N_2 atmosphere for 17 h. The reaction mixture was purified by preparative HPLC to yield **4-1b** (8.3 mg, 47 %) as a colorless powder.

Peptide-Dendron Hybrid 4-2. Dendritic azide **4-11** (10.2 mg, 0.00930 mmol) was dissolved in H_2O (110 μL) and transferred to a vial containing peptide **4-4** (5.5 mg, 0.0032 mmol), a premixed solution of $CuSO_4{\cdot}5H_2O$ (1.2 μL, 1 M solution in H_2O), and sodium ascorbate (2 mg, 0.01 mmol) in DMSO (110 μL). The reaction mixture was stirred at room temperature under a N_2 atmosphere for 90 h. The reaction mixture was purified by preparative HPLC to yield **4-2** (6.7 mg, 53 %) as a colorless powder.

Peptide-Linear Hybrid 4-16. Azide **4-15** (7.8 mg, 0.034 mmol) was dissolved in 150 μL 1 M TIRS·HCl buffer (pH 8) and transferred to a vial containing peptide **4-3a** (6.8 mg, 0.0040 mmol), $CuSO_4{\cdot}5H_2O$ (1.2 mg, 0.0048 mmol), and sodium ascorbate (2.5 mg, 0.013 mmol) in 150 μL of DMSO. The reaction mixture was stirred at room temperature under a N_2 atmosphere for 15 h. The reaction mixture was purified by preparative HPLC to yield **4-16** (3.8 mg, 44 %) as a colorless powder.

Peptide-Linear Hybrid 17. Azide **4-15** (5.1 mg, 0.0023 mmol) was dissolved in 1 M TRIS·HCl buffer (pH 8) (150 μL) and transferred to a vial containing peptide **4-4** (5.0 mg, 0.0029 mmol), a premixed solution of $CuSO_4 \cdot 5H_2O$ (1.5 μL, 1 M solution in H_2O), and sodium ascorbate (1.2 mg, 0.0061 mmol) in DMSO (150 μL). The reaction mixture was stirred at room temperature under a N_2 atmosphere for 15 h. The reaction mixture was purified by preparative HPLC to yield **4-17** (1.5 mg, 22 %) as a colorless powder.

4.5 References

1. Furuta, P.; Fréchet, J. M. J., Controlling Solubility and Modulating Peripheral Function in Dendrimer Encapsulated Dyes. *J. Am. Chem. Soc.* **2003,** *125*, 13173-13181.

2. DeMattei, C. R.; Huang, B.; Tomalia, D. A., Designed dendrimer syntheses by self-assembly of single-site, ssDNA functionalized dendrons. *Nano Lett.* **2004,** *4*, 771-777.

3. Maraval, V.; Caminade, A.-M.; Majoral, J.-P.; Blais, J.-C., Dendrimer Design: How to Circumvent the Dilemma of a Reduction of Steps or an Increase of Function Multiplicity? *Angew. Chem., Int. Ed.* **2003,** *42*, 1822-1826.

4. Douat-Casassus, C.; Darbre, T.; Reymond, J.-L., Selective Catalysis with Peptide Dendrimers. *J. Am. Chem. Soc.* **2004,** *126*, 7818-7826.

5. Lim, J.; Kostiainen, M.; Maly, J.; da Costa, V. C. P.; Annunziata, O.; Pavan, G.; Simanek, E. E., Synthesis of Large Dendrimers with the Dimensions of Small Viruses. *J. Am. Chem. Soc.* **2013,** *135*, 4660-4663.

6. Lhenry, S.; Jalkh, J.; Leroux, Y. R.; Ruiz, J.; Ciganda, R.; Astruc, D.; Hapiot, P., Tunneling Dendrimers. Enhancing Charge Transport through Insulating Layer Using Redox Molecular Objects. *J. Am. Chem. Soc.* **2014,** *136*, 17950-17953.

7. Melicher, M. S.; Walker, A. S.; Shen, J.; Miller, S. J.; Schepartz, A., Improved Carbohydrate Recognition in Water with an Electrostatically Enhanced β-Peptide Bundle. *Org. Lett.* **2015,** *17*, 4718-4721.

8. Miller, J. P.; Melicher, M. S.; Schepartz, A., Positive Allostery in Metal Ion Binding by a Cooperatively Folded β-Peptide Bundle. *J. Am. Chem. Soc.* **2014,** *136*, 14726-14729.

9. Melicher, M. S.; Chu, J.; Walker, A. S.; Miller, S. J.; Baxter, R. H. G.; Schepartz, A., A β-Boronopeptide Bundle of Known Structure As a Vehicle for Polyol Recognition. *Org. Lett.* **2013,** *15*, 5048-5051.

10. Daniels, D. S.; Petersson, E. J.; Qui, J. X.; Schepartz, A., High-Resolution Structure of a β-Peptide Bundle. *J. Am. Chem. Soc.* **2007,** *129*, 1532-1533.

11. Korendovych, I. V.; Kim, Y. H.; Ryan, A. H.; Lear, J. D.; DeGrado, W. F.; Shandler, S. J., Computational Design of a Self-Assembling β-Peptide Oligomer. *Org. Lett.* **2010,** *12*, 5142-5145.

12. Cheng, R. P.; DeGrado, W. F., Long-Range Interactions Stabilize the Fold of a Non-natural Oligomer. *J. Am. Chem. Soc.* **2002,** *124*, 11546-11565.

13. Collie, G. W.; Pulka-Ziach, K.; Lombardo, C. M.; Fremaux, J.; Rosu, F.; Decossas, M.; Mauran, L.; Lambert, O.; Gabelica, V.; Mackereth, C. D.; Guichard, G., Shaping quaternary assemblies of water-soluble non-peptide helical foldamers by sequence manipulation. *Nat. Chem.* **2015,** *7*, 871-878.

14. Nanda, V.; Koder, R. L., Designing artificial enzymes by intuition and computation. *Nat. Chem.* **2010,** *2*, 15-24.

15. Yu, F.; Cangelosi, V. M.; Zastrow, M. L.; Tegoni, M.; Plegaria, J. S.; Tebo, A. G.; Mocny, C. S.; Ruckthong, L.; Qayyum, H.; Pecoraro, V. L., Protein Design: Toward Functional Metalloenzymes. *Chem. Rev.* **2014,** *114*, 3495-3578.

16. Shu, J. Y.; Panganiban, B.; Xu, T., Peptide-polymer conjugates: from fundamental science to application. *Annu. Rev. Phys. Chem.* **2013,** *64*, 631-657.

17. Klok, H.-A., Peptide/protein-synthetic polymer conjugates: Quo vadis. *Macromolecules* **2009,** *42*, 7990-8000.

18. Shao, H.; Lockman, J. W.; Parquette, J. R., Coupled Conformational Equilibria in β -Sheet Peptide−Dendron Conjugates. *J. Am. Chem. Soc.* **2007,** *129*, 1884-1885.

19. Shao, H.; Parquette, J. R., Controllable Peptide–Dendron Self-Assembly: Interconversion of Nanotubes and Fibrillar Nanostructures. *Angew. Chem., Int. Ed.* **2009,** *48*, 2525-2528.

20. Shao, H.; Bewick, N. A.; Parquette, J. R., Intramolecular chiral communication in peptide-dendron hybrids. *Org. Biomol. Chem.* **2012,** *10*, 2377-2379.

21. Jang, W.-D.; Aida, T., Dendritic Physical Gels: Structural Parameters for Gelation with Peptide-Core Dendrimers. *Macromolecules* **2003,** *36*, 8461-8469.

22. Jang, W.-D.; Jiang, D.-L.; Aida, T., Dendritic physical gel: Hierarchical self-organization of a peptide-core dendrimer to form a micrometer-scale fibrous assembly. *J. Am. Chem. Soc.* **2000,** *122*, 3232-3233.

23. Sato, K.; Itoh, Y.; Aida, T., Columnarly Assembled Liquid-Crystalline Peptidic Macrocycles Unidirectionally Orientable over a Large Area by an Electric Field. *J. Am. Chem. Soc.* **2011,** *133*, 13767-13769.

24. Sato, K.; Itoh, Y.; Aida, T., Homochiral supramolecular polymerization of bowl-shaped chiral macrocycles in solution. *Chem. Sci.* **2014,** *5*, 136-140.

25. Percec, V.; Dulcey, A. E.; Balagurusamy, V. S. K.; Miura, Y.; Smidrkal, J.; Peterca, M.; Nummelin, S.; Edlund, U.; Hudson, S. D.; Heiney, P. A.; Duan, H.; Magonov, S. N.; Vinogradov, S. A., Self-Assembly of Amphiphilic Dendritic Dipeptides into Helical Pores. *Nature* **2004,** *430*, 764-768.

26. Percec, V.; Dulcey, A.; Peterca, M.; Ilies, M.; Miura, Y.; Edlund, U.; Heiney, P. A., Helical Porous Protein Mimics Self-Assembled from Amphiphilic Dendritic Dipeptides. *Aust. J. Chem.* **2005,** *58*, 472-482.

27. Percec, V.; Dulcey, A. E.; Peterca, M.; Ilies, M.; Ladislaw, J.; Rosen, B. M.; Edlund, U.; Heiney, P. A., The internal structure of helical pores self-assembled from dendritic dipeptides is stereochemically programmed and allosterically regulated. *Angew. Chem., Int. Ed.* **2005,** *44*, 6516-6521.

28. Percec, V.; Dulcey, A. E.; Peterca, M.; Ilies, M.; Sienkowska, M. J.; Heiney, P. A., Programming the internal structure and stability of helical pores self-assembled from dendritic dipeptides via the protective groups of the peptide. *J. Am. Chem. Soc.* **2005,** *127*, 17902-17909.

29. Percec, V.; Dulcey, A. E.; Peterca, M.; Ilies, M.; Nummelin, S.; Sienkowska, M. J.; Heiney, P. A., Principles of self-assembly of helical pores from dendritic dipeptides. *Proc. Natl. Acad. Sci. U. S. A.* **2006,** *103*, 2518-2523.

30. Peterca, M.; Percec, V.; Dulcey, A. E.; Nummelin, S.; Korey, S.; Ilies, M.; Heiney, P. A., Self-assembly, structural, and retrostructural analysis of dendritic dipeptide pores undergoing reversible circular to elliptical shape change. *J. Am. Chem. Soc.* **2006,** *128*, 6713-6720.

31. Percec, V.; Dulcey, A. E.; Peterca, M.; Adelman, P.; Samant, R.; Balagurusamy, V. S. K.; Heiney, P. A., Helical pores self-assembled from homochiral dendritic dipeptides based on L-Tyr and nonpolar alpha-amino acids. *J. Am. Chem. Soc.* **2007,** *129*, 5992-6002.

32. Percec, V.; Peterca, M.; Dulcey, A. E.; Imam, M. R.; Hudson, S. D.; Nummelin, S.; Adelman, P.; Heiney, P. A., Hollow spherical supramolecular dendrimers. *J. Am. Chem. Soc.* **2008,** *130*, 13079-13094.

33. Rosen, B. M.; Peterca, M.; Morimitsu, K.; Dulcey, A. E.; Leowanawat, P.; Resmerita, A.-M.; Imam, M. R.; Percec, V., Programming the supramolecular helical polymerization of dendritic dipeptides via the stereochemical information of the dipeptide. *J. Am. Chem. Soc.* **2011,** *133*, 5135-5151.

34. Kim, A. J.; Kaucher, M. S.; Davis, K. P.; Peterca, M.; Imam, M. R.; Christian, N. A.; Levine, D. H.; Bates, F. S.; Percec, V.; Hammer, D. A., Proton Transport from Dendritic Helical-Pore-Incorporated Polymersomes. *Adv. Funct. Mater.* **2009,** *19*, 2930-2936.

35. Kaucher, M. S.; Peterca, M.; Dulcey, A. E.; Kim, A. J.; Vinogradov, S. A.; Hammer, D. A.; Heiney, P. A.; Percec, V., Selective transport of water mediated by porous dendritic dipeptides. *J. Am. Chem. Soc.* **2007,** *129*, 11698-11699.

36. Amorín, M.; Pérez, A.; Barberá, J.; Ozores, H. L.; Serrano, J. L.; Granja, J. R.; Sierra, T., Liquid crystal organization of self-assembling cyclic peptides. *Chem. Commun.* **2014,** *50*, 688-690.

37. Lee, J.; Kim, J. M.; Yun, M.; Park, C.; Park, J.; Lee, K. H.; Kim, C., Self-organization of amide dendrons with focal dipeptide units. *Soft Matter* **2011,** *7*, 9021-9026.

38. von Gröning, M.; de Feijter, I.; Stuart, M. C. A.; Voets, I. K.; Besenius, P., Tuning the aqueous self-assembly of multistimuli-responsive polyanionic peptide nanorods. *J. Mater. Chem. B* **2013,** *1*, 2008-2012.

39. Appel, R.; Tacke, S.; Klingauf, J.; Besenius, P., Tuning the pH-triggered self-assembly of dendritic peptide amphiphiles using fluorinated side chains. *Org. Biomol. Chem.* **2015,** *13*, 1030-1039.

40. Appel, R.; Fuchs, J.; Tyrrell, S. M.; Korevaar, P. A.; Stuart, M. C. A.; Voets, I. K.; Schönhoff, M.; Besenius, P., Steric Constraints Induced Frustrated Growth of Supramolecular Nanorods in Water. *Chem.–Eur. J.* **2015**.

41. Rosen, B. M.; Roche, C.; Percec, V., Self-assembly of dendritic dipeptides as a model of chiral selection in primitive biological systems. *Topics in Current Chemistry* **2013,** *333*, 213-253.

42. Percec, V.; Leowanawat, P., Why Are Biological Systems Homochiral? *Isr. J. Chem.* **2011,** *51*, 1107-1117.

43. Percec, V., From synthetic macromolecules to biological-like complex systems. *Adv. Polym. Sci.* **2013,** *261*, 173-197.

44. Roche, C.; Su, H.-J.; Leowanawat, P.; Araoka, F.; Partridge, B. E.; Peterca, M.; Wilson, D. A.; Prendergast, M. E.; Heiney, P. A.; Graf, R.; Spiess, H. W.; Zeng, Z.; Ungar, G.; Percec, V., A supramolecular helix that disregards chirality. *Nat. Chem.* **2015**.

45. Percec, V.; Aqad, E.; Peterca, M.; Rudick, J. G.; Lemon, L.; Ronda, J. C.; De, B. B.; Heiney, P. A.; Meijer, E. W., Steric communication of chiral information observed in dendronized polyacetylenes. *J. Am. Chem. Soc.* **2006,** *128*, 16365-16372.

46. Roche, C.; Sun, H.-J.; Prendergast, M. E.; Leowanawat, P.; Partridge, B. E.; Heiney, P. A.; Araoka, F.; Graf, R.; Spiess, H. W.; Zeng, X.; Ungar, G.; Percec, V., Homochiral Columns Constructed by Chiral Self-Sorting During Supramolecular Helical Organization of Hat-Shaped Molecules. *J. Am. Chem. Soc.* **2014,** *136*, 7169-7185.

47. Marine, J. E.; Song, S.; Liang, X.; Watson, M. D.; Rudick, J. G., Bundle-forming α-helical peptide-dendron hybrid. *Chem. Commun.* **2015,** *51*, 14314-14317.

48. MacKenzie, K. R., Folding and Stability of α-Helical Integral Membrane Proteins. *Chem. Rev.* **2006,** *106*, 1931-1977.

49. Woolfson, D. N., The design of coiled-coil structures and assemblies. *Adv. Protein Chem.* **2005,** *70*, 79-112.

50. Apostolovic, B.; Danial, M.; Klok, H.-A., Coiled coils: attractive protein folding motifs for the fabrication of self-assembled, responsive and bioactive materials. *Chem. Soc. Rev.* **2010,** *39*, 3541-3575.

51. DeGrado, W. F.; Lear, J. D., Induction of peptide conformation at apolar/water interfaces. 1. A study with model peptides of defined hydrophobic periodicity. *J. Am. Chem. Soc.* **1985,** *107*, 7684-7689.

52. Buchko, G. W.; Jain, A.; Reback, M. L.; Shaw, W. J., Structural characterization of the model amphipathic peptide Ac-LKKLLKLLKKLLKL-NH_2 in aqueous solution and with 2,2,2-trifluoroethanol and 1,1,1,3,3,3-hexafluoroisopropanol. *Can. J. Chem.* **2013,** *91*, 406-413.

53. Shu, J. Y.; Tan, C.; DeGrado, W. F.; Xu, T., New design of helix bundle peptide-polymer conjugates. *Biomacromolecules* **2008,** *9*, 2111-2117.

54. Dube, N.; Presley, A. D.; Shu, J. Y.; Xu, T., Amphiphilic Peptide–Polymer Conjugates with Side-Conjugation. *Macromol. Rapid Commun.* **2011,** *32*, 344-353.

55. Presley, A. D.; Chang, J. J.; Xu, T., Directed co-assembly of heme proteins with amphiphilic block copolymers toward functional biomolecular materials. *Soft Matter* **2011,** *7*, 172-179.

56. Shu, J. Y.; Lund, R.; Xu, T., Solution Structural Characterization of Coiled-Coil Peptide–Polymer Side-Conjugates. *Biomacromolecules* **2012,** *13*, 1945-1955.

57. Lund, R.; Shu, J.; Xu, T., A Small-Angle X-ray Scattering Study of α-helical Bundle-Forming Peptide–Polymer Conjugates in Solution: Chain Conformations. *Macromolecules* **2013,** *46*, 1625-1632.

58. Danial, M.; Aleksandrowicz, J.; Pötgens, A. J. G.; Klok, H.-A., Site-Specific PEGylation of HR2 Peptides: Effects of PEG Conjugation Position and Chain Length on HIV-1 Membrane Fusion Inhibition and Proteolytic Degradation. *Bioconjugate Chem.* **2012,** *23*, 1648-1660.

59. Wilger, D. J.; Bettis, S. E.; Materese, C. K.; Minakova, M.; Papoian, G. A.; Papanikolas, J. M.; Waters, M. L., Tunable energy transfer rates via control of primary, secondary, and tertiary structure of a coiled coil peptide scaffold. *Inorg. Chem.* **2012,** *51*, 11324-11338.

60. Mahmoud, Z. N.; Grundy, D. J.; Channon, K. J.; Woolfson, D. N., The non-covalent decoration of self-assembling protein fibers. *Biomaterials* **2010,** *31*, 7468-7474.

61. Mahmoud, Z. N.; Gunnoo, S. B.; Thomson, A. R.; Fletcher, J. M.; Woolfson, D. N., Bioorthogonal dual functionalization of self-assembling peptide fibers. *Biomaterials* **2011,** *32*, 3712-3720.

62. Jain, A.; Buchko, G. W.; Reback, M. L.; O'Hagan, M.; Ginovska-Pangovska, B.; Linehan, J. C.; Shaw, W. J., Active Hydrogenation Catalyst with a Structured, Peptide-Based Outer-Coordination Sphere. *ACS Catal.* **2012,** *2*, 2114-2118.

63. Fu, L.; Liu, J.; Yan, E. C. Y., Chiral sum frequency generation spectroscopy for characterizing protein secondary structures at interfaces. *J. Am. Chem. Soc.* **2011,** *133*, 8094-8097.

64. Mermut, O.; Phillips, D. C.; York, R. L.; McCrea, K. R.; Ward, R. S.; Somorjai, G. A., In situ adsorption studies of a 14-amino acid leucine-lysine peptide onto hydrophobic polystyrene and hydrophilic silica surfaces using quartz crystal microbalance, atomic force microscopy, and sum frequency generation vibrational spectroscopy. *J. Am. Chem. Soc.* **2006,** *128*, 3598-3607.

65. Long, J. R.; Oyler, N.; Drobny, G. P.; Stayton, P. S., Assembly of α-helical Peptide Coatings on Hydrophobic Surfaces. *J. Am. Chem. Soc.* **2002,** *124*, 6297-6303.

66. Marine, J. E.; Liang, X.; Song, S.; Rudick, J. G., Azide-Rich Peptides Via an On-Resin Diazotransfer Reaction. *Biopolymers* **2015,** *104*, 419-426.

67. Shoemaker, K. R.; Kim, P. S.; York, E. J.; Stewart, J. M.; Baldwin, R. L., Tests of the helix dipole model for stabilization of α-helices. *Nature* **1987,** *326*, 563-567.

68. Fairman, R.; Shoemaker, K. R.; York, E. J.; Stewart, J. M.; Baldwin, R. L., Further studies of the helix dipole model: Effects of a free α-NH3+ or α-COO− group on helix stability. *Proteins: Struct., Funct., Genet.* **1989,** *5*, 1-7.

69. Pace, C. N.; Vajdos, F.; Fee, L.; Grimsley, G.; Gray, T., How to measure and predict the molar absorption coefficient of a protein. *Protein Sci.* **1995,** *4*, 2411-2423.

70. Woody, R. W., Aromatic side-chain contributions to the far ultraviolet circular dichroism of peptides and proteins. *Biopolymers* **1978,** *17*, 1451-1467.

71. Wang, Q.; Chan, T. R.; Hilgraf, R.; Fokin, V. V.; Sharpless, K. B.; Finn, M. G., Bioconjugation by Copper(I)-Catalyzed Azide-Alkyne [3 + 2] Cycloaddition. *J. Am. Chem. Soc.* **2003,** *125*, 3192-3193.

72. Tam, J. P.; Lu, Y.-A., Coupling Difficulty Associated with Interchain Clustering and Phase Transition in Solid Phase Peptide Synthesis. *J. Am. Chem. Soc.* **1995,** *117*, 12058-12063.

73. Cremer, G.-A.; Tariq, H.; Delmas, A. F., Combining a polar resin and a pseudo-proline to optimize the solid-phase synthesis of a 'difficult sequence'. *J. Pept. Sci.* **2006,** *12*, 437-442.

74. Patel, H.; Chantell, C. A.; Fuentes, G.; Menakuru, M.; Park, J. H., Resin comparison and fast automated stepwise conventional synthesis of human SDF-1 α . *J. Pept. Sci.* **2008,** *14*, 1240-1243.

75. García-Ramos, Y.; Paradís-Bas, M.; Tulla-Puche, J.; Albericio, F., ChemMatrix® for complex peptides and combinatorial chemistry. *J. Pept. Sci.* **2010,** *16*, 675-678.

76. Miranda, M. T. M.; Liria, C. W.; Remuzgo, C., Difficult Peptides. In *Amino Acids, Peptides and Proteins in Organic Chemisty: Building Blocks, Catalysis, and Coupling Chemistry*, Hughes, A. B., Ed.; Wiley-VCH, 2011; Vol. 3, pp 549-569.

77. Coin, I., The depsipeptide method for solid-phase synthesis of difficult peptides. *J. Pept. Sci.* **2010,** *16*, 223-230.

78. Tickler, A. K.; Wade, J. D., Overview of Solid Phase Synthesis of "Difficult Peptide" Sequences. In *Current Protocols in Protein Science*, 2007; Vol. 50, pp 18.8.1-18.8.6.

79. Suckau, D.; Resemann, A.; Schuerenberg, M.; Hufnagel, P.; Franzen, J.; Holle, A., A novel MALDI LIFT-TOF/TOF mass spectrometer for proteomics. *Anal. Bioanal. Chem.* **2003,** *376*, 952-965.

80. Grayson, S. M.; Jayaraman, M.; Fréchet, J. M. J., Convergent Synthesis and 'Surface' Functionalization of a Dendritic Analog of Poly(ethylene glycol). *Chem. Commun.* **1999**, 1329-1339.

81. Grayson, S. M.; Fréchet, J. M. J., Synthesis and surface functionalization of aliphatic polyether dendrons. *J. Am. Chem. Soc.* **2000,** *122*, 10335-10344.

82. Jayaraman, M.; Fréchet, J. M. J., A convergent route to novel aliphatic polyether dendrimers. *J. Am. Chem. Soc.* **1998,** *120*, 12996-12997.

83. Jee, J.-A.; Spagnuolo, L. A.; Rudick, J. G., Convergent synthesis of dendrimers via the Passerini three-component reaction. *Org. Lett.* **2012,** *14*, 3292-3295.

84. Liang, X.; Sen, M. K.; Jee, J.-A.; Gelman, O.; Marine, J. E.; Kan, K.; Endoh, M. K.; Barkley, D. A.; Koga, T.; Rudick, J. G., Poly(oxanorbornenedicarboximide)s dendronized with amphiphilic poly(alkyl ether) dendrons. *J. Polym. Sci., Part A: Polym. Chem.* **2014,** *52*, 3221-3239.

85. Niemietz, M.; Perkams, L.; Hoffman, J.; Eller, S.; Unverzagt, C., Selective oxidative debenzylation of mono- and oligosaccharides in the presence of azides. *Chem. Commun.* **2011,** *47*, 10485-10487.

86. Adinolfi, M.; Barone, G.; Guariniello, L.; Iadonisi, A., Facile cleavage of carbohydrate benzyl ethers and benzylidene acetals using the $NaBrO_3/Na_2S_2O_4$ reagent under two-phase conditions. *Tetrahedron Lett.* **1999,** *40*, 8439-8441.

87. Kim, H.-Y.; Lee, B.-I.; Cho, B.-K., Large-scale synthesis of water soluble non-ionic dendrons by stepwise extraction purifications. *Macromol. Rapid Commun.* **2008,** *29*, 1758-1763.

88. Gupta, S. S.; Kuzelka, J.; Singh, P.; Lewis, W. G.; Manchester, M.; Finn, M. G., Accelerated Bioorthogonal Conjugation: A Practical Method for the Ligation of Diverse Functional Molecules to a Polyvalent Virus Scaffold. *Bioconjugate Chem.* **2005,** *16*, 1572-1579.

89. Soriano del Amo, D.; Wang, W.; Jiang, H.; Besanceney, C.; Yan, A. C.; Levy, M.; Liu, Y.; Marlow, F. L.; Wu, P., Biocompatible Copper(I) Catalysts for in Vivo Imaging of Glycans. *J. Am. Chem. Soc.* **2010,** *132*, 16893-16899.

90. Hong, V.; Presolski, S. I.; Ma, C.; Finn, M. G., Analysis and Optimization of Copper-Catalyzed Azide- "Alkyne Cycloaddition for Bioconjugation. *Angew. Chem., Int. Ed.* **2009,** *48*, 9879-9883.

91. Chan, T. R.; Hilgraf, R.; Sharpless, K. B.; Fokin, V. V., Polytriazoles as Copper(I)-Stabilizing Ligands in Catalysis. *Org. Lett.* **2004,** *6*, 2853-2855.

92. Kumar, A.; Li, K.; Cai, C., Anaerobic conditions to reduce oxidation of proteins and to accelerate the copper-catalyzed "Click" reaction with a water-soluble bis(triazole) ligand. *Chem. Commun.* **2011,** *47*, 3186-3188.

93. Strohalm, M. *mMass*, 5.5.0. Available at: http://www.mmass.org/.

94. Rodionov, V. O.; Presolski, S. I.; Gardinier, S.; Lim, Y.-H.; Finn, M. G., Benzimidazole and related ligands for Cu-catalyzed azide-alkyne cycloaddition. *J. Am. Chem. Soc.* **2007,** *129*, 12696-12704.

95. Kolb, H. C.; Finn, M. G.; Sharpless, K. B., Click chemistry: Diverse chemical function from a few good reactions. *Angew. Chem., Int. Ed.* **2001,** *40*, 2004-2021.

96. Shu, J. Y.; Hodges, R. S.; Kay, C. M., Effect of chain length on the formation and stability of synthetic α-helical coiled coils. *Biochemistry* **1994,** *33*, 15501-15510.

97. Kochendoerfer, G. G.; Chen, S.-Y.; Mao, F.; Cressman, S.; Traviglia, S.; Shao, H.; Hunter, C. L.; Low, D. W.; Cagle, E. N.; Carnevali, M.; Gueriguian, V.; Keogh, P. J.; Porter, H.; Stratton, S. M.; Wiedeke, M. C.; Wilken, J.; Tang, J.; Levy, J. J.; Miranda, L. O.; Crnogorac, M. M.; Kalbag, S.; Botti, P.; Schindler-Horvat, J.; Savatski, L.; Adamson, J. W.; Kung, A.; Kent, S. B. H.; Bradburne, J. A., Design and Chemical Synthesis of a Homogeneous Polymer-Modified Erythropoiesis Protein. *Science* **2003,** *299*, 884-887.

98. Wolfe, A. L.; Duncan, K. K.; Lajiness, J. P.; Zhu, K.; Duerfeldt, A. S.; Boger, D. L., A fundamental relationship between hydrophobic properties and biological activity for the duocarmycin

class of DNA-alkylating antitumor drugs: Hydrophobic-binding-driven bonding. *J. Med. Chem.* **2013,** *56*, 6845-6857.

99. Ouchi, M.; Inoue, Y.; Liu, Y.; Nagamune, S.; Nakamura, S.; Wada, K.; Hakushi, T., Convenient and efficient tosylation of oligoethylene glycols and the related alcohols in tetrahydrofuran-water in the presence of sodium hydroxide. *Bull. Chem. Soc. Jpn.* **1990,** *63*, 1260-1262.